The creation of a reservoir in the White Volta River, Ghana: An analysis of the impact on river morphology

Master's thesis report

May 2012

Author:
Joost van der Zwet

TU Delft

HKV CONSULTANTS

The creation of a reservoir in the White Volta River, Ghana: An analysis of the impact on river morphology

Master's thesis report

A thesis submitted for the degree of Master of Science
Delft University of Technology
Faculty of Civil Engineering and Geosciences
Department of Water Management
Section of Water Resources

May 2012

Author:
Joost van der Zwet

Graduation committee:

Prof. Dr. Ir. N.C. van de Giesen	- Delft University of Technology, CE, Watermanagement
Dr. T.A. Bogaard	- Delft University of Technology, CE, Watermanagement
Dr. Ir. C.J. Sloff	- Delft University of Technology, CE, Hydraulic Engineering
Ir. P. Termes	- HKV Consultants

Preface

This report marks the end of my study Watermanagement at the faculty of Civil Engineering and Geosciences at Delft University of Technology. I enjoyed this period, which was full of interesting courses and the enthusiasm and commitment of both staff and students was encouraging to me.

In this Master's thesis I was able to apply the knowledge I have gained in the fields of hydrology and water resources management. Additionally, I could integrate these fields with morphology, geology and hydraulics, which made this a dynamic project. Furthermore, the applied relevance of the topic, the construction of a dam in Northern Ghana, motivated me very much. Especially the field research has been an amazing experience; the interaction with the people, the daily methodological improvisations and the unexpected situations made this an unforgettable time.

I would like to acknowledge some people who were helpful to me during the process of my Master's thesis. First, I would like to thank the members of my graduation committee: Paul Termes for his daily supervision and functional and detailed commentary; Prof. Nick van de Giesen for suggesting the subject, introducing me to HKV consultants and his useful advise; Thom Bogaard and Kees Sloff for the valuable discussions. I would also like to thank HKV for giving me this opportunity, the Lamminga fonds for their financial support and the Water Research Institute in Accra for providing the measurement equipment and facilities. My parents deserve many thanks for their support, in many ways, and their confidence in me to choose my own path in life. Last, I would like to thank my dear Jacqueline for her love, patience and continuous support and encouragement.

Executive summary

There are plans for the construction of a multi-purpose dam in the White Volta River near Pwalugu in northern Ghana. The reservoir that will be formed should be beneficial for hydropower generation, irrigation and fishery. Up to now there has been no research into the morphological consequences of the creation of this reservoir. In this study the rate and location of sedimentation in the reservoir and the erosion of the riverbed downstream of the dam are investigated. Sedimentation could lead to a loss of storage capacity having less water available for hydropower generation and irrigation purposes. Delta deposition (i.e. sedimentation of coarse sediment in the upstream part of the reservoir) could lead to higher water levels in the river upstream, causing an increased risk of flooding. Erosion of the riverbed downstream of the dam could lead to decreased water levels in the downstream reach. This could provoke riverbank collapse and have negative effects on agriculture due to lowering of groundwater levels. Possibly bridges downstream could be damaged by scouring of the foundations. The aim of this research is to understand the large-scale morphological processes and to give first order estimations of the morphological changes. Additionally, the sediment balance of the White Volta catchment is investigated to estimate landscape erosion. The method consists of a literature study, a field study and a morphological model (SOBEK) of the White Volta River.

The total sedimentation in the intended reservoir has been analysed by determining the yearly sediment transport of the White Volta River. The estimation is based on field measurements, conducted in September 2011 at a location close to the proposed dam site, supplemented with a literature study and theoretical transport formulas. The yearly average sediment inflow appeared to be ± 1 million ton/year. The theoretical trap efficiency of the reservoir is nearly 100%, so it is assumed that all sediment will be deposited. If all sediment settles in the active storage of the reservoir, this would mean a storage loss of 3% per 100 years. The impact of this storage loss on the functions of the reservoir is considered negligible.

The delta deposition (i.e. sedimentation of coarse material) and the erosion downstream of the dam have been estimated using SOBEK RE, a 1D software package capable of solving the hydrodynamic, sediment transport and morphological equations. The model parameters followed from the field research. The delta deposition depends on the water level variation in the reservoir. If the water level varies between maximum and minimum operative level, the reservoir will vary in length over 40 km and most of the delta deposition will occur in this region. The delta deposition is propagating in both upstream and downstream direction. Due to upstream propagation the riverbed level upstream of the reservoir will also increase. After 50 years, the effect is restricted to ± 30 cm just upstream of the lake and has damped out at the border of Burkina Faso. The water levels will slightly increase during high flows. More research is needed to analyse the increased risk of flooding.

Erosion of the riverbed downstream of the dam will occur. The released flow through the dam is expected to be sediment-free. As the sediment concentration is lower than the sediment carrying capacity, the river will take up sediment and the bed will experience erosion. The riverbed level could decrease by 20-30 m in 50 years just downstream of the dam. The erosion rate is reducing in downstream direction, but propagating in time. After ± 30 years a bridge near Pwalugu could be affected. The erosion could be limited locally if any coarse layers are present beneath the riverbed.

The erosion rate depends on the released flow through the dam, which is determined by the operational strategy. Spillage could occur when the reservoir gets completely filled. These high flows will have a substantial negative effect on the erosion. Spillage cannot be completely prevented, but the risk could be reduced by ensuring that the lake is at minimum level at the start of the rain season. The drawback of this solution is a decreased energy generation, as the lake will not fill up completely during dry years.

The sediment balance of the White Volta catchment is based on sediment deposition and erosion rates. During the dry season there is a supply of Saharan dust into the catchment by so-called Harmattan winds. During the rain season eroded material is flowing out of the catchment as suspended sediment in the White Volta River. The Harmattan dust deposition rate has been derived from literature. The sediment deposition and erosion rate are equal (± 15 mm/1000 years), therefore there is no net landscape erosion in the White Volta catchment. Some parts might be eroding and some parts accumulating, but on average there is equilibrium.
To analyse if there are areas more prone to erosion, the origin of deposited sediment on the riverbanks was analysed. This sediment has been collected during the field research in September 2011 and subsequently the texture and mineralogy have been analysed. This has been compared to the composition of the soil in the catchment and the composition of Harmattan dust. Both compositions were derived from literature. The texture of the deposited sediment on the riverbanks appeared to be mainly silt and clay. The mineralogy of the sediment is quartz, feldspar and kaolinite. As these minerals are abundant in the soil as well as in Harmattan dust, no definite conclusions can be drawn on the origin of the sediment.

The general conclusion is that the creation of a reservoir will have morphological effects in the reservoir and downstream of the dam. In the intended reservoir sedimentation will occur, but the effect on the functions of the reservoir is negligible. Delta deposition will mainly occur within the reservoir and partly in the upstream riverbed. As the sand will be spread out over a large distance the riverbed increase will be limited. The effect on the water levels in the river should be further investigated. There will be significant erosion of the riverbed close to the dam. In the future the riverbed erosion could damage Pwalugu bridge. Other negative consequences such as bank collapse and the draw down of groundwater levels could occur locally.

Applying sediment management strategies could reduce the impact on the river morphology. Possible measures to reduce the erosion and sedimentation rates include dredging or sluicing of high-turbidity currents. The factors that are most determining the results of this study are the riverbed composition and the suspended sediment load. In order to obtain more accurate results, model refinement should start with collecting more data in the field.

Contents

List of tabels

List of figures

1 Introduction

1.1 Background

For several decades there are plans for constructing a multi-purpose dam in the White Volta River in Ghana. The reservoir that will be formed should be beneficial for hydropower generation, irrigation and fishery. A prefeasability study (COB, 1993) has lead to an optimal location and dimension of the dam, based on an economical analysis of costs and revenues. The World Bank is interested to invest in this project and will probably carry out a feasibility study in the near future.

This Master's Thesis research, which is executed in cooperation with HKV CONSULTANTS, is aiming to give an estimation of the morphological consequences of the creation of a reservoir. Up to now there has been no research on this subject. It is expected that sediment transported by the river will be trapped in the reservoir. This could eventually lead to a loss of storage capacity and therefore affecting the functions of the reservoir. There are also morphological consequences expected downstream of the dam: the riverbed will experience erosion as the sediment-free water will try to restore the sediment carrying capacity.

The area of research is located in the north-eastern part of Ghana. The reservoir that will be formed is presented in Figure 1.1. As part of the research, field measurements have been carried out downstream of the intended dam (Pwalugu) and upstream of the reservoir, in Nangodi (Red Volta) and Yarugu (White Volta).

In 2011 and 2012 HKV has developed a flood early warning system for northern Ghana. As part of this project a hydraulic model of the White Volta River has been created.

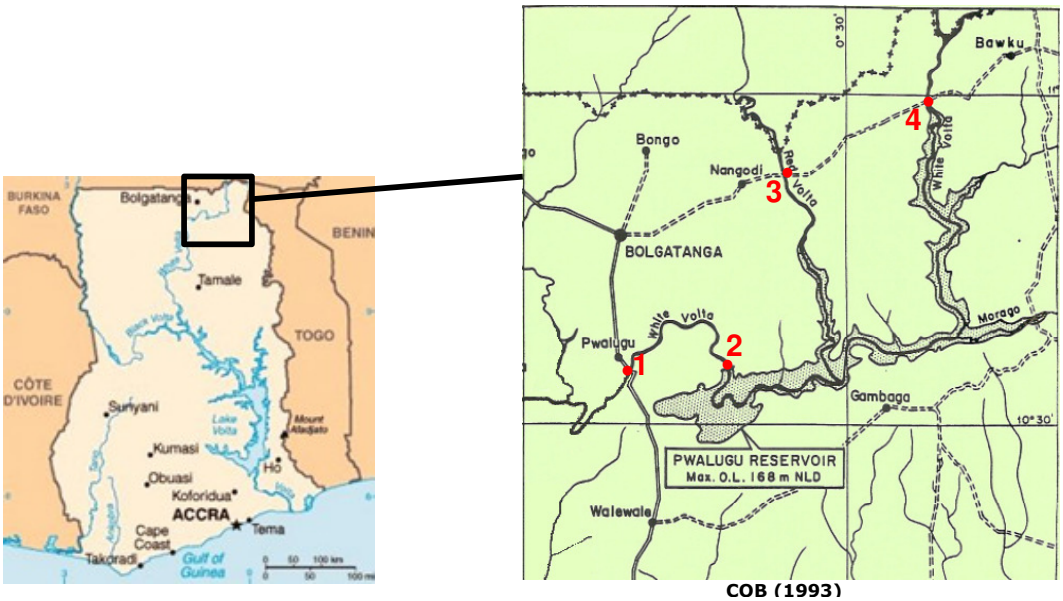

Figure 1.1 Intended reservoir, Northern Ghana. 1 = Pwalugu (White Volta), 2 = proposed dam site, 3=Nangodi (Red Volta), 4=Yarugu (White Volta)

1.2 Research objective

The main objective of this research is to make an estimation of the sedimentation in the intended reservoir at Pwalugu and the erosion of the riverbed downstream of the dam. As this is the first research carried out on this specific subject, the aim is to give a preliminary analysis of the morphological consequences. Further research should refine both the results and method used.
First, the sediment transport load of the White Volta river has to be estimated. A distinction has to be made between wash load (silt, clay) and bed material load (sand) as they have different settling characteristics. By using a morphological model the rate and location of sedimentation in the reservoir could be estimated, as well as the bed erosion downstream. The parameters of the model will be derived from a field study, in combination with a literature study. As the morphological consequences depend on the operation of the dam, different operational scenarios will be investigated.

Another objective is to make an estimation on catchment erosion, by setting up a sediment balance between Harmattan dust deposition[1] and sediment transport through the White Volta river.

1.3 Research questions

The main research question is: **What are the effects on river morphology with the creation of a reservoir near Pwalugu?** This main research question is divided into several sub questions:

- What is the rate and location of sedimentation inside the reservoir?
    - How much sediment will flow into the reservoir?
    - What is the trap efficiency of the reservoir?
    - What is the proportional sediment input of the White Volta River, Red Volta River and lateral inflow?
    - What is the siltation in the reservoir?
        - What is the proportion of wash load to the total sediment input?
    - What is the delta deposition in the reservoir?
        - What is proportion of bed material load to the total sediment input?
    - How do operational strategies of the dam affect sedimentation?
    - What is the effect of sedimentation on the storage capacity of the reservoir?

- What is the rate and location of bed erosion downstream of the dam?
    - What is the effect of operational strategies of the dam on the erosion?
    - How does erosion develop in time?

- What is the sediment balance of the White Volta catchment area?
    - What is the origin of the sediment transported by the river?
    - What is the Harmattan dust deposition rate?
    - Does texture/mineralogy of the sediment compare with that of Harmattan dust?

[1] During the dry season Saharan dust is deposited in the White Volta catchment, by sediment-laden Harmattan winds

1.4 Report outline

This report starts with the theoretical background on sediment transport and sedimentation in reservoirs, chapter 2.
In chapter 3 the topological and morphological characteristics of the White Volta basin are described, containing a literature study on Harmattan dust deposition and sediment transport through the White Volta river.
Chapter 4 contains information on the intended dam and reservoir. Hereby the objectives of the reservoir, the decision making process for this particular location and the dimensions of both dam and reservoir are discussed.
In chapter 5 the main method, results and conclusions of a four-week field study in northern Ghana are presented, details are available in Appendices.
The conclusions of the field study are used in chapter 6, where the morphological consequences are modelled in a 1D- hydrodynamic software package SOBEK RE.
In chapter 7, the accuracy of the model and fieldwork results are addressed in a discussion.
The main conclusions are summarized in chapter 8. In this chapter there will also be feedback on the research questions.
In chapter 9 recommendations on a sediment management strategy are given. Finally recommendations are done for further research. This concerns future fieldwork, ideas on improvement of the model and other subjects that, in relation with the construction of the dam, could be investigated with this model.

2 Sedimentation in reservoirs

In this chapter the general theory on sedimentation in reservoirs is presented. First the theory on sediment transport is discussed, followed by different mechanisms of sedimentation and the general impact of sedimentation on river morphology.

2.1 General theory on sediment transport

Water flowing through a riverbed exerts forces on the grains. At a certain critical velocity, the particles will start to move. When flow velocity increases more sediment will move and sediment transport takes place. Particles are lifted and dragged forward by the flow force. Sediment can be transported either as bed load or as suspended load (Figure 2.1). Bed load is defined as the transport of bed material by rolling, sliding and jumping close to the riverbed. Suspended load is defined as the transport of sediment that is suspended in the fluid for some time. Sediment transport can also be classified based on the origin of the sediment. Material originating from the riverbed itself is called bed material load, which can be transported either as bed load or in suspension. All suspended material finer than the bed material is called wash load. This is considered to be eroded material from the upstream catchment area. Transport of wash load does not only depend on the transport capacity of a river, but also on the sediment availability.

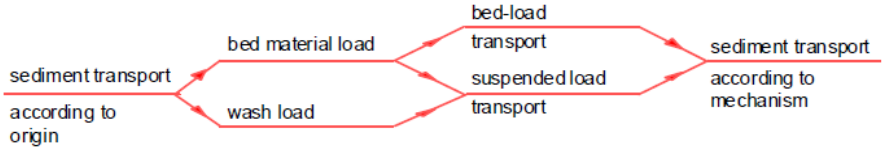

Figure 2.1Classification of sediment transport (Jansen, 1979)

The bed material load can be estimated based on flow conditions and bed material composition in the local cross-section. The most commonly used prediction formulas will be discussed in chapter 2.1.2. In order to get a quick insight into the morphological behaviour, a simplified formula can be used, $s = m \cdot u^n$ which states that bed material load at a location in the cross-section (s) is a power function (n>3) of the local flow velocity (u). n and m are constants determined by flow parameters and the particle size distribution of the bed material.

Often, suspended load transport is not just determined by the transport capacity at the local cross-section, but determined by supply from the upstream reach (washload). For this, an empirical relationship between discharge and sediment concentration can be used. The most commonly used relationship is a rating curve in the form of a power function (e.g. Walling (1974, 1977) and Church (1975)).

$$C = a \cdot Q^b$$

in which C is the suspended sediment concentration in mg/l, Q is the water discharge in m^3/s and a and b are empirically derived regression coefficients. The accuracy of the sediment rating curve is often low, which can be attributed to variations in sediment supply and sediment depletion. These changes in sediment availability result in so-called hysteresis effects

(Asselman, 1999). These hysteresis effects can be either clockwise (Figure 2.2) or counter-clockwise (Figure 2.3).

- Clockwise hysteresis loops may be caused by, among others, sediment depletion in the channel system (Church, 1975; Spott, 1994) or the increased portion of base flow during the recession limb of the hydrograph (Walling, 1974; Wood, 1977).

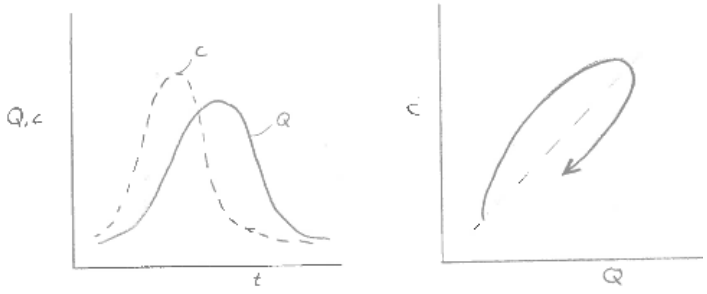

Figure 2.2 Clockwise hysteresis

- Anti- or counter-clockwise hysteresis occurs less frequently, but is often prominent when sediment originates from a distant source (Heidel, 1965) or when the valley slopes form the most important sediment source (Walling, 1979; Klein, 1984). (Sarma (1986) and Ashbridge (1995) mention the high rate of bank collapse just after passage of the flood peak, which may result in counter-clockwise hysteresis.

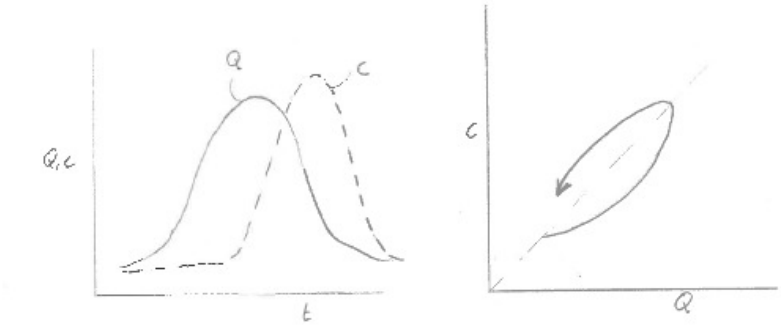

Figure 2.3 Counter clockwise hysteresis

Asselman (1999) measured clockwise hysteresis of suspended sediment in the Rhine River and concludes that sediment depletion occurs during a hydrological year and during individual floods. It is hypothesized that sediment had been deposited under low flow conditions. During high flows the temporary stored sediment was eroded and the amount of available sediment had decreased. The same clockwise hysteresis has been found by Amos (2004) in the Burdekin River (Australia), which discharge pattern, catchment characteristics and climate is comparable to the White Volta River. There was not one dominant mechanism, but the sediment concentration was a combination between hydraulically limited and supply-limited transport, making estimation of sediment flux from discharge data difficult. Picouet (2001) found positive hysteresis in the Niger River during the hydrological year. He relates this to decreasing sediment availability and to an increased portion of the base flow during the recession limb of

the hydrograph. In the White Volta River clockwise hysteresis has been observed (see chapter 5.3.1).

2.1.1 Measuring sediment transport

Bed load transport

Bed load transport can be measured directly using mechanical bed load samplers, like the Helly Smith or the Bed Load Transport Meter Arnhem (Boiten, 2008). With these instruments a net is pressed on the riverbed, trapping sediment moving over or close to the bed. Bed load transport can be influenced locally due to the appearance of dunes and ripples (Figure 2.4). A changing bed form is an indication that the bed load is variable both in space and time. In that case, measurement of bed load transport needs to be executed extensively, both temporally and spatially, in order to give an accurate estimation.

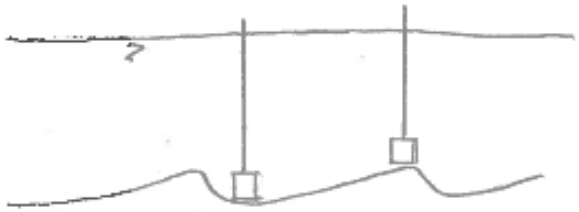

Figure 2.4 Bed load measurements on dunes

Sometimes dune tracking methods are used; the propagation of bed forms is measured with an echo sounder and subsequently bed load transport is calculated using formulas for dune propagation. Another possibility is to dredge a channel and measure the rate of filling or progress of the upstream edge.

Suspended sediment transport

Suspended sediment load is determined by measuring the discharge and the suspended sediment concentration. For direct measurement of suspended concentration it is important to consider that the concentration is highest at the bottom and decreases in upward direction. As the flow velocity is lowest at the bottom and increases in upward direction, the suspended sediment load profile has a bell shape (Figure 2.5)

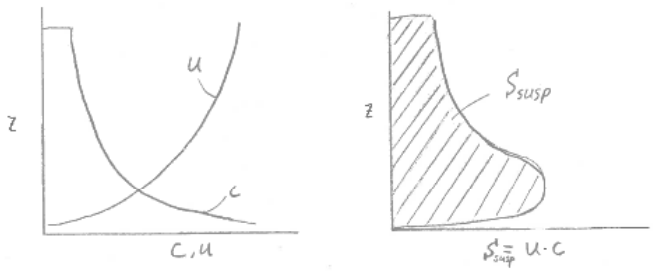

Figure 2.5 Concentration, velocity and sediment transport profiles

There are different ways to measure the suspended sediment concentration with mechanical sampling instruments:

- Point-integrated (PI) sampling devices measure concentrations in points or portions of the vertical. That way a total sediment profile can be created.
- Depth-integrating (DI) samplers are designed to collect one sample over the entire depth, by transiting the stream vertical at a uniform rate.
- Surface dip (SD) technique collects a sample from the water surface. This is the fastest and cheapest way of sampling, but the concentration is underestimated, as the concentration is lowest near the surface. To estimate the average sediment concentration, a correction factor (>1) should be derived. This can be done by comparing SD measurements with PI or DI measurements.

A different way to sample the suspended load is by using optical or acoustical methods. The main advantage compared to the mechanical samplers, is that they enable continuous measurements without interfering the flow pattern. In practice, the optical and acoustical sampling methods can only be used in combination with mechanical samplers to collect water samples for calibration (Boiten, 2008).

2.1.2 Sediment transport formulas

Several authors have derived empirical formulas for estimation of bed material load. In Appendix A the formulas of Engelund-Hansen (total load), Peter-Meyer-Müller (bed load) and Van Rijn (suspended load and bed load) are explained. These formulas assume that the amount and grain size of sediment in transport depends on hydraulic parameters (e.g. bed shear stress, velocity) and local bed composition. Sediment availability is not taken into account. These predictive formulas can therefore not be applied to predict wash load.

Several authors have proposed models for prediction of suspended sediment. Van Sickle (1983) developed a supply-based model, which computes sediment transport as a function of water discharge and the amount of sediment in storage. During a flood, erosion occurs and the sediment in storage decreases. This results in lower sediment concentrations during the falling limb of the hydrograph, than during the rising. By applying this model to the river Rhine, Asselman (1999) produced better estimates of instantaneous suspended sediment concentrations during high discharge events. It is mentioned that the major restriction to the model is that sediment in stock at the start of the season should be known, as well as the timing of sediment supply. Picouet (2001) developed a simple conceptual model that is very similar to the supply-based model and proved to give better estimates than a normal rating curve.

2.2 Reservoir sedimentation

When a river enters a reservoir the flow velocity decreases. As a result the sediment transport capacity decreases and sediment starts to settle. The coarsest sediment particles having the highest settling velocity will settle in the upstream part of the reservoir to form delta deposits. The finer sediment will be transported further into the reservoir, either by non-stratified or by stratified flow (turbidity currents). The different processes are shown in Figure 2.6 and will be explained below. Sediment can also enter a reservoir by landslides or shore erosion, but these processes are not considered here, because the occurrence is unpredictable.

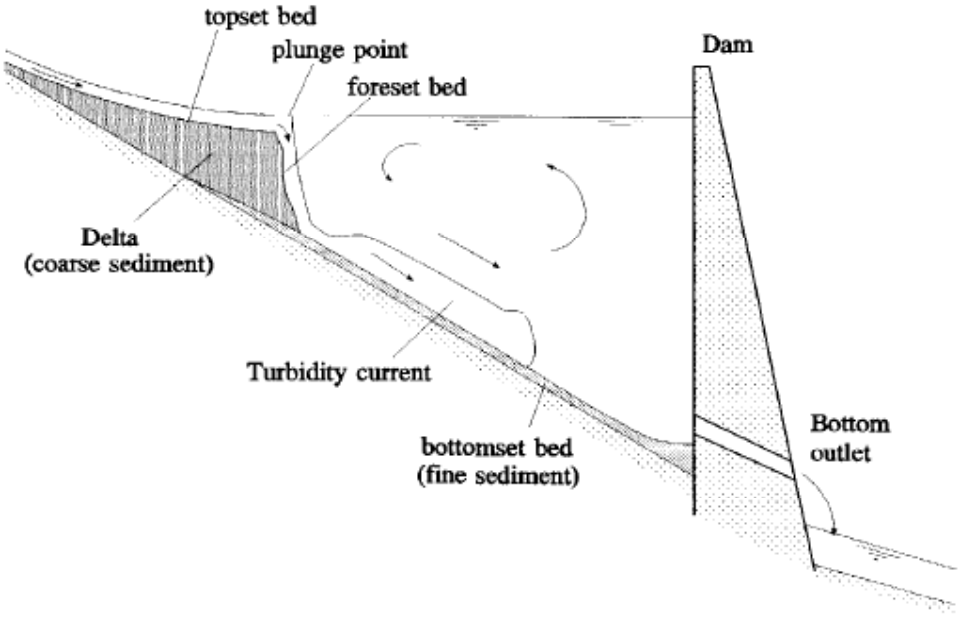

Figure 2.6 Sediment deposits in reservoirs (Sloff, 1997)

2.2.1 Delta deposits

The delta deposit usually has a steep ridge, which is called the foreset. At this point the flow velocity decreases drastically, due to the large cross-sectional area. Bed load is settling directly below the knick point of the delta front. Sediment then avalanches from the foreset, such that it remains steep. As a result the foreset is moving in downstream direction. The delta deposit also propagates in upstream direction. This is a self-sustaining effect: the bed level increase causes more pronounced backwater curves, the velocities become lower and sediment starts to settle earlier, increasing the bed level, etc.
In case of water level variation, the delta deposit could be eroded again during low water levels. Channels could be carved out through the deposited sediments. This could result in a matrix of fine sediment and sand fingers, frequently with a number of entrapped pools. This type of delta is usually an unattractive swamp, sandy waste or thixotropic mass (Sloff, 1991). Fine sediments in suspension will move further down, settling downstream of the foreset (i.e. creating the bottomset bed).

2.2.2 Density currents

Fine sediment in suspension can be transported into deeper parts of the reservoir by density currents. These low velocity currents on the bottom of the reservoir can be developed when there is a turbidity difference between inflowing water and the fresh water in the reservoir. The heavier inflowing water could plunge down and propagate underneath the ambient fresh water by stratified flow. When a turbidity current arrives at an obstacle to the flow, notably at a dam, it will deposit its suspended particles, forming a muddy pond. (Sloff, 1991)

2.2.3 Non-stratified flow

Sedimentation of fine sediment, homogeneously present in the reservoir can be calculated theoretically. The fall velocity of a particle (w_s) depends on the balance between submerged weight and hydraulic resistance and can be described by Stokes law. Assuming laminar conditions in a reservoir, Stokes law can be written in the following form:

$$w_s = \frac{\Delta g}{18\nu} D^2 \quad \text{for } 1<D<100\ \mu m$$

If the geometry of the reservoir is known, the residence time (T) of the water can be calculated, assuming that there is complete mixing thus no short-circuiting is occurring.

$$T = \frac{V}{Q}$$

With:
V = Average volume of the reservoir
Q = Average yearly discharge

Given the total depth of the reservoir (h) it can be stated that a certain particle will be settled to the bottom if $w_s > h/T$ (Figure 2.7). This gives the following relation for a critical particle diameter D:

$$D > \sqrt{\frac{h}{T}\frac{18\nu}{\Delta g}}$$

With:
h = average water level in the reservoir
v = kinematic viscosity = $1 \cdot 10^{-6}$ m^2/s
Δ = relative density = 1.65
g = gravitational acceleration = 9,81 m/s^2

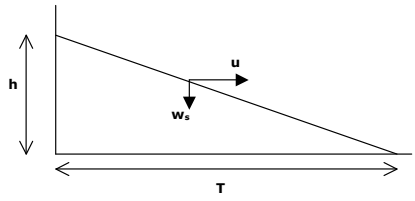

Figure 2.7 Settling of a sediment particle

Given the residence time (T) and the water depth (h) all particles bigger than D will be settled. Also a portion of smaller particles could be settled, as h is the maximum possible distance to be travelled to settle. Most particles are already closer to the bottom when they start to settle.
It is important to note that this formula only counts for laminar settling in a still fluid. In reality there could be turbulence created by wind or currents, which would reduce the settling velocity. The proposed formula is therefore a very rough approximation of the settling of a particle. If the particle size distribution is known, the formula could give an indication of the amount of sediment that will be trapped in the reservoir.

2.2.4 Trap efficiency

The trap efficiency of a reservoir is the ratio of incoming sediment load that is retained in the reservoir to the total inflow of river sediment (C. Sloff, 1991). When the particle size distribution is known, a very rough estimation of trapped sediment can be calculated using the formula presented in the previous paragraph. Also empirical methods exist to predict the trap efficiency, presented graphically (Figure 2.8). Brune (1953) developed a method to determine trap efficiency based on the residence time of the reservoir, which is the ratio of the reservoir capacity (V_R) and the annual inflow (Q_A). This method is only useful for storage-type reservoirs. Another method is Brown's curve (Brown, 1958), which determines the trap efficiency based on the ratio of the original capacity (V_R) and the watershed area.

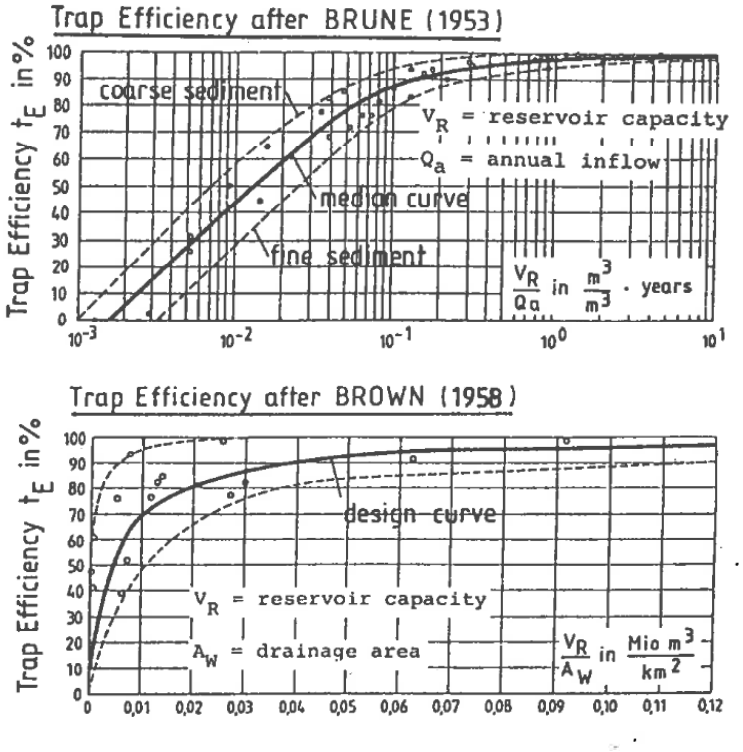

Figure 2.8 Empirical Trap Efficiency relationships

2.3 Consequences of reservoir sedimentation

A wide range of sediment-related problems can occur due to sediment trapping. In this research the most important morphological consequences are described:

- **Loss of storage capacity**

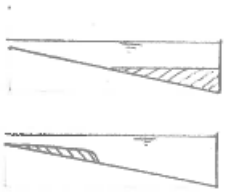

Due to sedimentation the storage capacity of the reservoir will reduce. A distinction has to be made between active and dead storage. The active storage is the reservoir capacity that can be used for the functions of the reservoir, like hydropower, irrigation or flood control. The dead storage is the reservoir capacity below minimum operative level. Fine sediments could end up in the dead storage of the reservoir, therefore not having an effect on the functions of the reservoir until the dead storage has been filled up. Delta deposition will have an immediate effect on the useful storage capacity and therefore on the functions.

- **Channel agradation**

Delta deposition will not only deplete reservoir storage but can also cause channel aggradation extending many kilometres upstream from the reservoir pool. When the riverbed upstream of the reservoir rises, the water level will also rise. This can increase flooding of the floodplains thereby harming communities, infrastructure and agriculture. If delta areas become heavily vegetated, the upstream flood levels can be further elevated because of increased hydraulic roughness, and the vegetation can trap sediment promoting additional aggradation (Morris, 1979).

- **Downstream erosion**

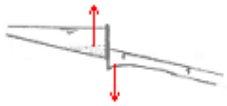

The bed level change downstream of the dam is determined by the released flow and the sediment concentrations.
Due to sediment entrapment in the reservoir, the released discharge through the dam contains less sediment. If the sediment concentration is lower than the sediment carrying capacity, riverbed erosion will occur. The river tends to reach a new equilibrium with a transport capacity corresponding to the released sediment concentration, by decreasing its slope (Sloff, 1991).
The storage of water in the reservoir damps the downstream flood waves and discharge dynamics. Any sediment release from the dam (for example through bottom outlets) may even cause sedimentation in case of erosion. As the released sediments will probably be finer than the original riverbed material the grain-size distribution may be modified.
Riverbed erosion has many negative effects: coarsening of the bed can make it unsuitable as ecological habitat and spawning site for both native and introduced species. Channel degradation can increase both bank height and bank erosion rates, increase scour at downstream bridges, lower water levels at intakes, reduce navigational depth in critical locations, and lower groundwater levels in riparian areas, adversely affecting both wetlands and agricultural areas (Morris, 1997).

Other consequences of sediment trapping could be impairment of navigation caused by delta formation, abrasion of hydropower turbines by sediment particles (in case the deposited

sediment near the dam reaches the intakes of the turbines) or negative effects on ecosystems. These consequences are not treated in this report.

2.4 Measures

If sedimentation is affecting the functions of a reservoir, measures can be taken to reduce sedimentation. The most popular methods are hydraulic flushing and sluicing:

- Sediment could be flushed out of the reservoir by increasing the flow, in a way that the deposited sediment at the bottom is resuspended and discharged through bottom outlets of the dam. When water levels are brought down partially, there will only be an effect close to the dam. Complete draw down of the water levels until the original river flow is obtained, would give best results. The drawback is that energy generation stops will occur and the reservoir might not be filled up again (Sloff, 1991).
- Sluicing means that sediment-laden inflow is released before it can settle. This could be applied in case of high-density currents at the bottom of the reservoir. These currents could be sluiced through the dam by opening bottom outlets (Sloff, 1991).

It is also possible to remove deposited sediment by dredging. However flushing or sluicing is preferred above dredging because of higher costs involved (Sloff, 1991).

3 White Volta basin

In this chapter the geographical and morphological characteristics of the White Volta basin are described. First the topology, geology, climate and water resources management of the White Volta catchment are described. Hereafter the main characteristics of the White Volta River that are of importance for this research are discussed. The morphological characteristics are described containing a literature study on Harmattan dust deposition and sediment transport through the White Volta River. Finally the morphological impact of the creation of the Volta Lake is elaborated.

3.1 Characteristics

3.1.1 Physical features

The White Volta basin is a sub catchment of the Volta basin. The other sub catchments are the Black Volta basin, the Oti river basin and the Lower Volta basin (Figure 3.1). The White Volta basin covers the largest part of northern Ghana and ± 25 % of Burkina Faso. The main river stems are the Red Volta and the White Volta, who both have their origin in Burkina Faso. It is in general a low relief basin, with elevations ranging from 42 m to 537 m. The channel slopes within Ghana range from 16 cm/km to 34 cm/km.

3.1.2 Geology

In Figure 3.2 the geology of the Upper East Region of Ghana is presented (Hap, 2009). The geology consists of three types of rocks: Extrusive rocks, intrusive rocks and sedimentary rocks. Extrusive rocks are formed when hot magma from inside the earth flows out onto the surface and cools down quickly. These volcanic rocks consist of fine crystals due to the fast cooling process. Intrusive rocks are formed when magma is slowly pushed up from inside the earth. The cooling process is taking much longer than for extrusive rocks. The magma crystallizes into large cystals, like present in granite. Sedimentary rocks are formed by deposition of sediment. Before being deposited, sediment was formed by weathering and erosion in a source area, and then transported to the place of deposition by water, wind, ice or mass movement (Wilson, 2010).

There is a clear geological divide in the area between the three rock types. Extrusive rocks (Figure 3.2, green) are mainly present in the region between Nangodi and Pwalugu and consist mainly of basalt. Intrusive rocks (Figure 3.2, pink) are mainly present in the north-east, downstream of Yarugu. Sedimentary rocks (Figure 3.2, brown/yellow) are present in the southern part of the Upper East Region. There is a clear divide between sedimentary and in/extrusive rocks, visible as an almost straight line from east to north. A large part of the White Volta River (upstream of Pwalugu) flows through this region dominated by sedimentary rocks. The finest-grained rock is present closest to the riverbed (mudstone). On the floodplains the rocks are larger grained (fine grained sandstone). The left bank of the river in this area is bordered by a steep ridge. South of the ridge there is a plateau. The rock type at the plateau is medium-grained sandstone (Figure 3.2, yellow).

Figure 3.1 Volta River basin

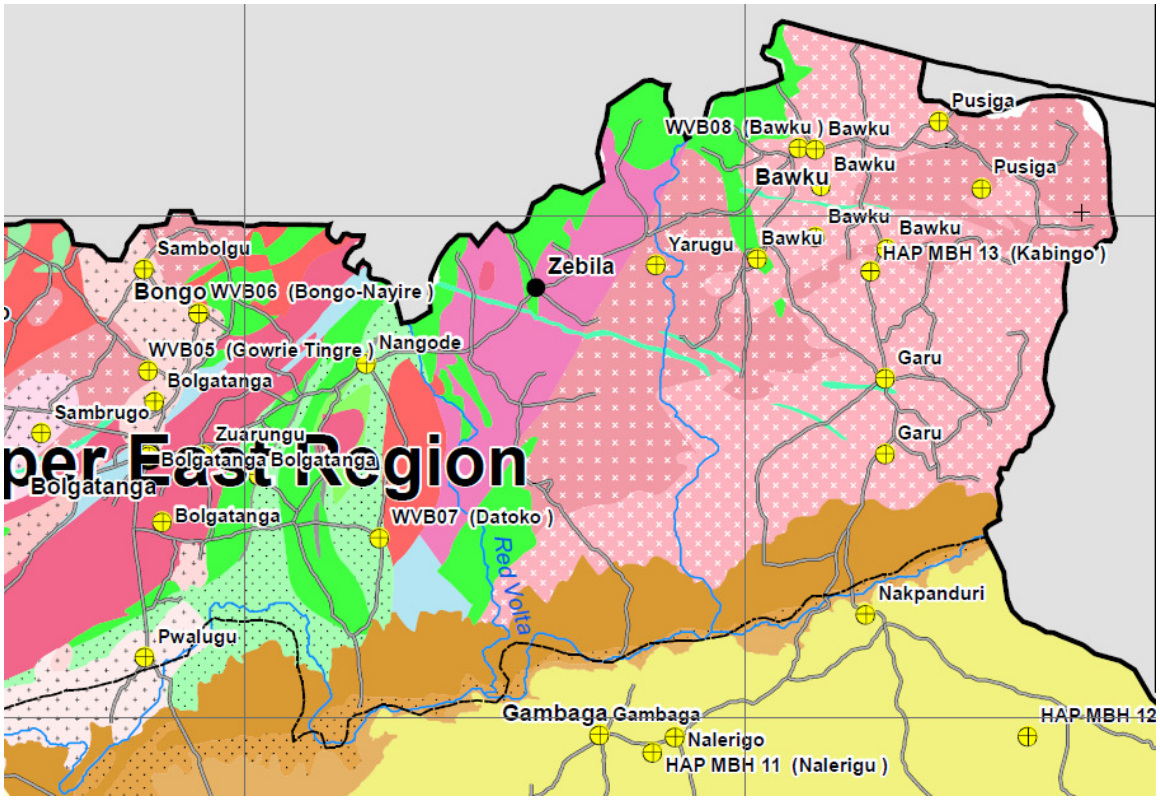

Figure 3.2 Geology, Upper East Region, Ghana With Pwalugu (White Volta River), Nangode (Red Volta River) and Yarugu (White Volta River)

3.1.3 Climate

The climate can be characterized by average high temperatures and a pronounced dry and wet season. As the catchment is located near the equator and as elevations are low, the average annual temperature never drops below 25 °C. In the southern part of the catchment the wet season takes from May to November with a rainfall intensity of ± 1200 mm/year. The rainfall intensity decreases in northward direction. At the northern edge of the catchment in Burkina Faso the duration of the wet season is four months (June-September) and the intensity is ± 600 mm/year (Andah, 2003). During the wet season the southwestern Monsoon winds are transporting moist air from the Gulf of Guinea into the continent. During the rest of the year a dry-dust laden 'Harmattan' wind is blowing from northeastern direction. The region where the Monsoon and Harmattan winds meet is called the Inter Tropical Convergence Zone (ITCZ), which moves across the Volta basin during the year. There is vigorous frontal activity in this zone, causing heavy rain events and thunderstorms (Barry, 2005).

3.1.4 Water resources management

Ghana has a fast growing economy and population, which is leading to a rapidly increasing demand for water in industries, agriculture and for human needs (Andah, 2003). During the dry season (November – March) water resources are scarce, due to a rainfall deficit. This can be observed in Figure 3.3 (HKV, 2011a). In this period the potential evapotranspiration exceeds the rainfall. The creation of a reservoir could improve the water availability during the dry season. In the rain season floods occur frequently (HKV, 2012). The impact of the floods will increase in the future because of the growing economy and population. The creation of a reservoir could attenuate the high flood peaks by (partially) storing flood waves in the reservoir. In 1968 the Akosombo dam was constructed in southern Ghana, creating the Volta Lake, being one of the largest man-made lakes in the world (Figure 3.1). The primary purpose of this dam is hydropower generation, providing energy for the largest part of the country, the secondary purpose is irrigation. In 1994 another multipurpose dam has been built further upstream along the White Volta River in Burkina Faso. The 41m high Bagré dam is in operation since 1994 and also serves hydropower, irrigation and fishery industry. Apart from these two major dams, a considerable amount of small reservoirs are present in tributaries of the White Volta River in both northern Ghana and Burkina Faso. For the rural population in the Upper East Region of Ghana, the presence of a small reservoir is an important means of overcoming minor droughts (Van de Giesen, 2005).

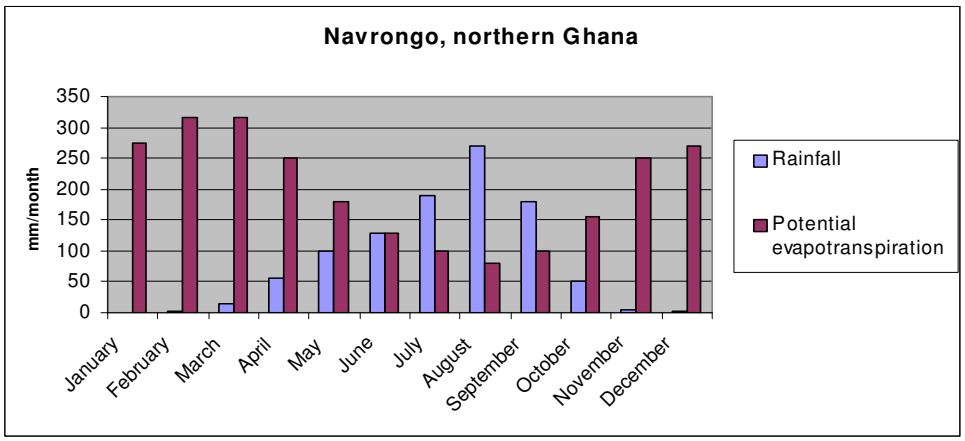

Figure 3.3 Average monthly rainfall and potential evapotranspiration, Navrongo

3.2 White Volta River

Along the White Volta River and its tributaries in Ghana there are 11 gauging stations. Most of the hydrological data is collected by the Hydrological Service Department (HSD). They operate and maintain the gauging stations. In most cases voluntary observers take measurements of the water levels by reading the staff gauges three times a day. At some gauging stations there is an automatic water level recorder present. The water levels are converted to discharges with rating curves, which are determined by the HSD (HKV, 2011b). The average yearly discharge of the White Volta River is highly variable (Figure 3.4) (COB, 1993). Extremely wet years can be followed by extremely dry years. The reliability of the discharge data at Pwalugu is unknown.

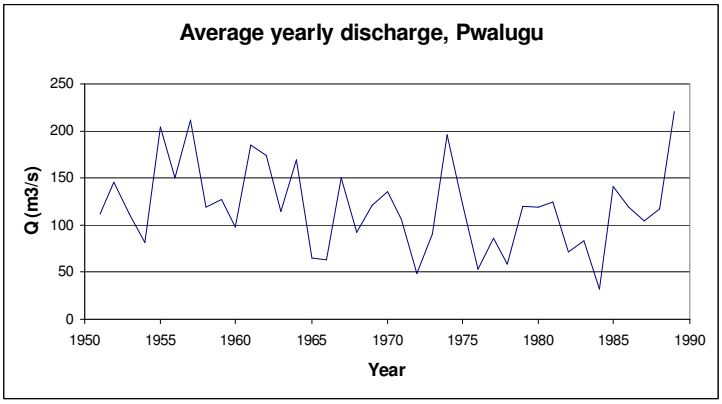

Average yearly discharge, Pwalugu	
Number of years	54
Average discharge (m^3/s)	118.6
Standard deviation (m^3/s)	39.8
Maximum discharge (m^3/s)	221,1
Minimum discharge (m^3/s)	32.2

Figure 3.4 Average yearly discharge, Pwalugu (COB,1993)

The discharge patterns for Pwalugu and Yarugu in the period 2003-2007 are presented respectively in Figure 3.5 and Figure 3.6. The discharge series are based on 6-hourly measurements. This particular series has been selected because it appeared to be the most reliable data set from a series of ± 50 years. Any data gaps or outliers have been filtered out (HKV, 2012). During the dry season the river becomes completely dry, due to high evapotranspiration rates and insufficient rainfall to generate runoff. In the wet season there are generally several flood peaks. The water level can rise and drop a few meters a day. The maximum discharges in Yarugu are comparable to Pwalugu, but the duration of the floods is shorter.

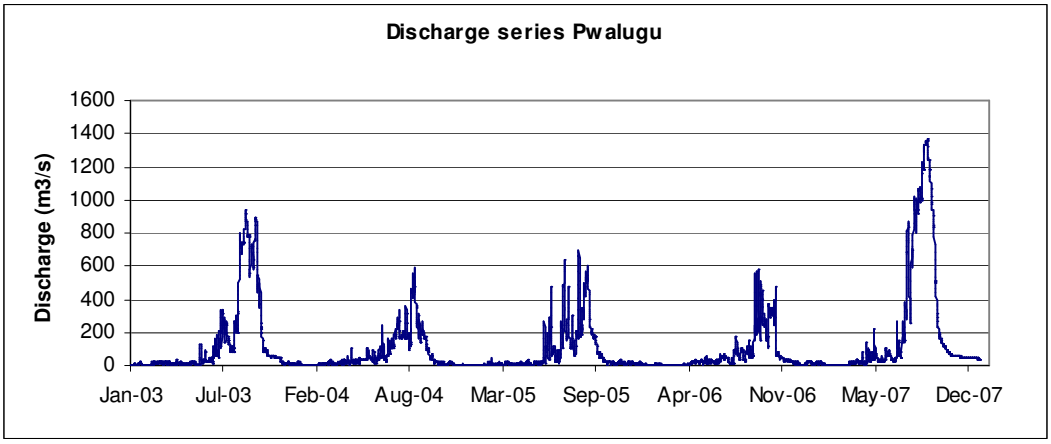

	Q_{ax} (m3/s)
2003	132
2004	68
2005	79
2006	63
2007	210

Figure 3.5 Discharge series White Volta river, Pwalugu

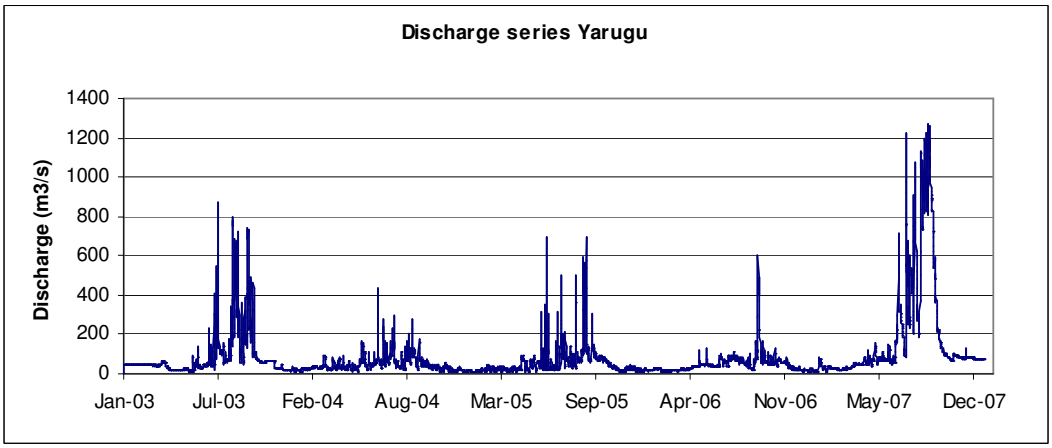

	Q_{ax} (m3/s)
2003	83
2004	47
2005	55
2006	46
2007	189

Figure 3.6 Discharge series White Volta river, Yarugu

In Figure 3.7 the flow duration curves are presented. It can be observed that the yearly discharge is concentrated in a small period. For example, for Pwalugu only 18% of the total time the discharge exceeds 200 m3/s. However within this small period around 60% of the total yearly discharge is taking place. This has been calculated by integrating all discharges higher than 200 m^3/s and dividing this by the total volume of water transported in the period 2003-2007. It can be stated that 60% of the total yearly discharge is taking place in only 18% of the time. The bank full discharges at Pwalugu and Yarugu are respectively 1000 m^3/s and 700 m^3/s (HKV, 2012). This means that the banks of Pwalugu and Yarugu are flooded for respectively 2% and 3% of the total time.

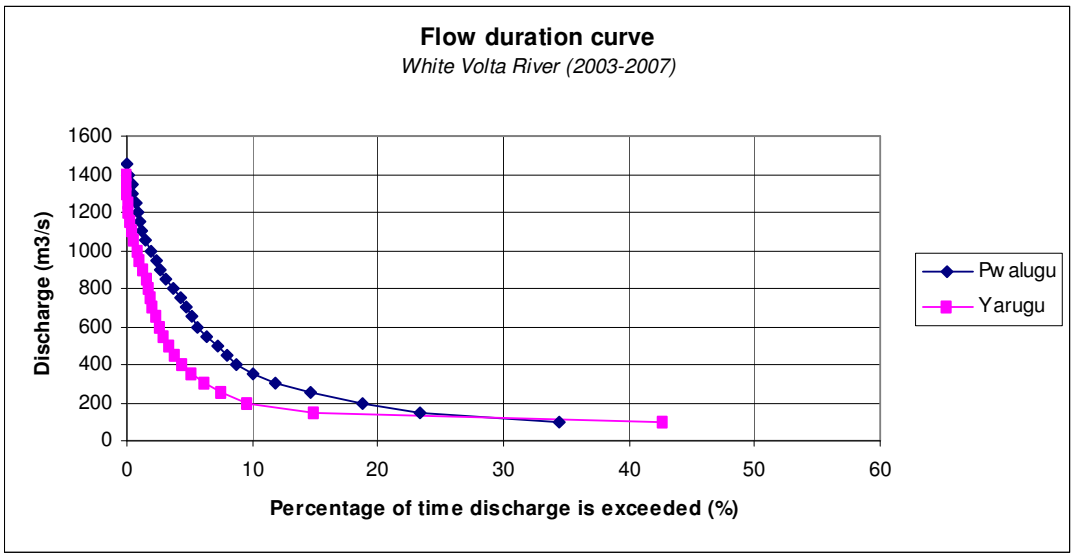

Figure 3.7 Flow duration curve White Volta River ,Pwalugu (2003-2007)

The discharges are derived from water levels by using a rating curve. However that way the hysteresis effects are neglected. The effects of hysteresis can be analyzed using Jones curve:

$$q = q_e \sqrt{1 + \frac{1}{c \cdot i_b} \frac{\partial h}{\partial t}}$$

with:
q_e = Chezy uniform flow (m^2/s)
c = flood wave celerity (m/s)
i_b = average slope of the riverbed
dh/dt = change of water level in time (m/s)

The flood waves in the White Volta River between Yarugu and Pwalugu have a peaked character. Water level variations of 3 meters in one day as indicated in Figure 3.8 are common.

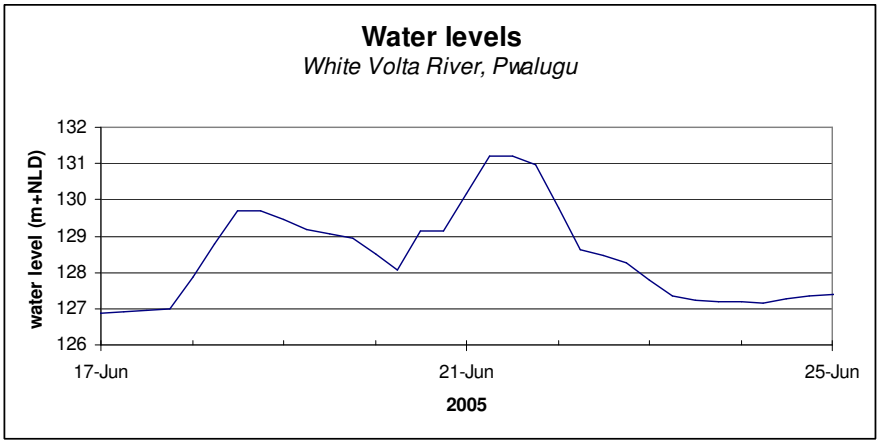

Figure 3.8 Water level variation of 3 m in one day, White Volta River (Pwalugu)

The average slope of the riverbed (i_b) between Pwalugu and Yarugu = 0.00027 (COB, 1993). The average celerity of the floodwave between Pwalugu and Yarugu is estimated on 0.85 m/s. This has been determined based on the distance between the Pwalugu and Yarugu gauging stations (145 km) and the time shift between the peak water levels at both stations (2 days) (HKV, 2012). With a dh/dt of 3m/day (=$3.47 \cdot 10^{-5}$ m/s), positive during the rising stage and negative during the falling stage, Jones formula reads:

Rising stage: $q = q_e\sqrt{1+0.15} = 1.07q_e$

Falling stage: $q = q_e\sqrt{1-0.15} = 0.92q_e$

The discharge difference between the rising and falling stage is ± 15%. It can be concluded that the hysteresis effect in this region is significant. This can be explained by the modest slope of the riverbed, low flood celerities and high water level variations in time. However, compared to the accuracy of about 20% of the flow measurements on which the rating curves are based, the hysteresis effect is of minor importance.

3.3 Catchment morphology

The morphological behaviour of the catchment is determined by erosion and deposition of material within the catchment. Erosion occurs due to shear stresses of wind or runoff. Eroded material could be transported as suspended sediment through the river system. Dust deposition from outside the catchment occurs by aeolian transport. In this paragraph literature reviews on Harmattan dust deposition and on sediment transport are presented.

3.3.1 Harmattan dust

During the dry season Harmattan dust is deposited in the White Volta catchment. In the period November to March, storm activities in the Bilma and Faya Largeau area in the Chad basin raise large amounts of dust into the atmosphere, which is carried southwest by the predominant winds (e.g. Kalu, 1979; Mc Tainsh, 1980; Mc Tainsh, 1982; d'Almieda, 1986). The Saharan dust trajectories in West Africa are shown in Figure 3.9.
Awadzi (2005) measured the dust deposition during the years 2000-2005. The measured dust deposition rate was 20 ton/km^2/year in the north of Ghana, decreasing in southern direction to 5 ton/m^2/year in the south. Assuming a bulk density of 1300 kg/m^3 this implies a deposition rate of 15 mm/1000 years in Northern Ghana. The mean particle diameters found were 13.4 µm in the north to 6.1 µm in the south. He (2007) measured the dust deposition using the same technique in 2001 and the results turned out to be very similar to the measurements carried out by Awadzi (2005). In both studies, the dust was collected on plastic mats with fiber grass, which should give a good representation of the predominant savannah vegetation in the catchment. Tiessen (1991) found dust deposition rates between 12 and 27 g/m^2 in northern Ghana during the Harmattan seasons of 1987/88 and 1988/89. The dust was collected in funnels at heights between 1 and 5 m above the ground surface.

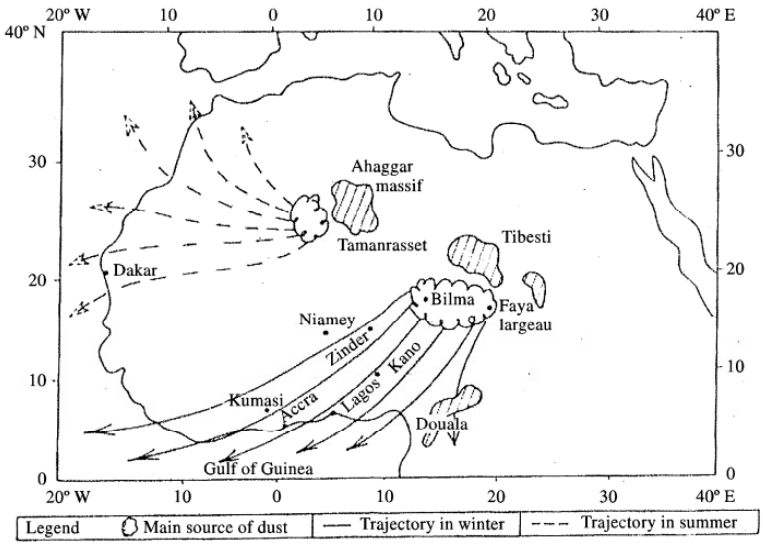

Figure 3.9 Saharan dust trajectories in West Africa (Kalu, 1979)

Several authors investigated the mineral composition of Harmattan dust in order to determine the origin. Tiessen (1991) compared dust collected during a local storm with that from a Harmattan storm. He found out that the composition and appearance of Harmattan dust is clearly different from local dust: the Harmattan dust contained mainly quartz and the local dust mainly feldspar. This conclusion is challenged by He (2007), who state that the composition of Harmattan dust is a mixture of Saharan and local dust. Feldspars, together with quartz were the main components found in Harmattan dust, but the relative contents varied in different zones in Ghana. This variation is consistent with changes in the relative content of the feldspars in the topsoil, indicating a substantial local contribution to the Harmattan dust. Lyngsie (2011) compared the composition of deposited dust during a Harmattan season and during a Monsoon season and found strong similarities in the elemental and mineral composition. He concludes that all dusts settled in Ghana are mainly of local origin. According to Lyngsie the influences of arid sediments are insignificant and the dust has been highly diluted on its path from Chad to Northern Ghana. Based on these researches it can be concluded that it is very difficult to distinguish Harmattan dust from local dust based on mineralogy. However it can be concluded that there is consensus that the Harmattan dust deposition rate is in the range of 12-27 ton/km^2/year.

3.3.2 Sediment transport

In Ghana, data on suspended sediment yield are limited due to the lack of logistic support for systematic sediment sampling activities (Akrasi, 2011). Nippon Koei (COB, 1993) found sediment concentrations in the range of 5 to 30 mg/L. The peaks are sharp indicating that the sediment transport process is dynamic (Figure 3.10). The average sampling interval of once every ten days is therefore probably too long. Peaks could have been missed. Nothing is known on the sampling and analysis methods used by Koei. It is important to mention that the Bagré dam and Akosombo dam, which could influence the sediment transport, were not built yet in 1966.

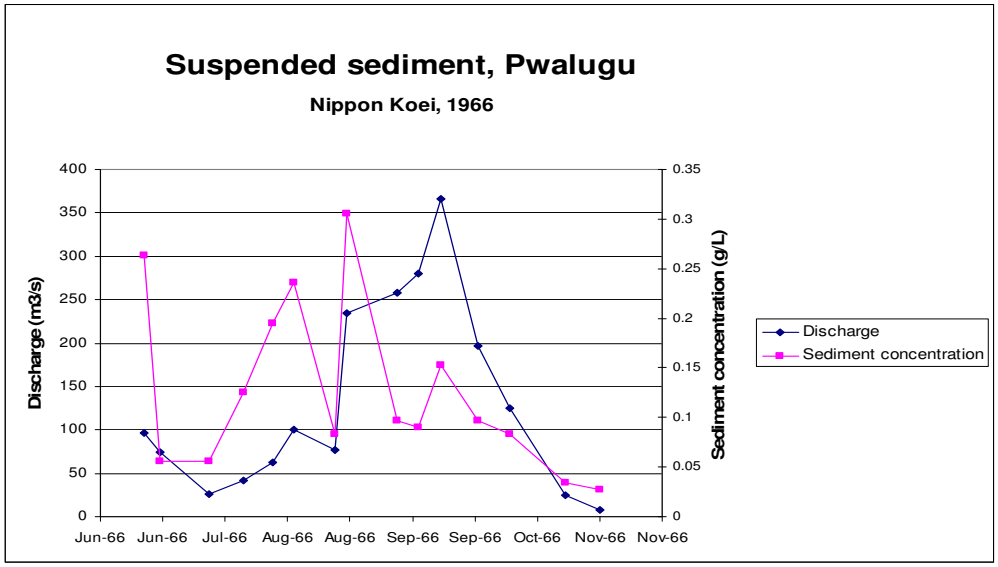

Figure 3.10 Suspended sediment measurements in 1966 (COB,1993)

Akrasi (2005) collected suspended sediment samples at six gauging stations in the White Volta catchment, in order to estimate the total sediment input into Lake Volta. During the years of 1994-1995, suspended sediment concentrations were measured using the surface-dip method (see chapter 2.1.1). To correct for the underestimation of surface dip samples, a correction factor of 1.25 is used. This factor was based on correction factors found in rivers in South Africa and Algeria. The water research institute (WRI) has provided the measurements from Pwalugu gauging station carried out by Akrasi freely to the author. In Figure 3.11 the suspended sediment concentration is plotted versus the discharge for 1994-1995.

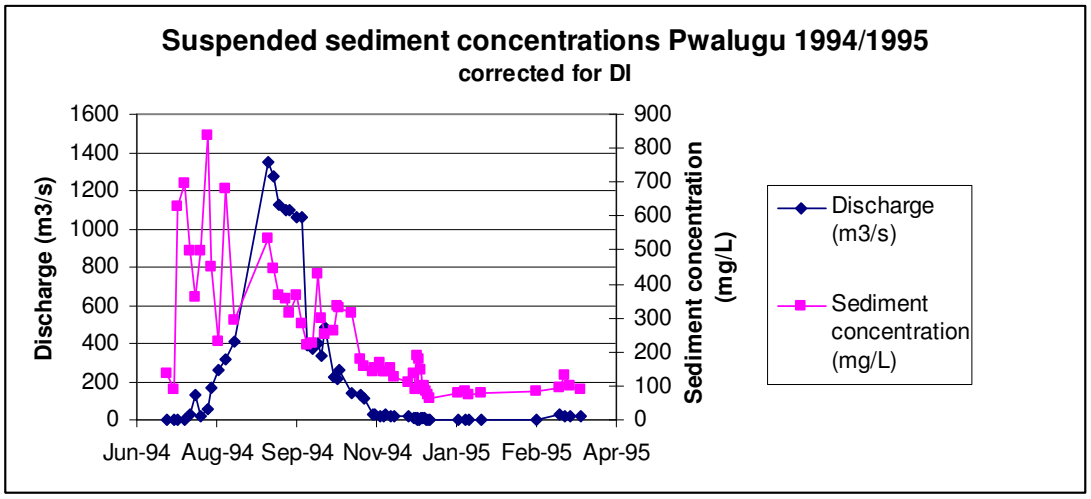

Figure 3.11 Suspended sediment measurements in 1994 (Akrasi, WRI)

The suspended sediment concentrations at Pwalugu are in the range of 100 – 800 mg/L and are characterized by sharp peaks. The concentrations are maximal at the start of the wet season and decrease over the year. This indicates sediment depletion over the season. It is important to realize that the frequency of discharge measurements is less than the timescale of one flood peak (Figure 3.5). For example, there is a 15-day gap between measurements in August 1994.

Discharge or sediment peaks could have been missed in this period. The total suspended sediment load during this hydrological year is 2 million ton/year.

The sediment yield of a catchment (Y) can be calculated by dividing the suspended sediment load (S) over the catchment area (A).

$$Y\left[ton/ha/year\right] = \frac{S\left[ton/year\right]}{A\left[ha\right]}$$

The catchment area upstream of Pwalugu is 57000 km^2 (COB, 1993). In 1994-1995 the sediment yield would be 0.35 ton/ha/year. Adwubi (2009) assessed the sediment yields of four small reservoirs in the northern part of Ghana. The sediment inputs into the reservoir have been calculated by executing bathymetric surveys and comparing the storage volumes to the design storage volumes. An inverse relationship has been derived between the sediment yield (Y) and catchment area (A): log (Y) = 1.310 A$^{-0.43}$ with r^2=0.71 (Figure 3.12). Based on this relation the sediment yield of Pwalugu (A=57000 km^2) would be ±1 t/ha/year. The uncertainty of this extrapolation is very high.

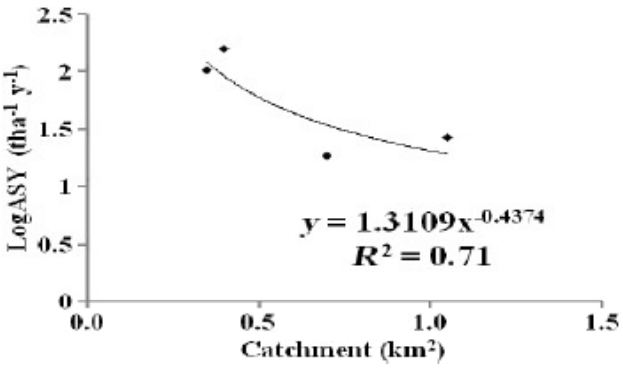

Figure 3.12 Relationship between area-specific sediment yield (ASY) and catchment area for four small reservoirs (Adwubu, 2009).

3.3.3 Lake Volta

In this paragraph the morphological impact of the construction of the Akosombo dam in the Volta River in 1968, forming Lake Volta, is analysed. This is done in order to give an approximation of possible morphological changes due to the intended dam near Pwalugu.

- **Sedimentation in Lake Volta**

The Volta lake has a maximum storage volume of 148 km^3. Not much is known about siltation rates of Lake Volta. Generally, it is assumed that siltation is not an issue, because of its large size (Akrasi, 2005). Whether delta deposition occurs and whether there are turbidity currents is unknown. Nothing could be found in literature on these subjects. Satellite image analysis on the upstream part of the Volta Lake did not give any insight into delta deposition.

- **Morphological effect downstream of Akosombo dam**

Ly (1980) investigated the role of the Akosombo dam in causing coastal erosion in Central and Eastern Ghana. It is stated that before construction of the dam, the Volta River was a major

agent of transportation of sediments to the shoreline. The general direction of long shore drift is eastwards. The sand fraction that reached the sea was carried to the east of the river mouth and deposited as beach ridges. The sand present in the dunes appeared to be of continental origin. After construction of the Akosombo dam sand supply to the sea reduced. Ly (1980) compared the retreat of the shoreline before and after construction of the dam in 1968 based on aerial photographs and maps from the period 1923 - 1976. The shoreline seemed to be characterized by a general recession before construction of the dam (±2.2 m/year). After construction of the dam, the shoreline retreat west of the river mouth remained the same, while the retreatof the eastern shoreline has increased from 4 m/year to 8 m/year. It has to be mentioned that these results are based on only few maps of limited quality and different scales. More extensive research of the present shoreline retreat is required in order to test the hypotheses of Ly (1980). On Landsat satellite images it can be observed that the sandbanks at the mouth of the Volta River are reducing in size (Figure 3.13, Figure 3.14, Figure 3.15). This observation confirms the hypothesis that sand supply from the Volta River is reduced. However shoreline reduction is not visible at the satellite images from the period 1972-2011.

Figure 3.13 Volta mouth, 14 November 1984

Figure 3.14 Volta mouth, 14 January 1991

Figure 3.15 Volta mouth, 9 November 1999

4 Case: Reservoir near Pwalugu

4.1 Introduction

The intended dam near Pwalugu would be the third multi-purpose dam in the White Volta River. In 1968 the Akosombo dam was built in southern-Ghana, creating the Volta Lake, one of the largest man-made lakes in the world (Figure 3.1). The dam was built with the main objective of hydropower-generation and nowadays the dam provides energy for most of the country. The Volta River Authority (VRA) is the energy generator and supplier. They are also responsible for the environmental impacts of Lake Volta on the towns and people bordering the lake. In 1994 the Bagré dam has been built further upstream in Burkina Faso. This dam also serves hydropower and irrigation.

In 1991 a pre-feasibility study has been carried out into the creation of a new reservoir in the White Volta River in the northern part of Ghana (COB, 1993). This study has been conducted by the French consultants Coyne et Bellier, commissioned by the Volta River Authority (VRA). The main two reasons for creation of another reservoir are:

- Increasing total power and energy generation capability within Ghana.
- Creating a source of generation close to the northern end of the national power distribution system, and thus relieving operational problems with energy transmission between the northern regions of Ghana to the main generation centres located in the south.

Apart from the increase of energy generation potential, economical benefits will come from irrigation development in the White Volta valley and fishery development along the newly created lake. The main drawback for the creation of a reservoir is the environmental impact. People living in the valley will have to be rehabilitated and valuable forest reserves will be flooded. The creation of a lake will therefore enhance mitigation costs. Another drawback is the negative effect on energy generation capacity in Lake Volta. The capacity will decrease, as the average inflow into Lake Volta will be reduced due to water loss through evaporation at the surface of the new lake and through irrigation purposes.

In the prefeasibility study three possible sites for a dam, Kulpawn, Pwalugu and Daboya (Figure 4.1), have been compared on economical feasability. Social, ecological and morphological impacts have not been considered. The economical comparison is based on total construction costs (civil works, equipment and engineering), environmental costs (mitigation), and benefits from energy generation, fishery and irrigation. The best alternative turned out to be Pwalugu. For the Pwalugu alternative, the valley that will be converted into a lake is a scarcely populated forest reserve. Compared to the other two alternatives, 10 times less people will have to be rehabilitated. The economical consequences for the loss of forest reserve are not quantified in the prefeasibility study. Therefore it is not clear if a financial compensation is needed. Evaporation losses in the reservoir are less than the other alternatives, because the surface to volume ratio is lowest.

In the near future, the Pwalugu alternative will be studied at feasibility stage. This will be commissioned by the World Bank, who are eager to invest in economical development of the relatively poor northern region in Ghana. Apart from the aforementioned advantages, the dam could also contribute to flood control. Presently HKV is working out a flood early warning system

for the White Volta River, based on a hydraulic model of the White Volta River and a hydrological model of the White Volta catchment. These models could be used to estimate the flood control perspective.

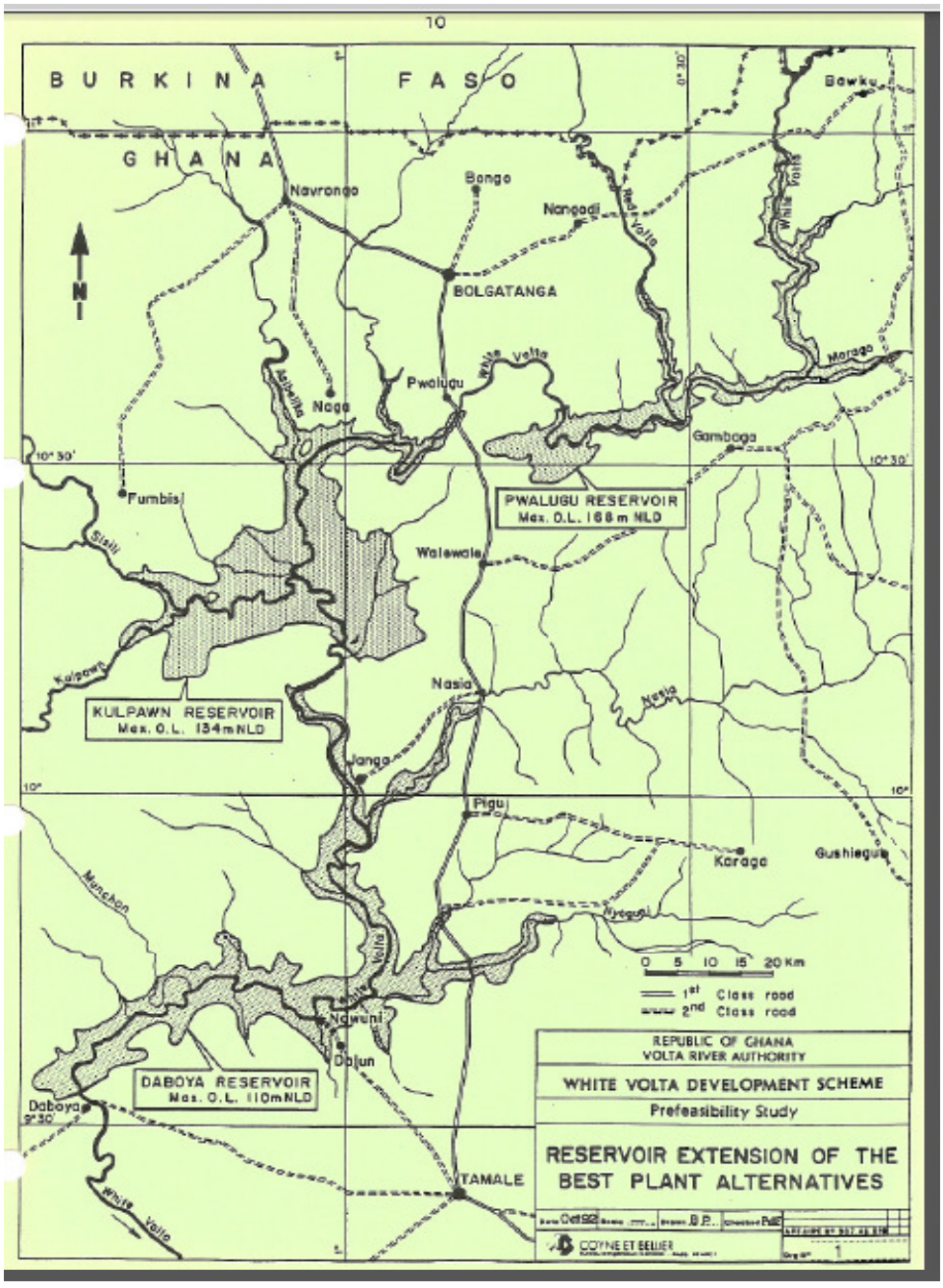

Figure 4.1 Corresponding reservoir when a dam would be built in Daboya, Kulpawn or Pwalugu (COB, 1993)

4.2 Dam and reservoir characteristics

In this paragraph first the topographical characteristics of the reservoir are described, followed by characteristics of the dam itself.

4.2.1 Reservoir characteristics

The area where the reservoir will appear is relatively shallow. A small increase in dam height will therefore have a large impact on:

- the embankment volume of the dam
- the reservoir area and therefore the total mitigation costs
- the storage volume and therefore the energy generation potential

In the prefeasibility study (COB, 1993) the optimal height of the dam has been determined based on a balance between construction and mitigation costs and revenues. The maximum and minimum operative level have been determined on 168 m +NLD and 154.4 m +NLD. In Figure 4.2 and Figure 4.3 the total reservoir area at Maximum and Minimum Operative Levels are plotted on an Aster Digital Elevation Map with 30x30 m resolution. The reference plain of these maps is Mean Sea Level (MSL), while in this research the local Ghanaian reference plain (NLD) is used, which is 0.35 m higher. For the Aster elevation maps this does not make any difference, as the accuracy of the vertical elevation measurements is 1 m.

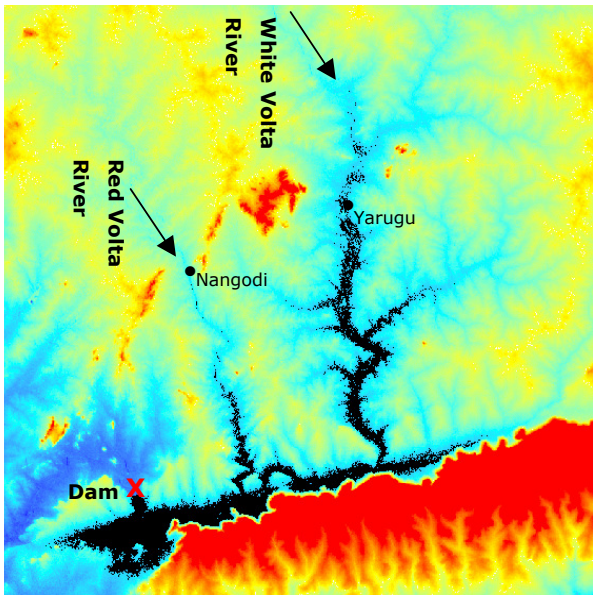

Figure 4.2 Pwalugu reservoir at max OL (168 m)

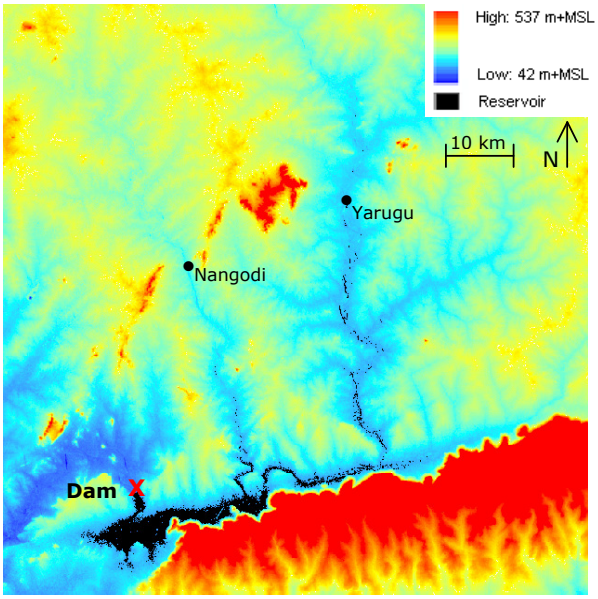

Figure 4.3 Pwalugu reservoir at Min OL (154,4 m)

The surrounding area of the Pwalugu reservoir consists of forest reserve. The area is relatively flat, except for the southern side, which is bordering a steep ridge (Figure 4.2). Water and sediment inputs into the reservoir are coming from the White Volta river, the Red Volta River and from lateral discharge of smaller streams. On average every 2 km a small stream is joining the White Volta River (HKV, 2012). The main ones are well visible in Figure 4.2 as tentacles. It is likely that delta deposition will occur at the mouths of these streams (Figure 4.4).

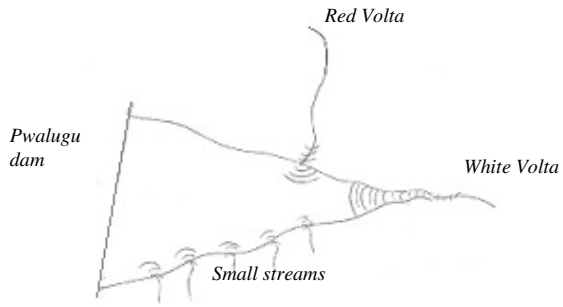

Figure 4.4 Delta deposition where streams enter the reservoir

The relation between volume, surface area and water levels has been investigated in ArcGIS using the Aster DEM. The volume and areas at Max OL and Min OL were 10% off compared to the values given by COB (1993). As the accuracy of the ASTER DEM is unknown, these values are corrected with 10%. The resulting volume/elevation (V/h) curves and surface area/elevation (A/h) curves are presented in Figure 4.5 and Figure 4.6. The lake volume below the inlet level of the turbines derived from the ASTER maps appeared to be $150 \cdot 10^6$ m^3.

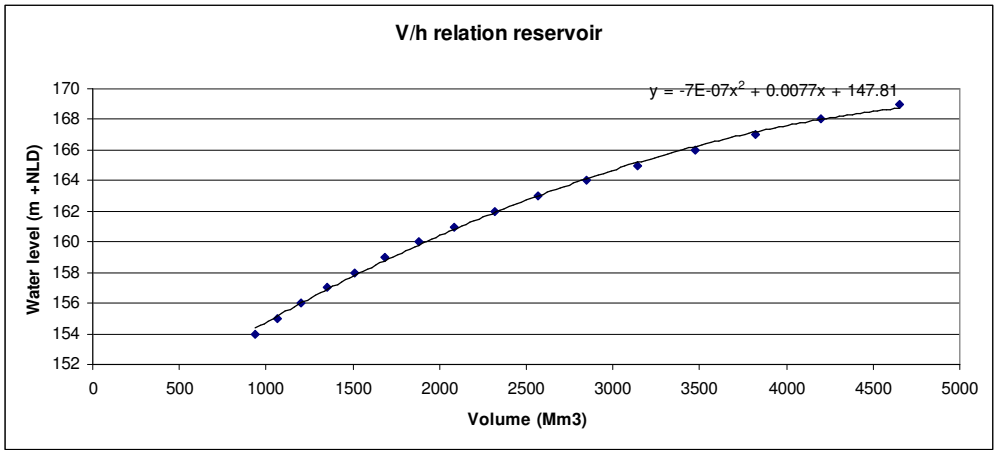

Figure 4.5 V/h relation reservoir

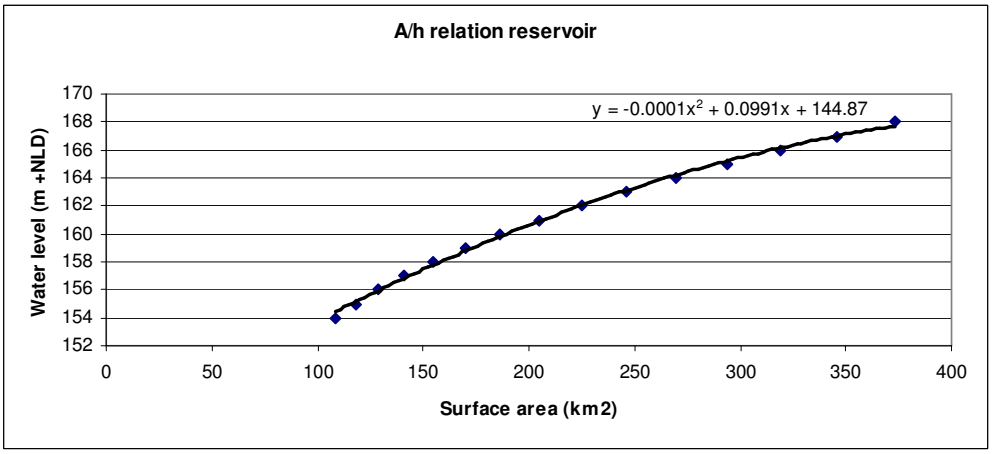

Figure 4.6 A/h relation reservoir

The minimum and maximum reservoir extent have been derived from the DEM and presented in Figure 4.7. At minimum extent the reservoir length is 75 km. Further upstream the river is inside the summer bed. At max OL the reservoir length is 115 km. Therefore the reservoir will vary 40 km in length. It is expected that delta formation will occur between the green and red dot and in case of backwater curves further upstream of the red dot in Figure 4.7. The characteristics of the intended reservoir are presented in Table 4.1.

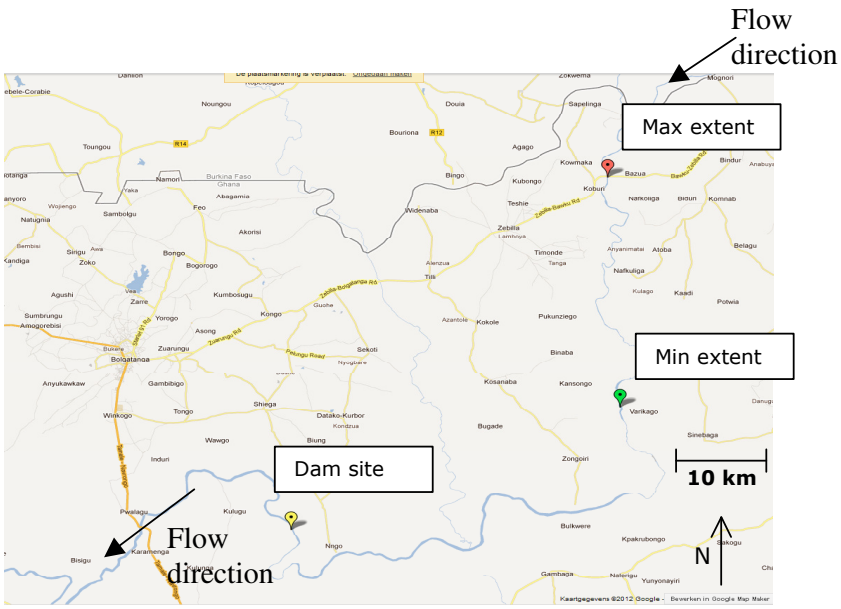

Figure 4.7 Pwalugu dam site and reservoir extent at Min OL and Max OL

Table 4.1 Pwalugu reservoir characteristics (COB, 1993)

Maximal operative level	168 m +NLD
Minimum operative level	154.4 m +NLD
Maximal reservoir capacity	4200 $\cdot 10^6$ m^3
Live storage	3260 $\cdot 10^6$ m^3
Dead storage	940 $\cdot 10^6$ m^3
Maximal reservoir area	380 km^2
Catchment area	57000 km^2
Evaporation rate	1134 mm/year
Annual inflow	3563 $\cdot 10^6$ m^3/year
Annual evaporation	430 $\cdot 10^6$ m^3/year

4.2.2 Dam dimensions

The dam will be equipped with turbines and a spillway, schematised in Figure 4.8. Hydropower will be generated by sluicing water through the turbines. In order to prevent sediment from damaging the turbines, the inlets are located at a certain height above the riverbed. As a result, a portion of the storage capacity cannot be used for hydropower generation (dead storage). When the reservoir level is below Minimum Operative Level (Min OL), the gates to the turbines are closed. When the water level exceeds the Maximum Operative Level (Max OL), water is discharged through the spillway. The dimensions of the dam and equipment are presented in Table 4.2

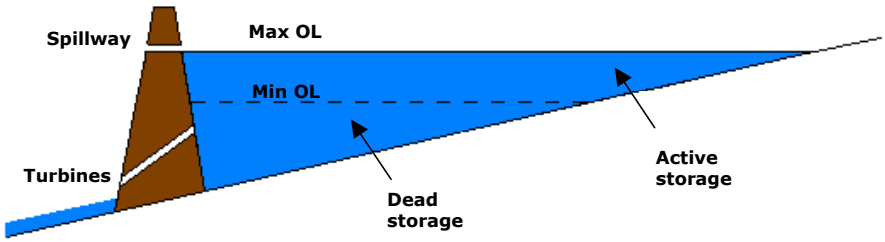

Figure 4.8 Pwalugu reservoir and dam schematisation

Table 4.2 Dam and turbine dimensions (COB, 1993)

Top level dam	171 m +NLD
Maximal operative level	168 m +NLD
Minimum operative level	154.4 m +NLD
Turbine gate level	145 m +NLD
Bottom level dam	130 m +NLD
Downstream water level	134 m +NLD
Number of turbines	2
Rated discharge (total)	170 m^3/s
Turbine capacity (total)	48 MW
Average energy generation	184 GWh/year

The formula for energy generation is described by:

$$P = \rho g Q H \eta \left[Watt \right]$$

in which:
ρ = 1000 kg/m^3
g = 9.81 m/s^2
Q = discharge through turbine (m^3/s)
H = head above turbine (m)
η = efficiency factor (-)

The energy generation capacity depends on the available head in the reservoir and the discharge through the turbines. With high water levels more energy can be produced, but the risk that water levels exceed Max OL and spillways need to be opened is higher. In the prefeasibility report (COB, 1993) it is advised that spillage should be avoided in order to make energy generation most beneficial. In practice it will be hard to prevent spillage from the dam, as the inflow is highly unpredictable and variable, as can be seen from the yearly average discharge of the White Volta River at Pwalugu (Figure 3.4).

4.2.3 Trap efficiency Reservoir

To predict which grain sizes will still be in suspension in the water leaving the reservoir, the formulas in chapter 2.2.3 are used. The input parameters for the Pwalugu reservoir follow from Table 4.1 and Table 4.2.

- $V_{average} = 0.5 \cdot \left(V_{\max} - V_{\min}\right) = 1630 \cdot 10^6\ m^3$

- $Q_{average} = 113\ m^3 / s$

- $h = 0.5 \cdot \left(h_{\max OL} + h_{\min OL}\right) = 31.2\ m$

The residence time (T) appears to be 167 days and the critical particle diameter (D) appears to be 1 μm. This suggests that only fine clays (D<1 μm) will still be in suspension when leaving the reservoir, while all other sediments would have been trapped in the reservoir. This is purely based on a theoretical formula for laminar settling in a still liquid, while in reality coarser sediments could also remain in suspension due to turbulence caused by wind and currents. Still it is an indication that most of the sediment could theoretically be trapped. Another assumption made is the residence time of 167 days. In reality short-circuiting could occur, enabling coarser sediment to remain suspended and be discharged through the dam. When determining the trap efficiency of the Pwalugu reservoir from the empirical Brune and Brown curves (chapter 2.2.4), the trap efficiency would be in both cases > 90 % for fine sediments and 100 % for coarse sediments. For the estimation of sedimentation in the reservoir and erosion downstream of the dam in chapter 5 and chapter 6 it is assumed that 100 % of the inflowing sediment is trapped in the reservoir. This would provoke the most severe sedimentation and erosion rates.

5 Fieldstudy

5.1 Introduction

5.1.1 Objective

In September 2011 a four week fieldwork period has been conducted in the Upper East region of Ghana. The main purpose of the field research was to quantify the sediment load of the White Volta River. At three different locations in the White Volta and Red Volta river suspended sediment transport measurements have been executed. As the measurements were done in September 2011, the suspended sediment transport had to be estimated for the rest of the year, to predict the total yearly sediment load. Previous measurements on suspended sediment transport within the catchment, as described in chapter 3.3.2 will be used to support the extrapolation. Another objective of the field study was to analyse the bed material at these three locations, which will be used as input into theoretical sediment transport formulas. These formulas are used in chapter 6 for modelling the delta deposition in the lake and the erosion downstream of the dam. Last, in order to make a well-founded prediction of the siltation rate, it is considered important to understand the morphological behaviour of the catchment. The sediment flows through different branches of the White Volta River, the origin of the sediment and the relation with Harmattan dust deposition have been analysed in this field research by comparing the texture and mineralogy of sediment depositions on the riverbanks with the composition of soils in the catchment and Harmattan dust.

5.1.2 Measurement locations

The main measurement location was the bridge over the White Volta near Pwalugu. This location is chosen, because of the following reasons:

- this location is close to the desired location of the dam
- there is an official gauging station with a stage-discharge curve
- previous measurements on sediment load have also been taken from this bridge.

Two more measurement locations were visited, Yarugu and Nangodi, located just upstream of the intended reservoir (Figure 5.1). Yarugu is situated along the White Volta river (± 150 km upstream of Pwalugu) at the upstream edge of the intended reservoir. The sediment transport at Yarugu can be considered as total sediment input into the lake through the White Volta branch. Nangodi is situated along the Red Volta River, which is a tributary of the White Volta River, joining the river ± 50 km upstream of Pwalugu. Sediment transport at Nangodi can be considered as sediment input into the lake through the Red Volta branch.

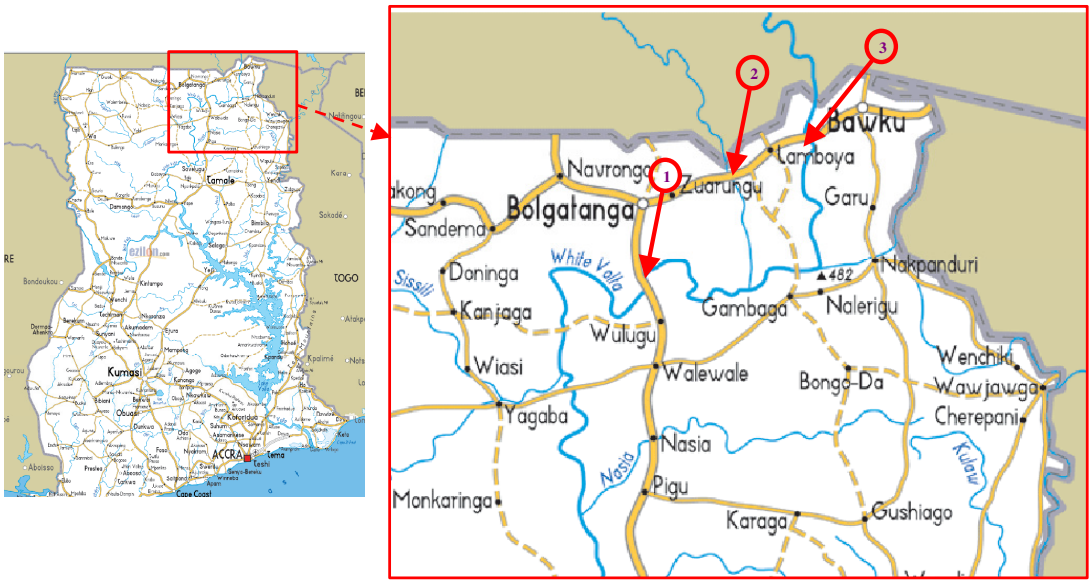

Figure 5.1 Northern Ghana, measurement locations: Pwalugu (1), Nangodi (2) and Yarugu (3)

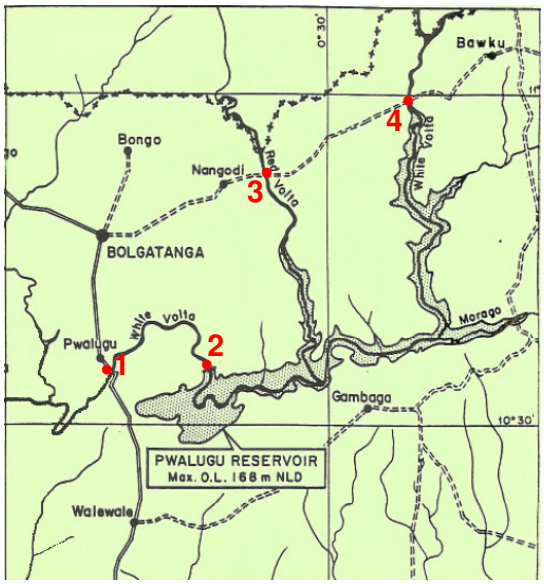

1 = Pwalugu (White Volta)
2 = Dam site
3 = Nangodi (Red Volta)
4 = Yarugu (White Volta)

Figure 5.2 Reservoir in case a 40 m high dam is built near Pwalugu (COB, 1993)

5.2 Method

A complete elaboration of the method used in this fieldwork can be found in Appendix B. In short, the following measurements have been executed:

Bed load
The bed load could not be measured with any accuracy. Therefore the bed load is estimated using theoretical formulas. Input into these formulas is the particle size distribution of the bed material. Bed material measurements have been executed with a bed material sampler. The particle size distribution has been determined by dry sieving analysis.

Suspended load
The suspended sediment concentration has been measured using a depth-integrating suspended sediment sampler. The suspended sediment load has been calculated by multiplying the concentration and the discharge.
Apart from depth-integrating samples, surface dip samples have been taken, in which water samples of the water surface are collected with a bucket. This is a very straightforward and fast way of sampling. However it is known that these surface dip samples underestimate the mean sediment concentration in the vertical, as the concentration is highest at the river bed, and decreases in upward direction (see chapter 2.1.2). Previous suspended sediment measurements in the White Volta River used the surface dip method with a certain correction factor derived from literature (see chapter 2.1.1). Part of the field research was aimed to investigate whether this correction factor is realistic.

Discharge
For Pwalugu, the discharge can be derived from a rating curve. At the bridges of Nangodi and Yarugu there are no operational gauging stations, so the discharge had to be measured. Due to the lack of professional equipment, an improvised float has been used. Validation of this improvised float method has been done at the gauging station of Pwalugu, by comparing the float method with the rating curve. Another reason to measure the discharge in Pwalugu is to analyse the effects of hysteresis. It is estimated that these effects are rather high, as the water level can drop or rise several meters per day (chapter 3.2).

Riverbank depositions
After every flood peak sediment depositions have been observed on the riverbanks. The texture and mineralogy of these samples have been analysed in order to tell the origin of the samples. The texture has been determined using the hydrometer method for fine sediments (silt/clay) in combination with dry sieving for the coarse sediment (sand) according to BS 1377: part 2:1990. The mineralogy of the samples has been analysed by x-ray diffraction (BrukerD5005 diffractometer) at the x-ray diffraction facility at Delft University of Technology (Faculty of Materials, Science and Engineering).

5.3 Results

A complete elaboration of the results of all field measurements can be found in Appendix B. The most important results are listed below.

5.3.1 Suspended sediment

During the period of measurement in September 2011 there were two flood waves. There had been one flood wave before the measurements had started. The results of the depth-integrated suspended sediment measurements are presented in Figure 5.3. A hysteresis pattern is observed during the flood waves: during increasing discharges (rising stage), the corresponding suspended sediment concentrations are higher than for the same discharges during the falling stage. During the day of maximum discharge (2 September) no suspended sediment measurements were taken. However it has been observed that the river looked most turbid that day, thus it is presumable that the suspended sediment concentration was maximal on September 2. The suspended sediment loads measured at Yarugu (White Volta) and Nangodi were roughly 50 % and 15 % of the suspended load measured at Pwalugu. Based on observations, the suspended sediment samples consisted mainly of silt/clay (washload) and contained only a small sand fraction. The surface dip samples contained no sand grains at all. The average correction factor for surface dip measurements is 1.33. A sediment rating has been created from all available suspended sediment measurements: S = 7.86*(Q)^1.2078. When applying the rating curve to 6-hourly discharge series for the period 2003-2007 (see chapter 3.2), the average yearly sediment load ≈ 1.1 M t/year. With a catchment area of 57000 km^2 the sediment yield = 0.19 t/ha/year.

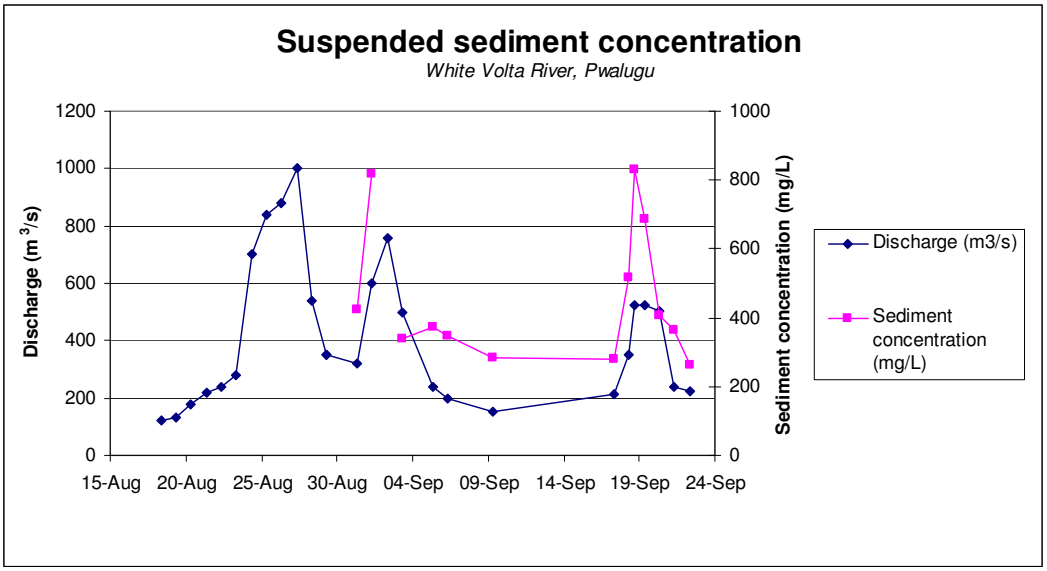

Figure 5.3 Sediment concentration and discharge in Aug/Sep 2011, Pwalugu

5.3.2 Bed load

The bed material measurements in Pwalugu show that there is a gradation of particle sizes over the cross-section: smallest grains were found in the inner bend and biggest grains were found in the outer bend. Flow velocities were smallest in the inner bend and highest in the middle section or in the outer bend (Table 5.1).

Table 5.1 Particle size distribution of the White Volta riverbed at Pwalugu bridge

	Av. D_{16}(mm)	Av. D_{50} (mm)	Av. D_{84}(mm)	Av. D_{90} (mm)
Inner bend	0.27	0.42	0.65	0.75
Middle section	0.40	0.70	1	1.2
Outer bend	0.75	1.4	3	4.5

The bed material load is estimated with three different theoretical formulas: Engelund Hansen (EH, total load), Meyer-Peter-Müller (MPM, bed load) and Van Rijn (VR, bed load and suspended load) (Figure 5.4). The predictions for bed load transport are almost equal for MPM and VR. There is a factor 5 difference between the total loads estimated by VR and EH. Van Rijn's suspended load is ± 1/3 of van Rijn's bed load, so this indicates that bed load transport is dominant. Based on criteria of applicability (Appendix A), the Engelund Hansen formula is valid for high flows (Q> 225 m^3/s) and Meyer-Peter-Muller for low flows (Q<400 m^3/s). The Shields number during this period of fieldwork are presented in Appendix B. The shields numbers are well above the critical Shields number. However during a large part of the dry season it is estimated that the critical Shields number will not be exceeded. The critical Shields number is included in MPM and VR, but not in EH. This means that EH will always result in some sediment transport, even at minimal discharges, while the sediment transport capacity estimated by VR and MPM could reduce to zero. The particle size distribution of the middle flow section has been used as input. When applying the particle size distribution of the inner bend, the loads would be ± 1.5 times higher.

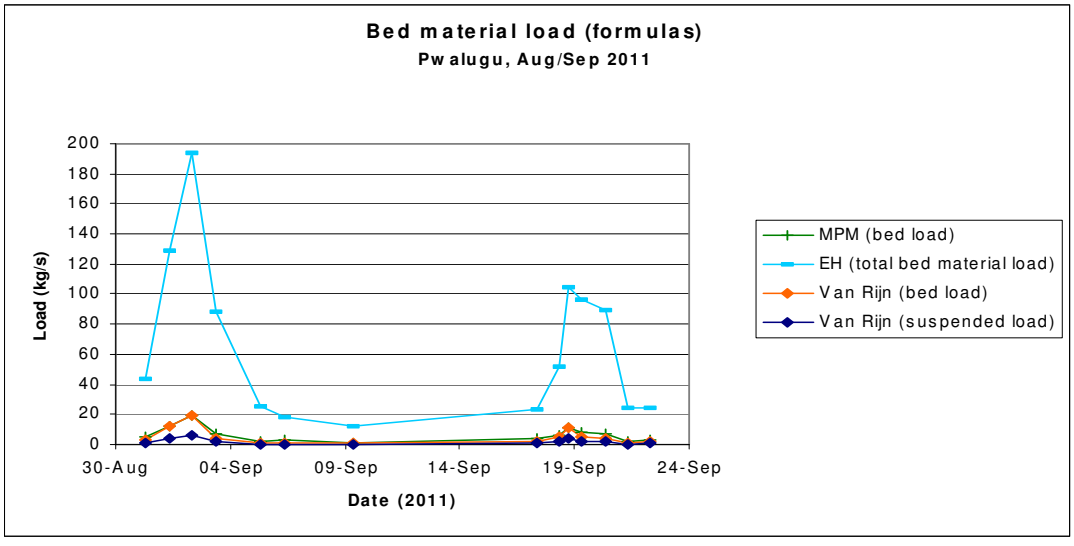

Figure 5.4 Bed material load (formulas) in Pwalugu, Aug/Sep 2011

5.3.3 Riverbank samples

The sand/silt/clay fractions of the riverbank samples are presented in Table 3.11. The following classification rules are used:

- Clay: D<0.002 mm
- Silt: 0.002<D<0.065 mm
- Sand: 0.065<D<2 mm
- Gravel: D>2 mm

Table 5.2 Particle size distribution of the riverbank samples

	Sand (%)	Silt (%)	Clay (%)
Pwalugu (after 1st flood wave)	13	60	27
Pwalugu (after 2nd flood wave)	19	62	19
Nangodi (after 1st flood wave)	40	48	12
Nangodi (after 2nd flood wave)	80	14	6
Yarugu (after 2nd flood wave)	70	24	6

After the first flood wave of 2011 a thick layer of sediment (4 cm) has been observed on the riverbanks of Pwalugu. As the sediment covered the vegetation, it is concluded that the sediment has been deposited recently. Texture analysis shows that the sediment deposited during the first flood wave of 2011 consists predominantly of silt and clay. After the second flood wave has passed the clay fraction has decreased. Sediment depositions have also been observed along the banks of the Red Volta River (Nangodi), after the first flood wave. However the sediment has disappeared after the second wave. This is confirmed by the results of the texture analysis presented in Table 5.2. After the first wave the river bank material consisted predominantly of silt and sand. After the second flood wave there is only a small fraction of fine sediment left behind. Based on observations, at Yarugu the amount of fine sediment on the banks has also decreased after the second flood.

The mineralogy (x-ray diffraction patterns) of the riverbank samples are presented in Table 5.3. The minerals found in the samples are quartz, albite, microcline and kaolinite. Quartz is one of the most abundant minerals in earths crust. Albite and microcline are feldspar minerals, respectively sodium and potassium rich. These minerals are common in granite rocks, which are present in the study area. Kaolinite is a clay mineral formed due to weathering of feldspar minerals and most abundant in areas with a tropical (hot and moist) climate.
The fractions of quartz, microcline and feldspar cannot explain the origin of the sediment, as all minerals are abundant in the whole study area.
Kaolinite appears to be present only in the samples taken at Pwalugu. This is explained by the particle size distribution, which indicates a large clay fraction. Kaolinite has not been observed in Nangodi or Yarugu, but probably the clay is present in the river, but hasn't been deposited on the banks. However, it could be the case that the kaolinite content is lower in the Red Volta River than in the White Volta River. Kaolinite is a white mineral, so this could explain why the color of the White Volta River is more white than the Red Volta River.

Table 5.3 Mineralogy riverbank samples

	P1	P2	P3	R1	R2	Y1
	Pwalugu 5/9 (bank)	Pwalugu 22/9 (bank)	Pwalugu old site 22/9	Nangodi (4/9) (muddy)	Nangodi 23/9 (fine sand)	Yarugu 23/9
Quartz	67 %	62 %	71 %	80 %	72 %	47 %
Albite:	16 %	21 %	11%	20 %	16 %	40 %
Microcline:	4 %	10 %	3 %	0 %	13 %	13 %
Kaolinite:	13 %	7 %	14 %	0 %	0 %	0 %
D16 (mm)	<0.001	<0.001	<0.001	0.01	0.06	0.02
D50 (mm)	0.017	0.03	0.02	0.05	0.15	0.1
D84 (mm)	0.05	0.07	0.05	0.1	0.27	0.28
Clay	30 %	21 %	23 %	13 %	7 %	10 %
Silt	34 %	59 %	62 %	48 %	14 %	30 %
Sand	12 %	20 %	15 %	39 %	79 %	60 %

5.4 Conclusions

5.4.1 Sediment measurements

- The suspended sediment concentrations measured in the White Volta River at Pwalugu in 2011 have the same order of magnitude as found by Nippon Koei in 1966 and Akrasi in 1994 at the same location. The concentrations are in the range of 100 mg/L to 800 mg/l.
- A flood wave through the White Volta River provokes a sharp sediment peak. This has also been observed in 1966 and in 1994. During the fieldwork hysteresis effects have been observed during the flood waves.
- There is sediment depletion during the hydrological year. This effect is visible in all three researches:
    - Akrasi measured the highest sediment concentrations during the first flood peak of 1994, while the discharge was moderately high.
    - Nippon Koei also measured high concentrations during the first flood peak in 1966, while discharge was only moderately high.
    - In the field research in 2011 no measurements have been done during the first flood wave. However it can be expected that the concentrations were maximal during the first flood wave, because much more sediment deposition has been observed on the banks, compared to the following peaks.
- The depth-integrated suspended sediment concentrations were on average a factor 1.33 higher than the concentrations measured by the surface dip method. The correction factor proposed by Akrasi (1.25) is of the same order of magnitude. It can be concluded that the sediment load based on Akrasi's surface dip measurements is realistic.
- The depth-integrated samples consist of both bed material load (sand) and washload (silt/clay), but the exact proportions are not known. The surface-dip samples consisted only of washload as no sand grains were observed in the samples. Theory shows that the washload concentration is minimal at the water surface and increases with the depth. Therefore the average washload concentration will be in between 75% (=1/1.33) and 100% of the suspended load. In order to avoid underestimation, all suspended sediment is considered to be washload.

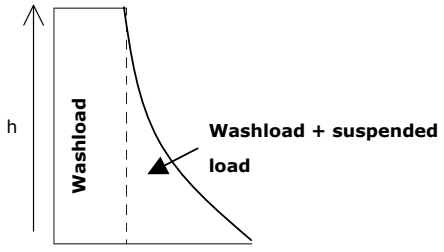

- Another indication of a high washload concentration are the sediment depositions on the riverbanks, which consist for ± 85 % of silt and clay, while the bed material consists of sand.
- The suspended sediment concentration appeared to be quite constant over the cross-section, even though flow velocities differ a factor 2 between the inner bend and outer bend. It looks like the higher flow velocities are counterbalanced by smaller grain sizes, in a way that the sediment transport is constant over the cross-section.

- A sediment discharge curve has been produced based on all available data: $S = 0.091 \cdot Q^{1.2078}$ in which S is the suspended sediment load (kg/s) and Q the discharge (m^3/s). When applying the rating curve to 6-hourly discharge series for the period 2003-2007 in Pwalugu (see chapter 3.2), the average yearly sediment load ≈ $1.1 \cdot 10^6$ ton/year. Total sediment load found by Akrasi was $2,0 \cdot 10^6$ ton/year, but the discharges in 1994 were above-average.
- With a porosity of 0.4 and a density of 2650 kg/m^3, the annual average input of suspended sediment is $6.9 \cdot 10^5$ m^3/year, of which at least 75% is washload. It can not be predicted how this sediment will be distributed over the reservoir bottom, however it is likely that the sediment will deposit everywhere, forming a blanket of mud at the bottom of the lake. If the sediment would be deposited equally over the reservoir area, the sedimentation rate would be 3 mm/year. It is very well possible that density currents will develop, which may bring the mud closer to the dam. If the mud deposition comes close to the inlet level of the turbines, the turbines could be damaged. The storage volume below the inlet level of the turbines is $150 \cdot 10^6$ m^3, so it would take ± 200 years to fill this up with sediment. If all sediment would remain in the active storage ($3260\ 10^6$ m^3), the annual storage loss would be 0.03 %/year.
- The sediment discharge relationship is not very reliable, as the hysteresis effect has not been taken into account. With the available data it is not possible to make two separate rating curves for rising and falling stages. This because, for the researches carried out in 1966 (COB, 1993) and 1994 (Akrasi, 2005), it was not known whether the measurements had been taken during the rising or falling stage, due to the low frequency of discharge measurements. Also sediment depletion has been observed so the sediment discharge relationship also depends on the number of floods that occurred before and the intensity of these floods.
- Based on a sediment balance between Pwalugu (White Volta, downstream of the intended dam), Yarugu (White Volta, upstream of the reservoir) and Nangodi (Red Volta, upstream of the reservoir), it is expected that roughly 50% of the total sediment input will enter the reservoir through the White Volta branch, 15% through the Red Volta branch and 35 % would originate from lateral inflow. This is a large proportion of lateral inflow, given the relatively small drainage area between the measurement locations.

5.4.2 Sediment formulas

- EH gives a reasonable estimation of the total load when compared to the field measurements. In Figure 5.5 the EH formula, the depth-integrated (DI) suspended sediment measurements and the washload estimation (DI/1.33) are compared. When comparing the formulas, the following relation holds:

  Total bed material load = bed load + suspended load - washload

  It can be concluded that EH gives a reasonable estimate of the total load (excluding washload) and the formula can be used in the morphological model without a correction factor.

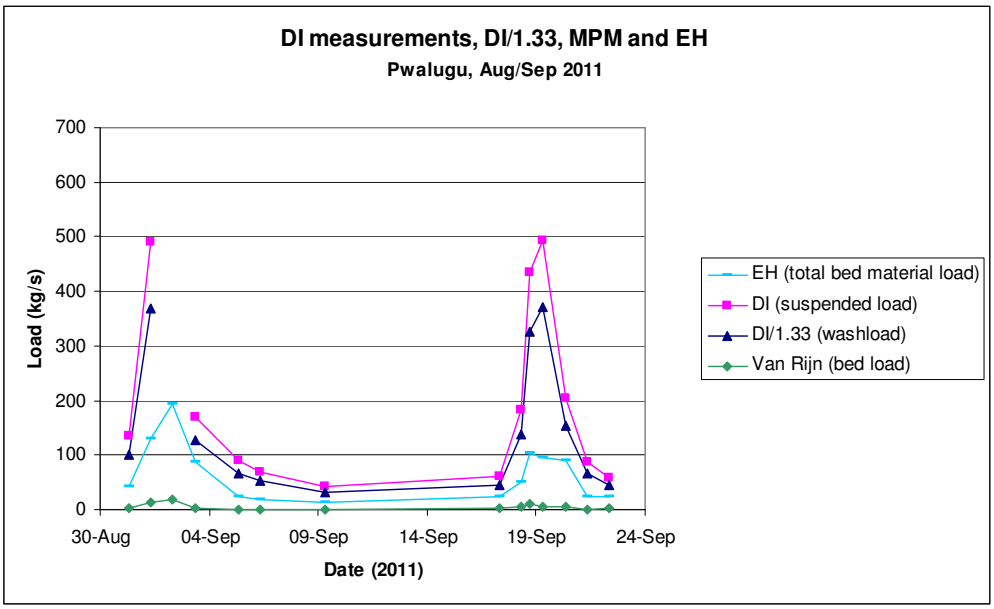

Figure 5.5 Sediment measurements compared to theoretical formulas

- EH can be applied for Q> 225 m^3/s. In the flood duration curves (Figure 3.7) it is observed that for Pwalugu and Yarugu this criterion is true for respectively 20 % and 10 % of the total time. During ± 90 % of the time MPM would be the better predictor. From the flood duration curves it has been calculated that the high flows (Q>200 m^3/s) account for up to 60 % of the total yearly discharge. As the high floods appear to be dominant, it is chosen to use EH in the morphological model.
- The above-mentioned formulas are applied to the bed material observed in the middle section of the White Volta River at the bridge of Pwalugu. It is not known whether this bed material is representative for the whole river reach. Possibly the bed material is different below the bridge, due to the non-uniform flow caused by the bridge piers. The particle diameters were smaller in the inner bend. When using these smaller particle sizes for the whole cross-section, the full transport through the cross-section would be approximately 1.5 times higher.
- Engelund-Hansen overestimates the total load during low flows. The reason is that the Shields critical shear stress for the start of movement is not implemented in the formula. That means that there will always be some sediment transport. For the Van Rijn and MPM formulas the sediment transport would stop at a certain moment when the Shields number is lower than the critical Shields number. It is estimated that the sediment transport capacity is overestimated in this research.

5.4.3 Landscape erosion

- The sediment yield of the White Volta is calculated on 0.192 t/ha/year, which equals an erosion rate of 13.5 mm/1000 years. As the Harmattan dust deposition is ± 15 mm/1000 years, there seems to be an equilibrium between erosion and deposition. Harmattan dust deposition is assumed to be equally divided over the catchment area. Erosion has usually a more local character. Therefore the flat areas might be accumulating and slopes might be eroding, but on average there would be equilibrium.

- Sediment entrapment in the upstream Bagré reservoir in Burkina Faso should be taken into account. If all inflowing sediment would be trapped in the Bagré reservoir, the measured sediment load at Pwalugu should be divided over a smaller catchment area (22000 km^2). In that case the sediment yield would be 0.46 t/ha/year and the erosion rate would be 32 mm/1000 years. The trap efficiency of the Bagré reservoir according to the empirical trap efficiency curves (Figure 2.8) is ± 90 %, but depends on the sediment management strategy. It is not known whether flushing or sluicing techniques are being applied.
- According to the yield/area relation derived from small reservoirs in northern Ghana (Awadzi, 2005) the yield should be ± 1 t/ha/year, but this would be an extrapolation with a high uncertainty.
- The texture of the sediment deposition on the banks of the White Volta is mainly silt. The average particle size of Harmattan dust is also characterized as silt. However this is not an evidence that the sediment has a Harmattan dust origin.
- The minerals found in the sediment deposited on the banks are quartz, feldspars and kaolinite. These materials are common in the catchment's soils and also in Harmattan dust. Therefore no definite conclusion can be drawn on the origin of the sediment.
- Kaolinite appears to be present only in the samples taken at the most downstream gauging station (Pwalugu). In the geological map (chapter 3.1.2) it can be seen that the White Volta River, just upstream of Pwalugu, flows through areas consisting of mudstone. This could be the reason for the high kaolinite content in the bank depositions. Kaolinite is a white mineral, so this could also explain why the color of the White Volta River is more white than the Red Volta River. However, the fact that no clay has been found on the banks further upstream (Yarugu and Nangodi) does not mean that there is no clay present in the river. It could simply be the case that clay has not been deposited on the banks at these measurement locations.

5.4.4 Elements of morphology of the White Volta catchment

The conducted field research is not sufficient to thoroughly understand the morphology of the White Volta catchment. However, an attempt is made based on the above-mentioned conclusions and field observations:

1) With the first severe rain events silt and clay accumulated in small streams (possibly Harmattan dust) is suspended and transported to the river.
2) Sediment is deposited on the riverbanks as soon as the discharge reduces. This can be explained by the following theory:
    a. The flood peaks in the upper White Volta River are very sharp, which can be seen by water levels rising and dropping a few meters within 1 day. This indicates a strong hysteresis effect between the discharge and the water levels (see chapter 3.2): for increasing water levels (rising stage) the discharge is higher than for water levels during the falling stage. When the water level is maximum, the discharge is already reducing and sediment will start to settle.
    b. The flow velocities on the riverbanks that are flooded are becoming smallest, because these riverbanks are usually relatively shallow lands with vegetation (grass, small bush, crops) and are located in the inner bend of the river. The suspended sediment will therefore most easily settle in this region, because of the low flow velocities. During the rising stage the water is high-concentrated, so the water that entered the floodplains and riverbanks will be able to deposit a thick layer of sediment.

3) When the next flood arrives, the settled sediment on the riverbanks is resuspended, as the water levels rise and velocities increase. This might be part of the reason that the water during the rising stage is high-concentrated. Another reason might be that sediment bars have developed behind obstructions and rapids. Also river pools, for example formed by sand banks as observed in Yarugu, could be temporal storage for fines. Finally, it is possible that part of the sediment is trapped in pores of rocky bed, and released again when turbulence increases due to a flood wave.
4) This resuspended sediment might be settled on the riverbanks again, further downstream, when the water level is dropping.
5) After a couple of flood peaks, the sediment layer on the riverbanks could become less and eventually disappears. This has been observed in Nangodi and Yarugu. The easily erodible material in the catchment has already been gone after the first flood wave. Therefore, with the second and third flood, there was less new wash load input into the river.

6 Modelling the river morphology

The construction of a reservoir in the White Volta River will certainly have consequences for the river morphology upstream and downstream of the dam. In the reservoir there will be sedimentation and downstream of the dam the riverbed will have to deal with erosion. As the trap efficiency of the reservoir is almost 100% it is assumed that both bed material load (sand) and washload (silt and clay) will settle in the reservoir. The sedimentation of washload (siltation) has been described in chapter 5. In this chapter the sedimentation of bed material load (delta deposition) as well as the riverbed erosion downstream of the dam will be estimated using SOBEK RE (version 2.52.007), an open channel 1D hydrodynamic numerical modelling system, which is capable of solving the equations that describe unsteady water flow, sediment transport and vertical bed level changes. The morphological formulas used in SOBEK RE are only related to sediment transport of bed material (sand), so the siltation could not be estimated with this model.

6.1 Model description

Both delta deposition and riverbed erosion are related to the operational strategy of the dam:

- The location of delta deposition depends on the water level in the reservoir. It is likely that the sediment will be deposited in the upstream part of the reservoir, where the flow velocities reduce drastically. However the upstream edge of the reservoir varies for ± 40 km if the water level varies between min OL and Max OL. This has been shown in Figure 4.7. The location of delta deposition will therefore depend on the operational strategy of the dam.
- The bed erosion depends on the release flow through the dam, because the sediment transport capacity is a function of the flow velocity (chapter 2.1). The release flow is the sum of the flows through the turbines and over the spillway. These fluxes are also determined by the operational strategy of the dam.

In order to analyse the effects of reservoir operation on the water levels in the lake and the release flow, a water balance model has been developed. In this model the reservoir operation can be simulated for a wide range of scenarios. Output of the reservoir model are a) the release flow (turbines + spillway) and b) the water levels in the reservoir. The input into the reservoir water balance model is the 5-year discharge series of Pwalugu (2003-2007), located 30 km downstream of the intended dam (Figure 3.5). The discharge series of Pwalugu can be considered as total inflow into the reservoir. (HKV, 2012).
The delta deposition in the reservoir has been modelled in SOBEK RE. The upstream part of the reservoir, where delta deposition is likely to take place (Figure 6.1), has been schematised. The water levels in the reservoir, resulting from the water balance model, are used as downstream boundary condition. The upstream boundary condition is a 5-year discharge series of Yarugu (chapter 3.2). The erosion of the riverbed downstream of the dam has also been modelled in SOBEK RE, separately from the upstream model. Here the downstream reach has been schematised, with the release flow as upstream boundary condition and the water level in the Lake Volta as downstream boundary condition. The model outline is presented graphically in Figure 6.1, Figure 6.2 and Figure 6.3.

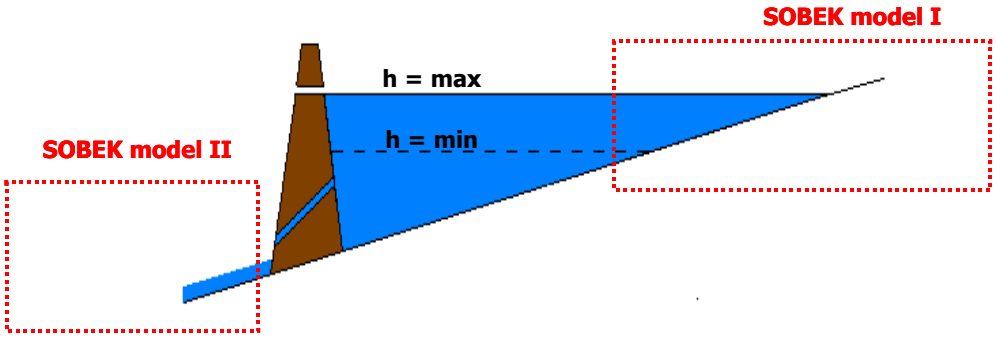

Figure 6.1 Upstream and downstream SOBEK model boundaries

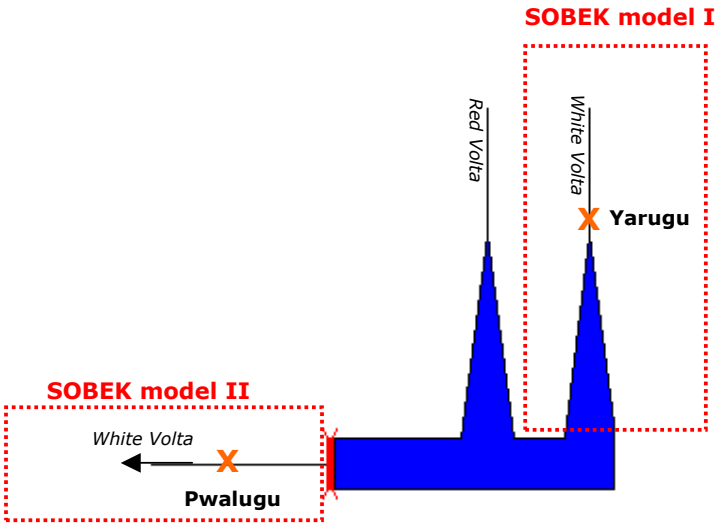

Figure 6.2 Topview study area with model boundaries

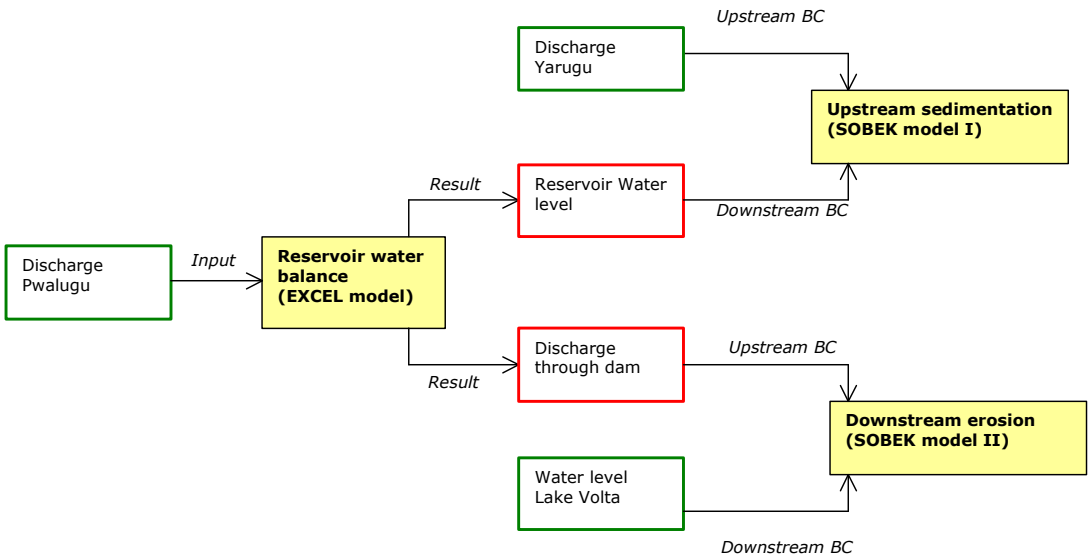

Figure 6.3 Model outline

Both models could have been joined together in one SOBEK model, if the dam would also have been modelled in SOBEK instead of using the water balance model. The reasons to chose two separate models are the following:

- The water balance model gives directly a clear view on the effect of operational strategies on the water levels in the reservoir and the release flow. Analysis of operational scenarios in SOBEK would be possible but would cost calculation time.
- The relation between storage volume (V) and water level (h) is incorporated in the water balance model using the V/h formula. This relation is exact. In SOBEK the right V/h relation can only be obtained by incorporating this in the reservoir geometry. This would be time-consuming and would never be more exact than the water balance.
- Only the upstream part of the reservoir has to be schematised, as this is the part where delta deposition occurs. That way calculation time is reduced. If one is interested in the effect of a certain scenario on only the up- or downstream reach, this can be investigated separately. This also saves calculation time.
- Evaporation rates can be included in the water balance model as a function of the lake surface.

6.1.1 Water balance model

For the reservoir a water balance has been set up:

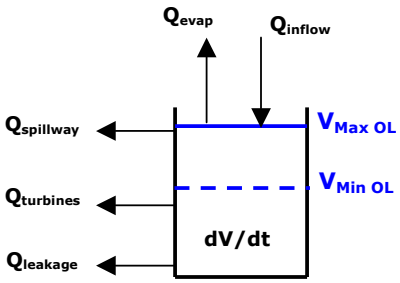

$$\frac{dV}{dt} = Q_{in} - Q_{uit}$$
$$= Q_{in\ flow} - Q_{turbines} - Q_{spillway} - Q_{evaporation} - Q_{leakage}$$

in which:

dV/dt: Change of reservoir volume over time (m^3/s)

Q_{inflow}: Time dependent inflow into the reservoir (m^3/s)

$Q_{evaporation}$: Evaporation rate, which depends on the surface area of the lake (m^3/s)
Annual evaporation loss = evaporation rate * reservoir area

$Q_{spillway}$: The volume leaving the reservoir by the spillway (m^3/s),
only active when $V>V_{MaxOL}$

$Q_{leakage}$: Water leaking through the earthen dam, through the gates, or infiltrating into the ground (groundwater recharge) (m^3/s)

$Q_{turbines}$: The discharge through the turbines, only active when $V_{MinOL} < V < V_{MaxOL}$ (m^3/s)

The outflow through the turbines ($Q_{turbines}$) is the variable of the model. In this model it is possible to choose either a constant flow through the turbines or a head dependent flow. It is assumed that the reservoir water levels vary between Min OL and Max OL. At Min OL the turbines are closed and at Max OL the spillways are opened (Figure 4.8). After filing in the fluxes in the water balance model, the volume will be calculated at every time step. This volume is converted to water levels using the V/h relation of the reservoir (Figure 1.1), as derived in chapter 4.2.1. The choice for the evaporation and leakage rates as well as further details on the model and scripts can be found in Appendix D.

6.1.2 Upstream SOBEK model

The model represents the river reach and the floodplains between minimum and maximum reservoir extent, as this is the reach where bed aggradation will occur. In order to understand the sedimentation process, the river has been schematised with a constant cross-section and slope. A more detailed representation of the geometry would mainly have local effects on sedimentation. The slope used in this model is the average slope between minimum and maximum reservoir extent, derived from riverbed measurements (HKV, 2012). The riverbed profile used is the one measured at Yarugu, because the discharge series are also measured at this location. Lateral inflow along the reach is neglected due to a lack of data. The average slope of the floodplain is derived from a DEM. The discharge series is the 6-hourly discharge series of Yarugu (period 2003-2007). The series are repeated up to 50 years. The bed material composition of the reach is based on riverbed material measurements from the bridge of Yarugu as described in Chapter 0. This is the main source of uncertainty of the model, as the riverbed material might be changing along the river reach. The downstream boundary conditions are the water levels in the reservoir, derived from the water balance model. More information on the model can be found in Appendix D.

6.1.3 Downstream SOBEK model

Similar to the upstream SOBEK model, the objective is to understand the large-scale morphological processes and to make first order estimations of the morphological changes. Therefore the river reach downstream of the dam has been schematised with a constant slope, cross-section, roughness and bed material composition. In reality the flow velocities are not constant in longitudinal direction due to a varying geometry and due to lateral inflow. The bed material might also be varying along the river, which would also have a direct impact on the erosion rate. However only one bed material measurement is available (Pwalugu gauging station), therefore implementing a detailed representation of the geometry would only suggest a high accuracy. In this model the river profile at Pwalugu gauging station is used. The reason is that also the riverbed material and the discharge series are measured at this location. The upstream boundary condition is the release flow of the dam, which has been derived in the water balance model. The downstream boundary condition is the average water level in Lake Volta. However, in reality the total discharge along the reach is increasing due to lateral inflow. The main tributaries of the White Volta River between the dam site and Lake Volta are presented in Figure 6.4. Downstream of Pwalugu the first main disturbance will occur at the inflow of the Sissili/Kulpawn River. The backwater effect of this reach will be reduced to 5 % at a distance of 30 km in upstream direction (HKV, 2012). Therefore it can be concluded that the schematisation with the constant geometry and without lateral inflow is valid for ± 60 km downstream of the dam. Further details on the model can be found in Appendix E.

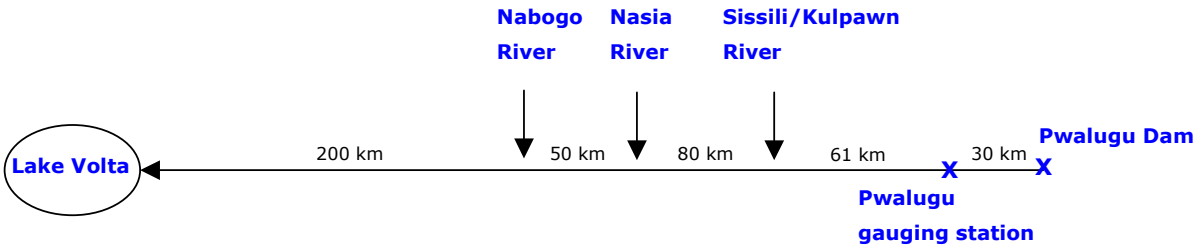

Figure 6.4 The White Volta River and tributaries between Pwalugu dam and Lake Volta.

6.1.4 Scenarios

As the location of delta deposition and the erosion of the riverbed downstream of the dam depend on the operation of the dam, different scenarios have been selected. These scenarios, as listed below, consist of both extreme and more realistic ones. The most extreme scenarios are chosen in order to know the geographical boundaries of the morphological impact. The more realistic scenarios should remain within the upper and lower boundaries defined by the extreme cases. The scenarios should give insight in the sensitivity of the system to different operational strategies.

- **Scenario 1** – **$Q_{in}=Q_{out}$ and $h = h_{max}$**
  The water level in the reservoir remains at Max OL all the time and all incoming discharge is directly released through the dam. This scenario is used to investigate the upstream boundary of the location of sediment deposition. The other purpose of this scenario is to estimate the maximal effect of erosion. It is expected that this unchanged discharge regime with sediment-free water will cause most erosion.

- **Scenario 2** – **$Q_{in}=Q_{out}$ and $h = h_{min}$**
  The water level in the reservoir stays at Min OL all the time. This scenario is used to determine the downstream boundary of delta deposition.

- **Scenario 3 – Constant regulated flow ($Q = 95\ m^3/s$)**
  The turbine flow is regulated by the reservoir manager to a constant value of 95 m^3/s. This is equal to the yearly average inflow minus evaporation losses. This would be a realistic scenario. The reservoir water balance model will show whether this constant flow will be possible in reality given the maximum and minimum operative levels. The water levels in the reservoir will range between min OL (154.4 m) and max OL (168 m).

- **Scenario 4 – Q(H) = max**
  The gates to the turbines will always be completely opened. The discharge is depending on the water level in the reservoir and will range in between 119 and 170 m^3/s (Appendix C). The water levels range between max OL and min OL.

- **Scenario 5 – Constant regulated flow ($Q = 79\ m^3/s$)**
  The outflow is chosen such that the reservoir levels will always stay above min OL. With this selected outflow, energy stops could be avoided for the given discharge series.

6.2 Results

6.2.1 Water balance model

The effect of operational strategies on the water levels in the reservoir and released flow through the dam has been analysed for scenario's 3, 4 and 5. The results of scenario 1 and 2 are straightforward (constant water level in the reservoir and inflow is equal to outflow) and will not be illustrated here. Also the yearly average energy generation has been calculated for several scenarios.

Scenario 3 – Qturb = constant (95 m^3/s)

In Figure 6.5 the relation between inflow, released flow through the dam and the water level in the reservoir is presented. During the three consecutive dry years (2004, 2005 and 2006) the inflow is insufficient to fill up the reservoir completely. There are 2 spills in 2003 and 2007 (blue peaks). The first spill (2003) is caused because the reservoir level at the start of the season was too high. The second spill (2007) occurs even though the reservoir was empty at the start of the season. There are two periods of energy generation stops (2006 and 2007), as the water levels reached min OL.

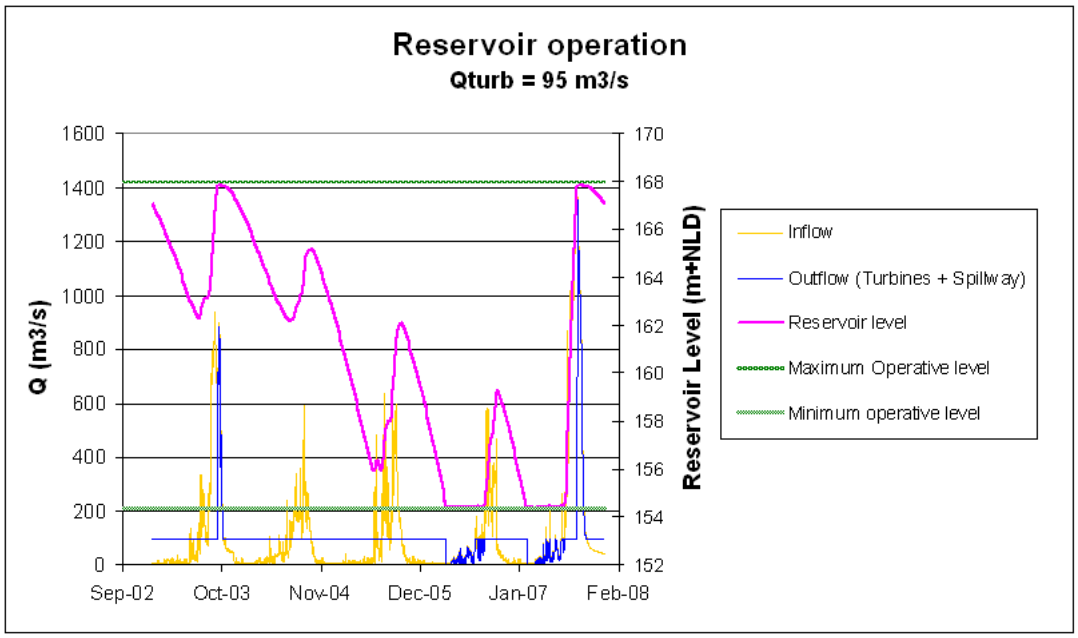

Figure 6.5 Water balance model, scenario 3

Scenario 4 – Q(H) = max

The discharge trough the turbines is maximal at Max OL (Q=170 m^3/s) and minimal at Min OL (Q=119 m^3/s). The average water levels are lower compared to scenario 3. That way, the discharge peak of 2003 can be stored in the reservoir without spillage occurring. The discharge peak of 2007 cannot be captured in the reservoir without spilling, even though discharge through the turbines is maximal. During dry years, there are long periods where no hydropower can be produced (Figure 6.6).

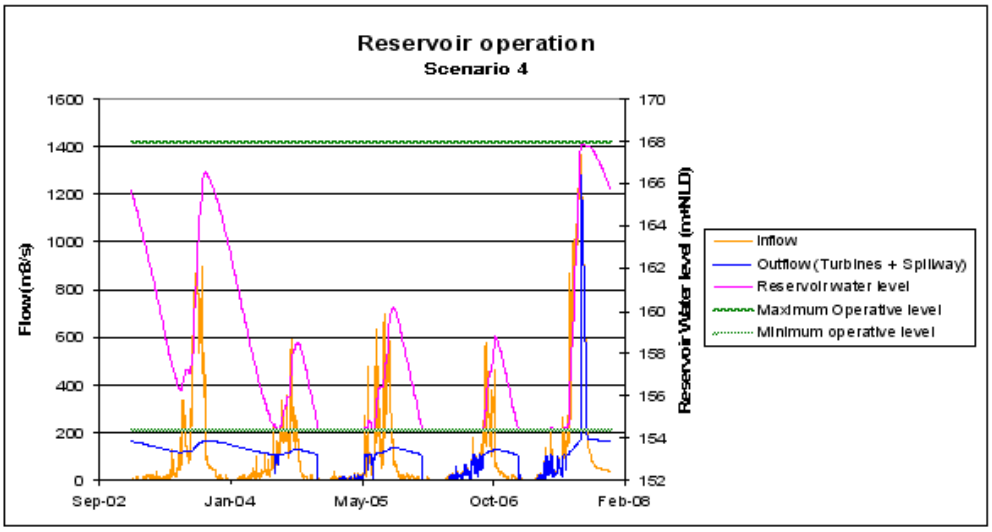

Figure 6.6 Reservoir operation scenario 4

Scenario 5 – Q=79 m^3/s

When Q is regulated at 79 m^3/s the water level remains above Min OL, so there are no energy generation stops (Figure 6.7). The total volume spilled in 2003 is higher than in the other scenarios. The reason for this is that the water level is higher when the flood arrives and the turbine flow is lower.

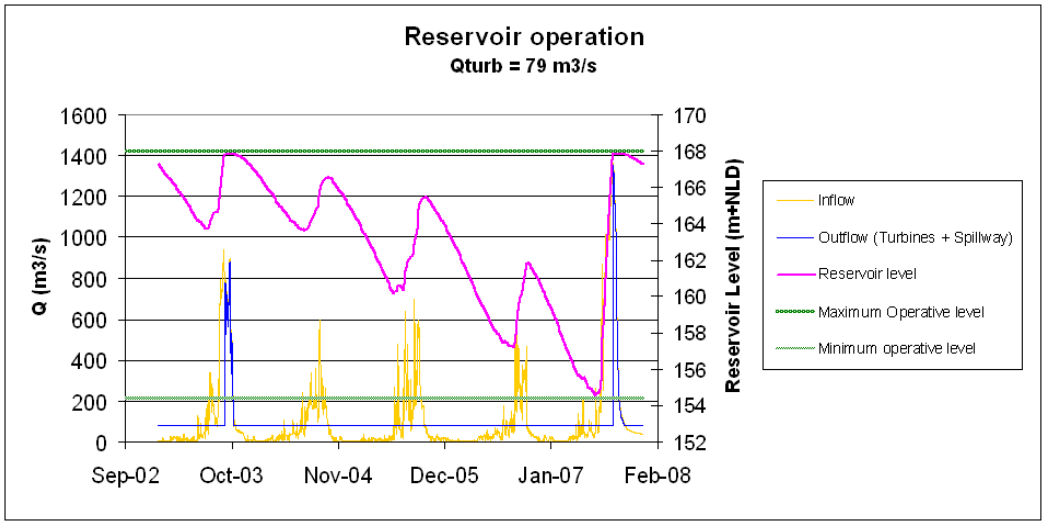

Figure 6.7 Reservoir operation scenario 5

Energy production

The average yearly energy generation has been calculated using the formula for energy generation (chapter 4.2.2). The water levels (h) and the turbine flow (Q) follow from the water balance model. The efficiency factor (η) is assumed on 0.9.

For scenario 4 (maximum flow through the turbines) the yearly average energy production is 108.5 GWh/year. If it is aimed to have a constant turbine flow instead, like in scenarios 3 and 5, the energy generation is presented in Figure 6.8 for desired constant flows between 60 m^3/s

and 200 m^3/s. Low, constant turbine flows will lead to higher average water levels in the reservoir, having a positive effect on energy generation. However in that case the spillway flows will be higher, which is a loss of energy. There appears to be an optimum turbine flow of 120 m^3/s (112 GWh/year). However in that case energy generation stops will occur. If generation stops have to be avoided and a constant discharge is desired, the results of scenario 5 show that the maximum turbine flow is 79 m^3/s. The energy production will in that case be 110 GWh/year.

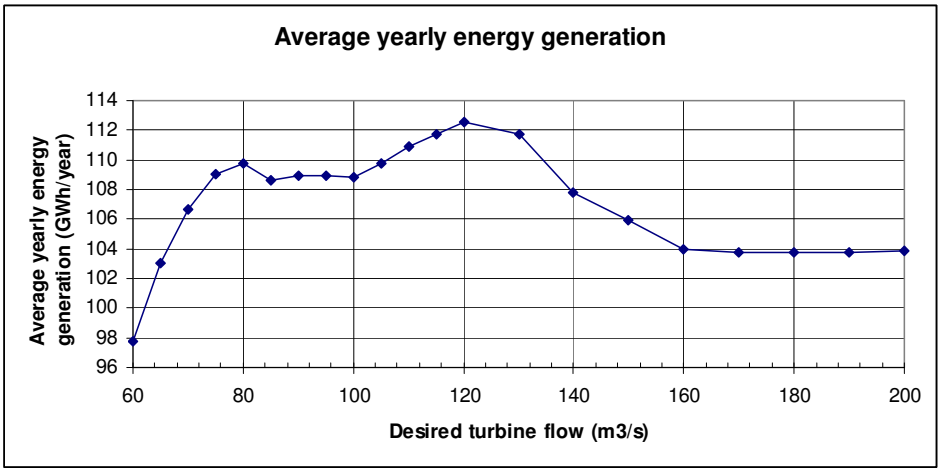

Figure 6.8 Average yearly energy generation for a range of desired turbine flows

6.2.2 SOBEK model I (bed aggradation)

In Figure 6.9 the bed aggradation is presented for scenario 1. The delta deposition is similar to theory (chapter 2.2.1). At the downstream end there is a sharp edge (foreset). The foreset is propagating in downstream direction. After 50 years the foreset will be located ± 10 km downstream of the upper boundary of the reservoir. The delta formation will also propagate in upstream direction. This is visible in Figure 6.10 where the evolution of delta formation is shown. For this scenario, most sedimentation will occur in the riverbed upstream of the reservoir. After 50 years the delta deposition will have propagated across the border with Burkina Faso.

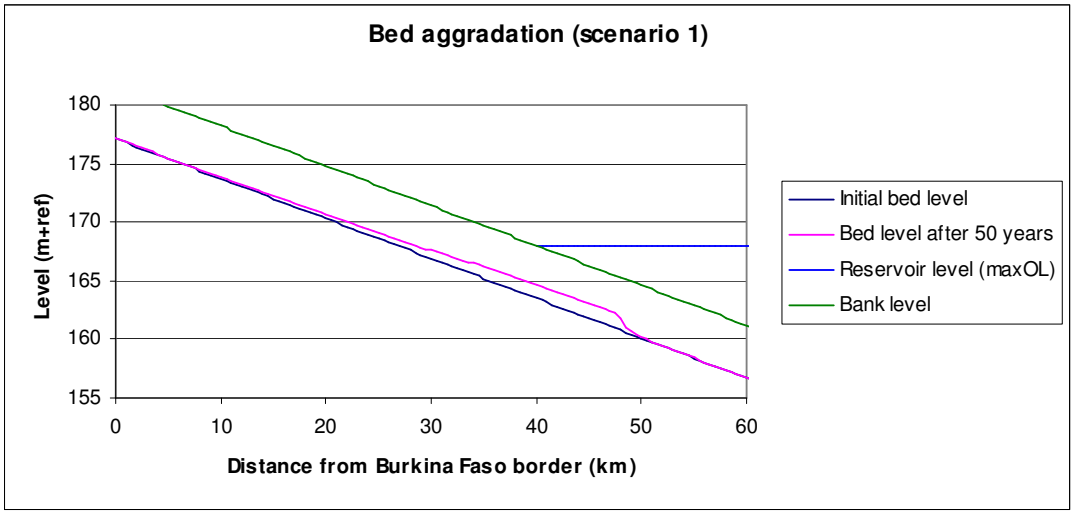

Figure 6.9 Delta deposition scenario 1

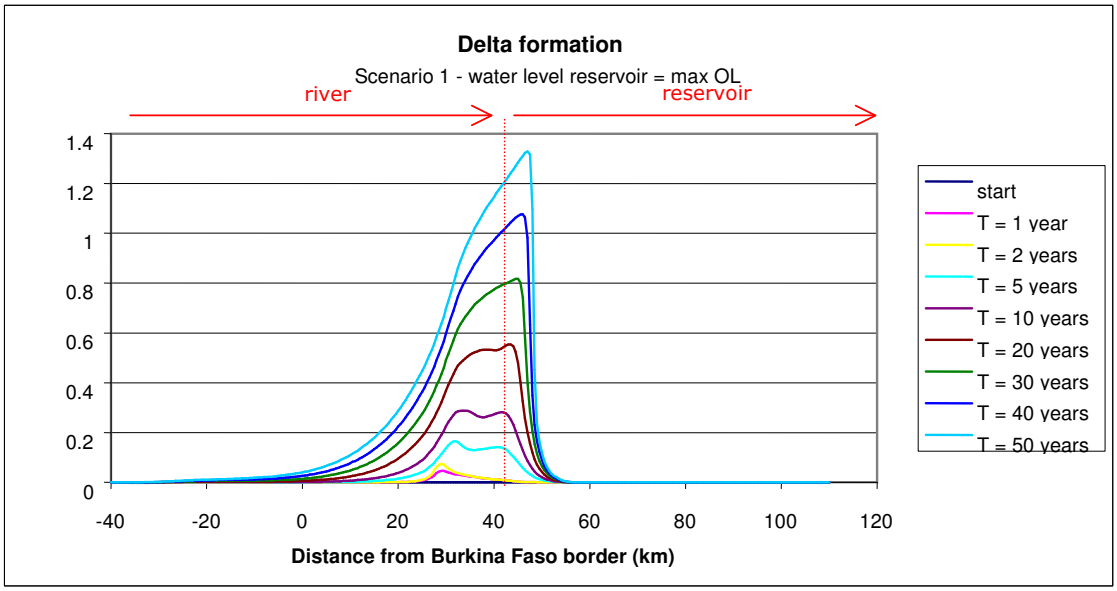

Figure 6.10 Bed level increase scenario 1

The delta formation for scenario 3 is presented in Figure 6.11. Due to the varying water level, most of the delta deposition occurs inside the reservoir. Only a small part of the total sedimentation occurs in the upstream river reach.

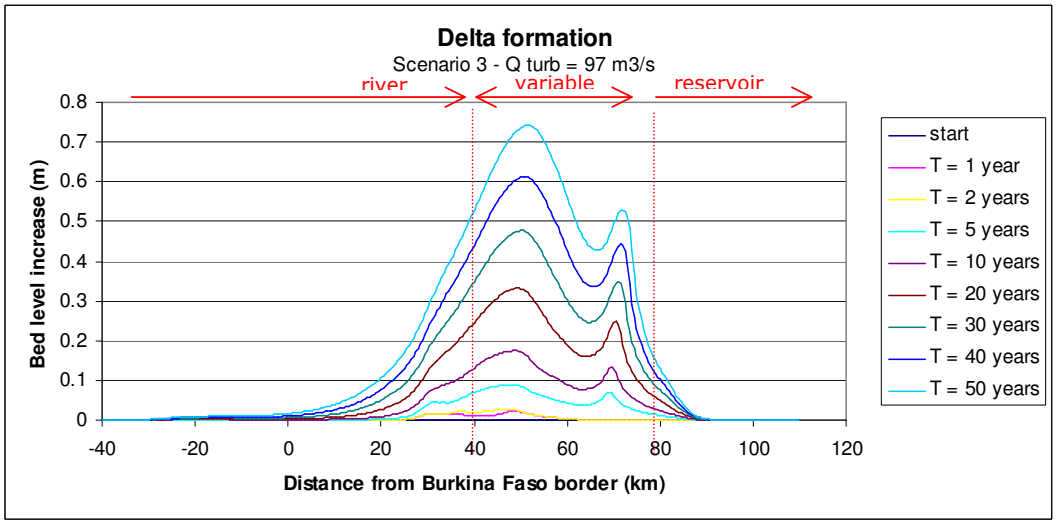

Figure 6.11 Delta formation scenario 3

The bed level increase after 50 years is compared per scenario in Figure 6.12. The total amount of deposited sediment is equal for all scenarios = $\Sigma(\Delta h \cdot \Delta x \cdot \text{width}) = 2.33 \cdot 10^6$ m^3 in 50 years. This is equal to 46600 m^3/year. When the water level in the reservoir is constant (scenarios 1 and 2), sedimentation is most concentrated: maximum bed level increase is 1.2 m after 50 years. When water levels vary between Max OL and Min OL (scenarios 3,4 and 5), the sedimentation is spread out over a larger distance. The location of deposition appears to be strongly related to the reservoir level: the lower the average reservoir level, the further downstream the sand will be deposited. Sedimentation will remain in between the geographical boundaries defined by scenarios 1 and 2. After 50 years, the sedimentation could be spread over a distance of 90 km. Delta deposits could reach the Burkina Faso border after about 50 years.

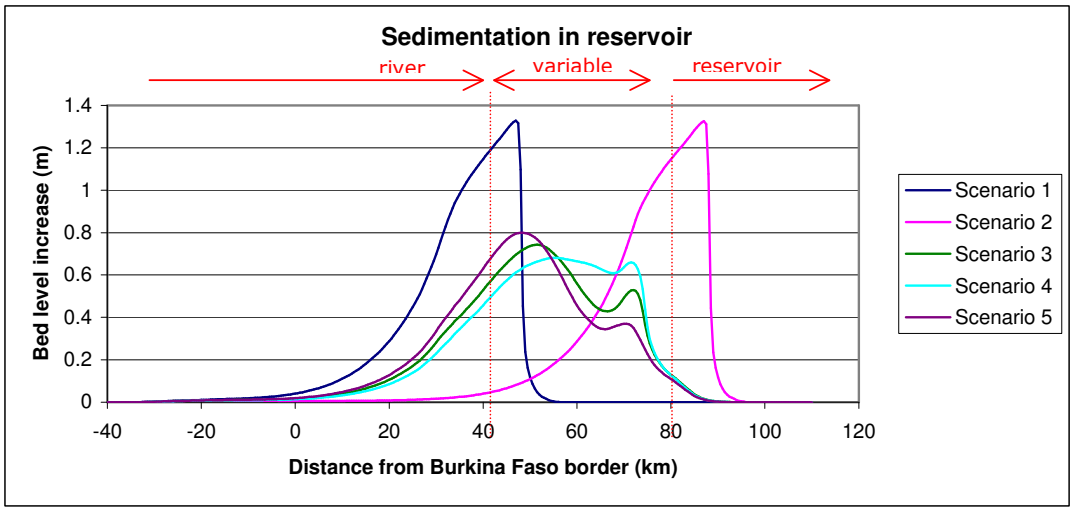

Figure 6.12 Delta deposition in the White Volta river after 50 years

The bed level increase for scenario 3 is presented in Figure 6.13. At Min OL the riverbed upstream of x = 65 km is not affected by the reservoir level. In the dry season there are periods where the river runs completely dry. In these periods the sand deposition can easily be investigated and eventually measures could be taken to remove the sediment using a shovel.

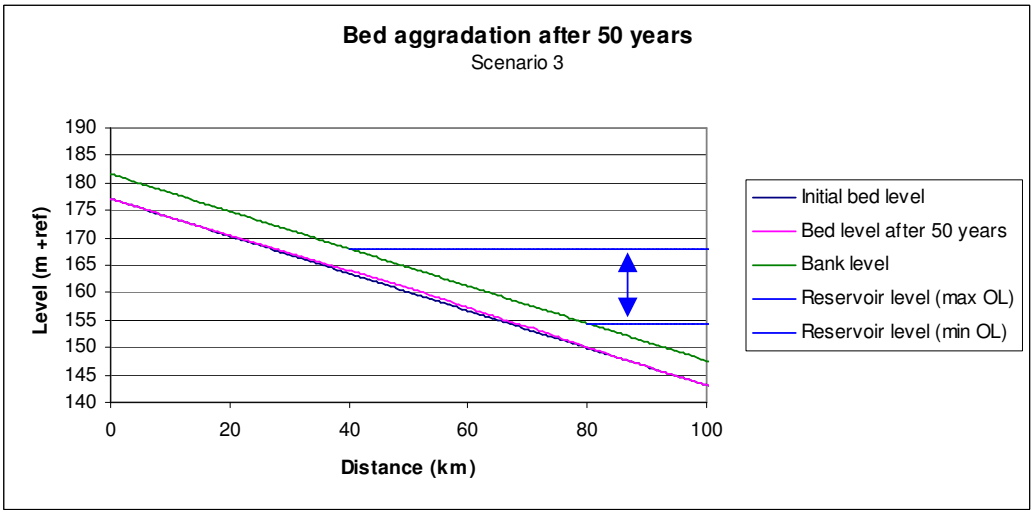

Figure 6.13 Delta deposition after 50 years, scenario 3

6.2.3 SOBEK model II (erosion)

The bed erosion for scenario 3 is shown in Figure 6.14. It is very well visible that erosion is maximal just downstream of the dam and that the erosion propagates in downstream direction. The other scenarios show a similar linear pattern of the evolution of erosion. About 30 km downstream of the dam there is an important bridge (Pwalugu). The riverbed at this location starts to erode after ± 30 years. The piers of the bridge might be suspect to scouring and the bridge could be in danger.

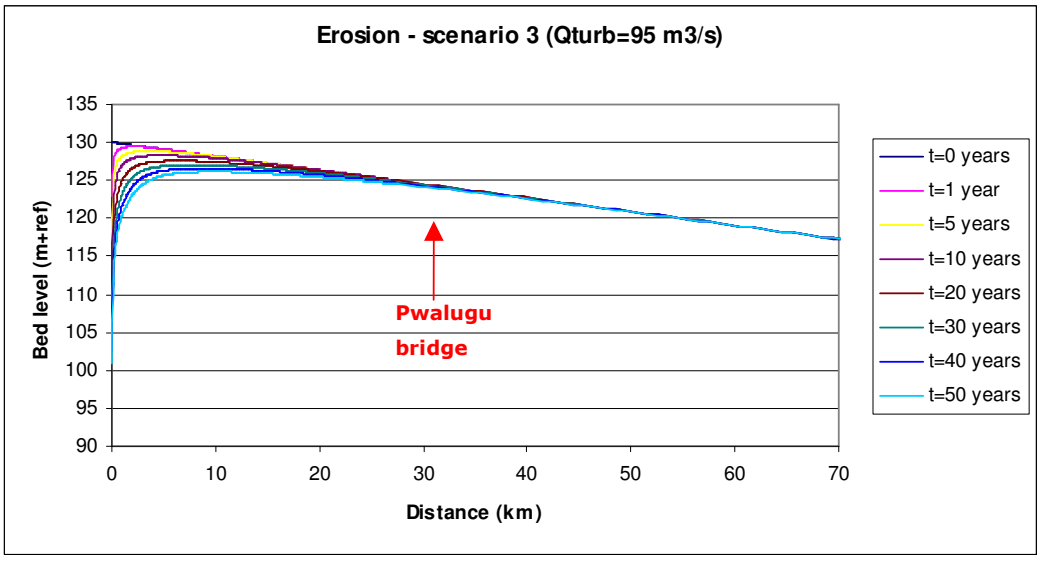

Figure 6.14 Bed erosion scenario 3

The bed erosion after 50 years is plotted in Figure 6.15. The erosion is maximal for scenarios 1 and 2 (inflow reservoir = outflow). These extreme scenarios have a peaked discharge pattern. These peaks are causing most erosion, which is logical as the formula for sediment transport is a power function of the velocity (s=m*u^n). For the more realistic scenarios (3,4 and 5) the erosion rates are similar. The erosion is maximal near the dam (± 20 m /50 years).

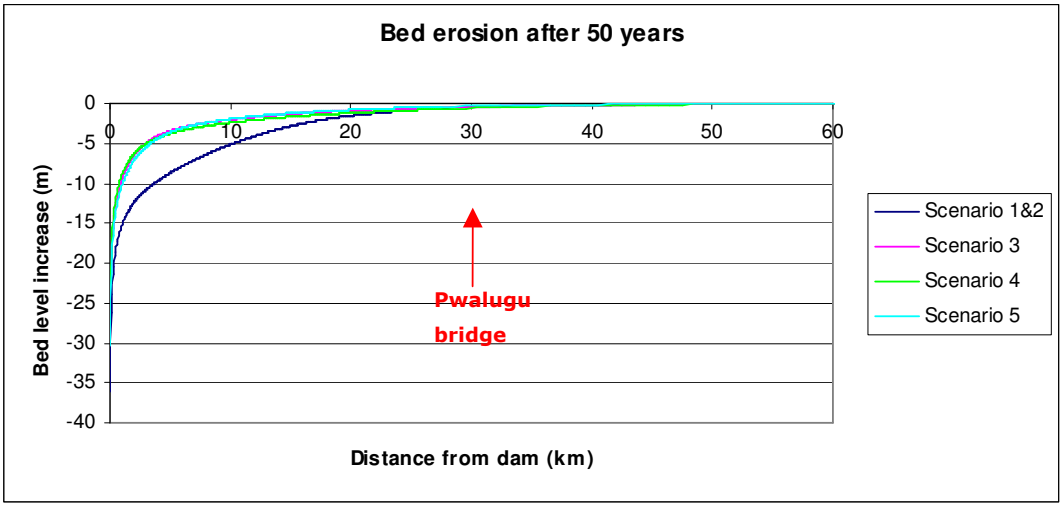

Figure 6.15 Bed level change after 50 years relative to the initial bed level

In Figure 6.16, the bed erosion for scenario 5 is plotted versus the discharge released through the dam. It can be seen that the spillage peaks cause most erosion; per spillage peak the bed level drops ± 25 cm. The constant discharge through the turbines of 79 m^3/s causes little erosion compared to the spillage peaks.

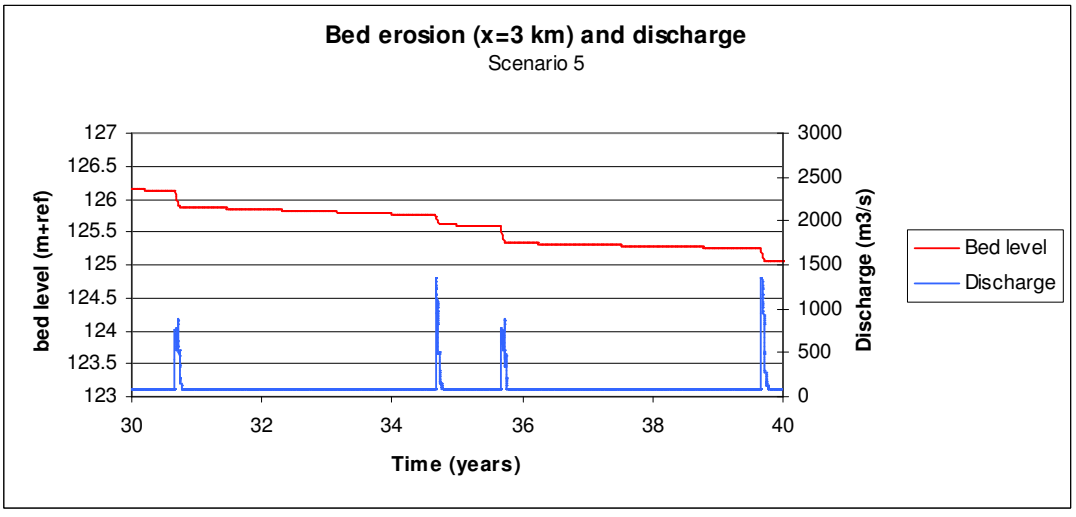

Figure 6.16 Bed erosion over time at 3 km downstream of the dam, scenario 5

The total impact of the spillage peaks generated in scenario 5 is shown in Figure 6.17. The results of scenario 5 are compared to a reference case without any spillage peaks. In this reference case the total outflow through the dam is equal to scenario 5, but averaged out over the entire period, giving a constant discharge of 95 m^3/s (for the given discharge this would only be possible if the Min OL would be lower). It appears that the spills account for 2.3 m/50 year extra erosion compared to the reference case without any spillage peaks.

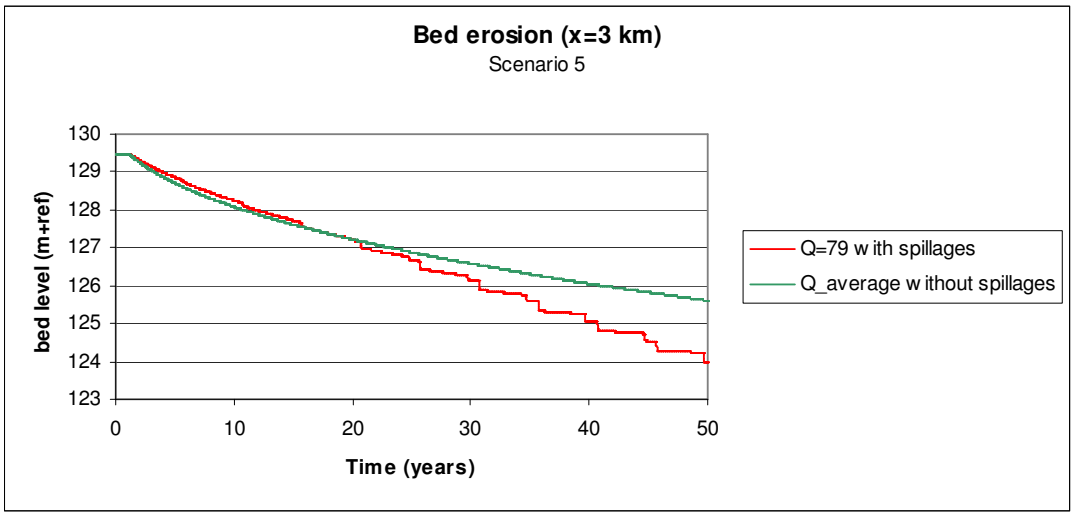

Figure 6.17 Influence of spillage peaks on bed erosion

In Figure 6.18 scenario 5 and the reference case without spillages after 50 years is plotted. It can be seen that avoiding spillage peaks would reduce the erosion rate near the dam by about 10 m.

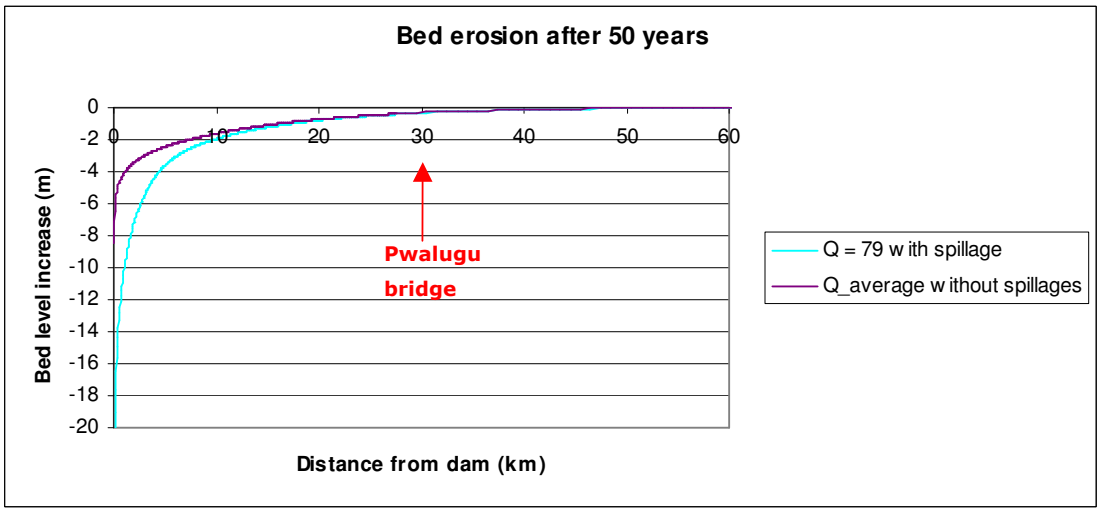

Figure 6.18 Bed erosion after 50 years

For scenario 5, the effect on erosion has been analysed when the discharge through the turbines is diverted 5 km downstream of the dam via a side channel. This is sometimes done in order to reduce erosion downstream of the dam. The spillages are still entering the river directly. The results (Figure 6.19) show that the bed level in the initial 5 km is ± 2 m higher. After 5 km the bed level is ± 30 cm lower than in the reference case. This effect holds on for 30 km.

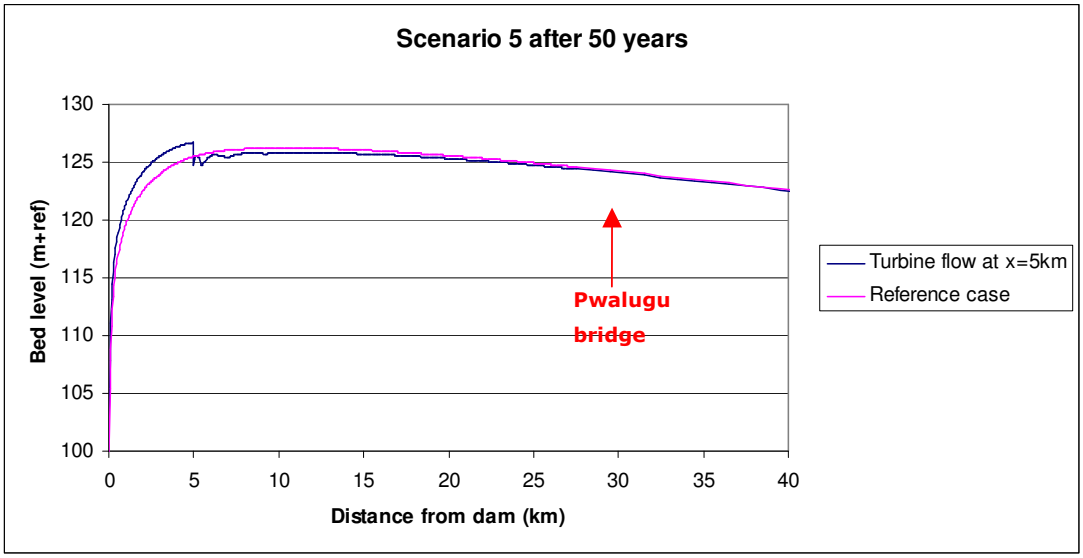

Figure 6.19 Bed erosion with turbine flow diversion channel at x = 5 km.

Another option to reduce the erosion locally could be to divert the spillway flow instead of the turbine flow. In Figure 6.20 the effect on the riverbed level is shown. The turbine flow enters the river just downstream of the dam and causes only 3 m erosion after 50 years. The spillway enters the river 5 km downstream of the dam and provokes an erosion of 10 m in 50 years. The erosion rate futher downstream will be higher, but the total riverbed erosion is exactly the same for both cases.

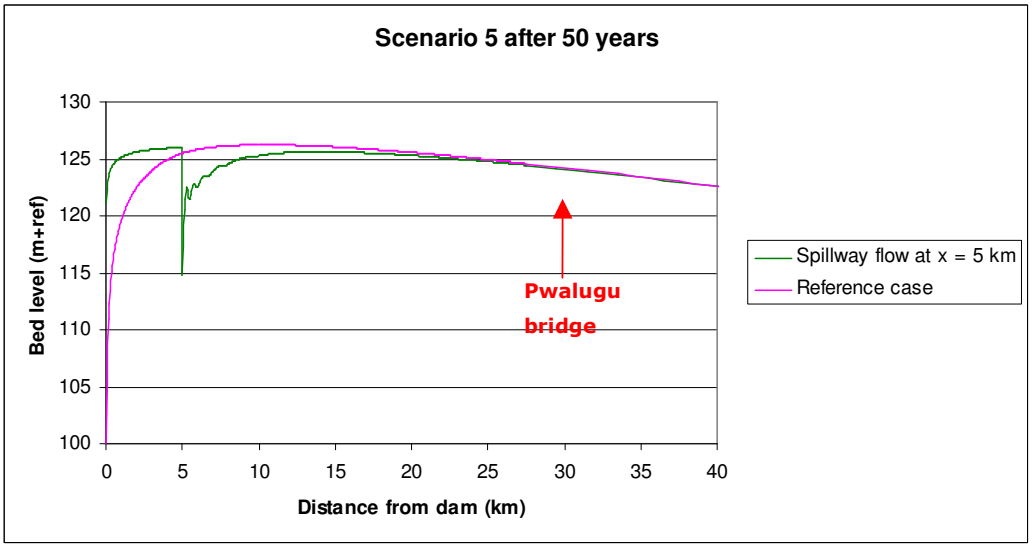

Figure 6.20 Bed erosion with spillway diversion channel at x=5km

6.3 Conclusions

6.3.1 Water balance

- When the discharge through the turbines is maximal (scenario 4), periods of energy generation stops are unavoidable. The risk on spillage is least, because the reservoir levels are drawn down as much as possible during the dry season. The drawback is that during consecutive dry years, the reservoir will not be completely filled, which leads to a reduction of hydro-power generation.
- Spillages are unavoidable, even when the reservoir level is drawn down to Min OL and discharge trough the turbines is maximal (scenario 4). The reason is that the large volume of water cannot be stored completely in the reservoir and the overcapacity cannot be discharged on time through the turbines.
- When the discharge through the turbines is set at the yearly average inflow minus evaporation (Q = 95 m^3/s), there will be energy generation stops during dry years.
- With a lower desired turbine flow of 79 m^3/s (scenario 5) there are no energy generation stops at all. The drawback is that spillages are higher, because of higher water levels when flood peaks arrive. The energy produced for this scenario is 110 GWh/year.
- Most energy can be produced (112 GWh) for a desired turbine flow of 120 m^3/s. However there will be periods where no energy can be generated. In this research the operational scenarios are restriced to constant flows through the turbines. When applying more advanced operating rules the generation could be higher. The average yearly energy generation is only 65 % of the design generation (184 GWh/year) calculated in the prefeasability study (COB, 1993). The operational strategy used in their calculations is not known.

6.3.2 Upstream reach (sedimentation)

- Total sedimentation of bed material load in the White Volta reach is $53 \cdot 10^6$ kg/year. With a porosity of 0.4 and a density of 2650 kg/m^3, the deposited volume would be 33000 m^3/year.
- The delta deposition is propagating in both up-and downstream direction. After ± 50 years, sedimentation could have reached the Burkina Faso border. The length of the reach where sedimentation occurs is maximally 90 km after 50 years.
- The maximum bed level increase after 50 years is 1.3 m, which will occur when the reservoir level would remain constant. However this is not a realistic scenario.
- For the more realistic scenarios, when water levels vary between Min OL and Max OL, the sedimentation will be more spread out. The maximum bed level increase after 50 years is in that case ± 0.8 m. Most sediment will be deposited inside the reservoir. Only a small portion will be deposited in the upstream river reach.
- In all cases there will be higher water levels in the upstream river reach during floods, due to bed level increase. This means an increased risk of flooding of the upstream floodplains, possibly harming communities.

6.3.3 Downstream reach (erosion)

- Erosion downstream of the dam is most severe for scenarios 1 and 2, where the outflow is not regulated. For more realistic scenarios (3,4 and 5) the results are comparable. Erosion just downstream of the dam is ± 20-30 m after 50 years. 5, 10 and 20 km downstream the erosion is respectively 4, 2 and 1 m /50 years.

- Erosion is most affected by spillage peaks. Avoiding spillage peaks could reduce sedimentation near the dam by 75 % compared to a case with 2 spillage peaks/5 year. In that case the Min OL has to be selected lower, because with the present settings spillage peaks are unavoidable.
- The water levels in the downstream reach will be more constant due to discharge regulation. High water levels will occur less frequently.
- At Pwalugu bridge the riverbed will start to erode after ± 30 years.
- The erosion can be reduced locally by diverting the turbine flow or the spillway flow via a side-channel to a location some distance downstream of the dam. However the total volume of eroded bed material will be exactly the same.

7 Discussion

The aim of this research was to get insight into the large-scale morphological processes and to give first order estimations of the river morphological changes. The use of the 1D model with schematized river reaches helped to understand these processes very well and enabled to draw conclusions on the estimated effects on the functions of the reservoir.
In reality the morphological processes are more dimensional and the geometry of the river and floodplains is not constant. However using a higher dimensional model or introducing a more detailed representation of the geometry would only have a local effect and would not change the first order estimations of sedimentation and erosion rates.
The total sedimentation and its effect on the storage capacity of the reservoir would not change if the geometry would vary, because all bed material load will settle in the reservoir anyway.
The local riverbed erosion is much determined by the composition of the riverbed. In this study the bed material is assumed to be uniform over the depth, while in reality there could be rocks or coarse material underneath the alluvial layer. This would limit the erosion process locally, but the consequence would be that the erosion further downstream would be more severe, as the river will restore the sediment carrying capacity. However the total erosion in the river reach would be the same.
More important than introducing more geometrical details in the model would be to have more information on the composition of the riverbed or the sediment load, because these are the most important factors determining the quantification of the morphological impact.

There are several uncertainties in both the model and the field measurements. Therefore the results can only be considered as first order estimations. The real values could very well be multiple times higher or smaller. The most important uncertainties are the following:

- The particle size distribution of the riverbed defines the sediment transport capacity of the river. As the measurements have been taken at a few locations and in a small period, the uncertainty is high. The bed material composition could be finer grained at the start of the season, leading to higher bed material loads, or could be variable along the river reach. More extensive measurements, both temporally and spatially, are required. Probably it would be better not to use the bed material below a bridge, because this could be influenced by a non-uniform flow pattern because of the presence of the piers.
- The suspended sediment measurements, defining the siltation rate of the reservoir, could be underestimated due to errors during sampling and analysis and the restricted number of measurements. However, the measurements were consistent and comparable with the results of other studies, so this suggests reliability.
- The chosen transport formula (Engelund-Hansen) overestimates the sediment load during low flows. Most of the time the flows are low, especially downstream of the dam, where the high peaks are attenuated. Most of the time the Shields numbers are in the low range, which indicates that MPM would be more appropriate to use than EH. In that case the sediment transport capacity could very well be 3 times lower and assuming linearity, the morphological changes would be reduced by a factor 3.
- The results of the models are based on a discharge series of the period 2003-2007. This is a realistic discharge series compared to the historical records. However, a longer time series could give a more realistic estimation.

- The trap efficiency of the reservoir is based on theoretical formulas assuming complete mixing. In reality short-circuiting could occur, leading to smaller residence times and thus lower trap effiencies. This would reduce sedimentation in the reservoir and bed erosion downstream of the dam.

The separation of the river system into an upstream and downstream SOBEK model provided quick and accurate results. The water balance model gave a good and quick insight into the impact of the operational scenarios on the water levels and the outflow through the dam. Simulating the whole system into one SOBEK model would be a more time-consuming process and not more accurate. Moreover, the water balance model has a high potential for future research on the optimal operational scenario and flood control.

8 Conclusion

In this chapter the conclusions of the fieldwork and morphological model results are summarized. Successively, the conclusions on reservoir sedimentation, riverbed erosion and the catchment sediment balance are dealt with. Finally, there will be an overall appreciation of the main research question: **What are the effects on river morphology with the creation of a reservoir near Pwalugu?**

Sedimentation in the reservoir

The transported sediment through the White Volta River consists of washload and bed material load. Washload is fine sediment (clay, silt) and causes siltation of the reservoir. Bed material load consists of fine-grained sand and causes delta deposition. The amount of suspended sediment flowing into the reservoir is ± $6.9 \cdot 10^5$ m^3/year. The fine material (silt/clay) is dominant in the suspended load (more than 75 %). With a trap efficiency of nearly 100 % it can be assumed that all fine sediment would be retained in the reservoir. As it is not known whether density currents will develop or non-stratified settling will be the main mechanism, it is not possible to estimate the location where sediment will be deposited. If all fine sediment would be spread evenly throughout the reservoir, the average siltation rate would be ± 3 mm/year. If density currents bring the sediment all the way to the dam and would be deposited as a wedge, it would take ± 200 years to fill up the reservoir up to the inlet level of the turbines.

The largest proportion of the washload will flow into the reservoir through the White Volta branch (± 50%) and roughly 15 % through the Red Volta branch. The rest (35%) is flowing into the reservoir by lateral inflow of small rivers. For the suspended sediment concentrations there seems to be a hysteresis effect during the flood waves. Moreover sediment concentrations appear to decrease throughout the year due to decreasing sediment availability in the river system. Asselman (1999) and Picouet (2001) observed the same mechanism. It can be stated that the highest sediment concentrations will usually occur during the rising stage of the first severe flood wave of the year.

Delta deposition will occur at the location where the White Volta River flows into the reservoir. The bed material load of the White Volta River upstream of the reservoir consists of fine-grained sand and is estimated on $3.3 \cdot 10^4$ m^3/year. All sand will be deposited. The exact location depends on the water level variation in the reservoir. If the water level in the reservoir is constant over the year, the deposition is most concentrated. The higher the variation of water levels, the more spread out will be the sediment deposition. If the water levels vary between maximum operative level (Max OL) and minimum operative level (Min OL) the reservoir pool will vary in length over 40 km and most of the delta deposition will occur in this region. The maximum bed level increase will be in the order of 1-2 m in 50 years. The delta depositions are propagating in both upstream and downstream directions. Due to upstream propagation the riverbed level upstream of the reservoir will also increase. After 50 years, the effect is restricted to ± 30 cm just upstream of the lake and has damped out at the border of Burkina Faso. As the bed levels increase, backwaters could provoke higher water levels in the river. The consequence is that a larger area will be flooded during periods of high flows, possibly harming communities near the river. However the area is not densely populated and occasional floods happen every few years, therefore the impact of increased water levels is assumed to be low. More research is needed into the upstream changes of the water levels to investigate the impact of these floods.

If all inflowing sediment (washload + bed material load) would be deposited in the active storage of the reservoir, this would mean an annual storage loss of 0.03 %/year. A reducing storage capacity has a negative effect on the energy generation potential, as less water can be

stored in the reservoir. However the storage loss of 3%/100 years is negligible. Moreover, if the lake level will be reduced to the minimum operative level at the start of the season, the total storage capacity will only be used during wet years. During dry years when the reservoir is not filling up completely, the storage loss due to sedimentation is irrelevant. Due to the uncertainties in the model and in the data the sediment input could very well be five times higher, but even then the storage capacity will only be reduced by 15% in 100 years. This is still not a serious problem. Sediment management strategies could eventually reduce the negative effects and increase the lifetime of the reservoir.

Riverbed erosion downstream of the dam

The water released through the dam is assumed to be sediment-free, as the theoretical trap efficiency is nearly 100 %. In order to restore the sediment carrying capacity the riverbed downstream of the dam will experience erosion. The erosion is most affected by spillage peaks, which is logical as the sediment transport capacity is a power function of the flow velocity. If there would be one or two spillage peaks per 5 years, which is a likely scenario, the erosion rate just downstream of the dam would be ± 20-30 meters / 50 years. This huge erosion rates will be very locally; at 5, 10 and 20 km downstream, the erosion rates would respectively be 4, 2 and 1 meters / 50 years. Possibly the erosion process is limited by coarse layers underneath the alluvial layer. In that case the erosion rate further downstream will be higher.

If no spillage peaks would occur, the erosion rate close to the dam would be reduced by 75 %. However, the reservoir water balance has showed that during a wet year (T ≈ 10 years), with the proposed active storage volume, spillage would be unavoidable. Reducing the risk on spillage by drawing down the water levels in the reservoir at the start of the season will have a negative effect on energy generation. There is a risk that the reservoir will not be filled completely during dry years. As a consequence, energy generation will be lower and eventually generation stops could occur. It is unknown whether energy generation stops are permissible. Possibly thermal energy could replace the hydropower energy during these periods. If the aim of the reservoir operation would be to provide a constant discharge without any energy generation stops, the maximum possible flow through the turbines would be 79 m^3/s, which is lower than the average inflow into the reservoir. The energy generation stops will occur most often, if the operational strategy would be to apply a maximum flow through the turbines. In that case the advantage would be that the spillage volumes would be lower, because the water level would be drawn down maximally every year. However it appeared that even in that case occasional spills are unavoidable.

The riverbed at the location of the bridge near Pwalugu will start to erode after ± 30 years after construction of the dam, which could endanger the foundations of the bridge. If the erosion process close to the dam would be stopped due to coarse layers or rocks, the river will continue to take up sediment and the erosion rate further downstream will be higher. In that case, the bridge will be in danger even sooner. Another possible consequence of erosion is bank collapse. The water levels in the river will be lower due to the changed discharge regime. Seasonal peaks are averaged out over the year. High water levels will occur only occasionally when spillage occurs and will be of shorter duration. These average low water levels could draw down groundwater levels affecting wetlands and agricultural areas along the White Volta River. However this effect seems to be only local; after 50 years the reach 30 km downstream of the dam will be affected. The erosion just downstream of the dam could be reduced if the flow through the turbines would be entering the river by a side channel some distance further downstream. However the total amount of eroded material would be exactly the same.

Catchment sediment balance

The sediment balance of the White Volta catchment is based on sediment input through Harmattan dust and sediment output by the washload transported by the White Volta River. When dividing the washload by the total upstream catchment area, the erosion rate would be 13,5 mm/1000 years. This is a low erosion rate, which could be explained by the topography of the White Volta catchment: the surface is relatively flat and well vegetated, so the erosion potential is not high. From literature it has been derived that the Harmattan dust deposition rate in northern Ghana is ± 15 mm/1000 years. This would imply that there would be no net erosion at all; sediment deposition and erosion would be in equilibrium. Harmattan dust deposition is more or less equally divided over the catchment area, while erosion usually has a more local character. Therefore the flat areas might be accumulating and slopes might be eroding, but on average there would be equilibrium. Eroded material originating from the upstream part of the White Volta catchment could possibly have been trapped in the Bagré reservoir. In that case the erosion rate would be a factor 2.5 higher (32 mm/1000 years).

The texture of the sediment deposits on the riverbanks of the White and Red Volta River mainly consists of silt. The mineralogy consists of quartz, feldspar and kaolinite. These minerals are abundantly present in the catchment's soils and also in Harmattan dust.

Kaolinite appears to be present only in the samples taken at the most downstream gauging station (Pwalugu). Just upstream of Pwalugu the White Volta River is flowing through soils consisting of mudstone. This could be the reason for the high kaolinite content in the bank depositions. Kaolinite is a white mineral, so this could also explain why the color of the White Volta River is more white than the Red Volta River. However, the fact that no clay has been found on the banks further upstream (Yarugu and Nangodi) does not mean that there is no clay present in the river. It could simply be the case that clay has not been deposited on the banks at these measurement locations. Therefore it is not possible to draw any definite conclusions on the origin of the sediment deposited on the riverbanks.

General

With the construction of a dam near Pwalugu, there will be morphological effects in the reservoir and downstream of the dam. In the intended reservoir sedimentation will occur, but the effect on the functions of the reservoir is negligible. Delta deposition will mainly occur within the reservoir and partly in the upstream riverbed. As it will be spread out over a large distance the riverbed increase will be limited. The effect on the water levels in the river should be further investigated. There will be significant erosion of the riverbed close to the dam. In the future the riverbed erosion could damage Pwalugu bridge. Other negative consequences such as bank collapse and the draw down of groundwater levels could occur locally.

9 Recommendations

Sediment Management Strategy

Based on the results of this report a sediment management strategy should be set up which should help limiting erosion, siltation and delta formation. A few recommendations are proposed. Further research is needed to investigate the feasibility of the strategy.

- In order to limit bed erosion downstream of the dam, spillage should be avoided. The best way to achieve this is drawing down the water level in the reservoir to minimum Operative Level (min OL) at the start of the rain season. That way the full reservoir storage capacity can be used to store the flood peak. However with the present min OL frequent spillages are unavoidable. Therefore it would be advised to investigate the feasability of the dam for a lower min OL.
- Delta depositions could be removed by dredging. If water levels are drawn down to min OL, a large part of the riverbed where sand has been deposited will become dry. Sand could be removed with a bulldozer. In case the sand could not be used for construction purposes, it could for example be loaded on a boat and released over the dam, creating a natural sand motor restoring the eroded bed downstream.
- In order to limit siltation in the reservoir, sluicing could be applied. The highest suspended sediment concentrations come in front of the first flood peak of the year. It could be an option to sluice these high-density currents directly through the dam. Water levels would have to be drawn down below min OL. The drawback would be that the reservoir would probably not be filled up again.

In summary, for sediment management purposes it would be advised to make sure that the water level in the reservoir is at min OL (and ideally even lower) before the start of the rain season. This would also be most beneficial for flood control. The drawback is that hydropower generation is most efficient with high water levels. A long-term economical analysis should balance the costs and benefits of the sediment management strategy. An intermediate solution could be to apply the strategy less frequently, for example once every five years.

Cooperation with Bagré dam (Burkina Faso)

To further optimise the operational strategy of the dam, more research has to be done into the influence of the working of the Bagré dam on the White Volta River discharge. If the operational strategy of the Bagré dam would be taken into account, discharge peaks could be estimated more accurately. Optimally, the Ghanaian and Burkina Faso energy companies could cooperate by tuning their operational strategies. The objective should be a maximum total energy generation of the total hydropower scheme, also including the Akosombo dam in southern Ghana. There is also more research needed in the trap efficiency of the Bagré dam. Based on theoretical formulas the trap efficiency is 90 %, but it is unknown whether sediment management strategies are applied.

Data improvement

The accuracy of the model strongly depends on parameters that have to be measured in the field. It is advised to set up a monitoring network for bed material measurements and suspended sediment measurements:

- Monitoring the suspended sediment concentrations give better insight into the variation over the year. Separate rating curves for rising and falling stages can be developed, as the effects of hysteresis seem to be significant. As the sediment concentration peaks have a small timescale, the sampling frequency must be

sufficiently high, ideally every day. During the dry season once every 2 weeks to 4 weeks should be sufficient. It is advised to use the surface dip technique. This is a very straightforward way of sampling, which could for example be executed by local gauge readers. Once in a while the correction factor should be optimised by executing depth-integrated samples. For example a professional organisation like the WRI could execute these measurements.

- For monitoring of bed material the sampling frequency should be based on the timescale of a flood peak. This would result in a frequency of once every week during the wet season and once every month during the dry season. Samples should better not be taken from a bridge, as the bridge could influence the local morphology. It is advised to use a boat or canoe and to take several samples per cross-section as the bed material appeared to vary over the cross-section.
- The bed load could also be measured by taking successive bed level measurements along a river reach. The changing bed forms indicate the bed load transport.

Model refinement

In continuation to the preliminary morphological research, the schematic model could be refined. The morphological processes could be investigated at a smaller scale, by making the geometry of the model more realistic. More cross-sections of the river and floodplains could be used, as well as lateral inflow by side streams. The cross-sections are already available by HKV. Instead of the 1D SOBEK model, a 2D or 3D model could be used taking into account the higher dimensional morphological processes. However, before adapting the model it is advised to collect more data on bed material composition, because that is the most important parameter in the model.

Model potential

This research aimed to estimate the morphological effects (i.e. erosion and sedimentation) of a reservoir. However, the developed models showed a wide range of other research possibilities:

1) The flood control potential could be analysed with the water balance model. The model already showed that most of the floods could be captured inside the reservoir, as long as the water levels are drawn down to min OL before the flood arrives. More extensive analysis could be carried out for different operational scenarios. The effects on flooding further downstream could be investigated making use of the hydraulic model of the White Volta River, developed by HKV. The release flow through the dam (water balance model) can be used as upstream boundary condition in the hydraulic model.
2) The energy generation capacity of the dam has been calculated for constant turbine flows in the reservoir model. The model can also be adapted to varying turbine flows (e.g. depending on the reservoir level). The optimal operational strategy yielding the highest total energy generation could be investigated.
3) The water levels of the upstream river reach could be analysed with the SOBEK model. Due to bed aggradation the water levels will increase. It is expected that backwaters will be propagating across the border with Burkina Faso. The future water levels could be compared with the present situation.

References

[Adwubi, 2009]. Adwubi A, Amegashie B.K, Agyare W.A, Tamene L, Odai S.N, Quansah C, Vlek P. Assessing sediment inputs to small reservoirs in Upper East Region, Ghana. Lakes & Reservoirs: Research and Management 14: 279-268. 2009.

[Akrasi, 1984]. Akrasi S.A, Ayibotele N.B. An appraisal of sediment transport measurement in Ghanaian rivers. Challenges in African hydrology and Water Resources (Proceedings of the Harare symposium). IAHS Publ. no. 144. July 1984.

[Akrasi, 2005]. Akrasi S.A. The assessment of suspended sediment inputs to Volta Lake. Lakes & Reservoirs: Research and management 10: 179-186. 2005.

[Akrasi, 2011]. Akrasi S.A. Sediment Discharges from Ghanaian Rivers into the Sea. West-African Journal of applied ecology. Volume 18. 2011.

[d'Almieda, 1986]. d'Almieda G. A. A model for Saharan dust transport. J. Climatol. appl. Meteorol. 25: 903–916. 1986.

[Andah, 2003] Andah W.E.I, Giesen N. van de, Biney C.A. Water, Climate, Food, and Environment in the Volta Basin. Contribution to the project ADAPT: Adaptation strategies to changing environments. http://www.weap21.org/downloads/ADAPTVolta.pdf.

[Amos, 2004]. Amos K.J, Alexander J, Horn A, Pocock G.D, Fieldings C.R. Supply limited sediment transport in a high-discharge event of the tropical Burdekin River, North Queensland, Australia. Sedimentology 51:145-162. 2004.

[Ashbridge, 1995]. Ashbridge D. Processes of river bank erosion and their contribution to the suspended sediment load of the River Culm, Devon. Sediment and Water Quality in River Catchments pp. 229-245. 1995.

[Asselman, 1999]. Asselman N.E.M. Suspended sediment dynamics in a large drainage basin: the River Rhine. Hydrological Processes 13, 1437-1450. 1999.

[Awadzi, 2005]. Awadzi T.W, Breuning-Madsen H. Harmattan dust deposited in Ghana within 2000-2005.

[Barry, 2005]. Barry B, Obuobie E, Andreini M, Andah W, Pluquet M. The Volta River basin: Comparative study of river basin development and management. Comprehensive assessment of water management in agriculture. http://www.iwmi.cgiar.org/assessment/files_new/research_projects/River_Basin_Development_and_Management/VoltaRiverBasin_Boubacar.pdf.

[Boiten, 2008]. Boiten W. Hydrometry 3rd edition: A comprehensive introduction to the measurement of flow in open channels. CrC press/Balkema ISBN 0415467632. 2008.

[Brown, 1958]. Brown C.B. Sediment transportation. In: Rouse, H. (ed.) Engineering hydraulics, Wiley, New York. 1958.

[Brune, 1953]. Brune G.M. Trap efficiency of reservoirs. Trans. Am. Geoph. Union, Vol.34, no.3. 1953.

[Church, 1975]. Church M, Gilbert R. Proglacial fluvial and lacustrine environments, glaciofluvial and glaciolacustrine sedimentation. Soc. Econ. Paleontol. Minerol. (Spec. Publ.) 23:40-100. 1975.

[COB, 1993]. Coyne et Bellier. White Volta Development Scheme. Prefeasibility Study. Prefeasibility Report For Volta River Authority. February 1993.

[De Vriend, 2004]. Vriend H.J. de. Lecture notes CT3340 River Engineering. TU Delft. 2004.

[EH, 1967]. Engelund F, Hansen E. A monograph on sediment transport in alluvial streams. Teknisk Forlag, Kopenhagen. 1967.

[HAP, 2009]. Hydrogeological Assessment Project of the Northern Regions of Ghana. Interim Hydrogeological Atlas. Canadian international development agency. July, 2009.

[He, 2007]. He C, Breuning-Madsen H, Awadzi T.W. Mineralogy of dust deposited during the Harmattan season in Ghana. Danish Journal of Geograpy 107(1): 9-15. 2007.

[HKV, 2011a]. North Ghana sustainable development, disaster prevention and water resources management. Flood hazard assessment White Volta. Inception report. HKV Report PR2147. August 2011.

[HKV, 2011b]. North Ghana sustainable development, disaster prevention and water resources management. Flood hazard assessment White Volta. Field trip report and river characteristics. HKV Report PR2147. November 2011.

[HKV, 2012]. North Ghana sustainable development, disaster prevention and water resources management. Flood hazard assessment White Volta. Survey Report. HKV Report PR2147. January 2012.

[Jansen, 1979]. Jansen P. Ph. et al. Principles of River Engineering. The non-tidal alluvial river. Pitman London 1979.

[Kalu, 1979]. Kalu A. E. The African dust plume: Its characteristics and propagation across West Africa in winter. Saharan dust: Mobilization, transport, deposition pp.95–118. Wiley, New York. 1979.

[Klein, 1984]. Klein M. Anti clockwise hysteresis in suspended sediment concentration during individual storms. Catena 11: 251-257. 1984.

[Liebe, 2005]. Liebe J, van de Giesen N, Andreini M. Estimation of small reservoir storage capacities in a semi-arid environment: A case study in the Upper East Region of Ghana. Physics and Chemistry of the Earth 30 448-454. 2005.

[Ly, 1980]. Ly C.K. The role of the Akosombo dam on the Volta River in causing coastal erosion in Central and Eastern Ghana (West Africa). Marine Geology 37: 323-332. 1980.

[Lyngsie, 2011]. Lyngsie G, Awadzi T, Breuning-Madsen H. Origin of Harmattan dust settled in Northern Ghana - Long transported or local dust? Geoderma 167-168. November 2011.

[Mc Tainsh, 1980]. Mc Tainsh G. Harmattan dust deposition in northern Nigeria. Nature 286: 587–588. 1980.

[Mc Tainsh, 1982]. Mc Tainsh G, Walker P.H. Nature and distribution of Harmattan dust. Z. Geomorphol. N.F. 26: 417–435. 1982.

[Morris, 1997]. Morris G.L, Fan J. Reservoir Sedimentation Handbook: Design and management of dams, reservoirs and watersheds for sustainable use. McGraw-Hill, New York, USA. ISBN 0-07-043302-X. 1997.

[MPM, 1948]. Meyer-Peter E, Müller R. Formulas for bed load transport. Proc. IAHR, Stockholm, Vol. 2, paper 2, pp. 3964. 1948.

[Picouet, 2001]. Picouet C, Hingray B, Olivry J.C. Empirical and conceptual modelling of the suspended sediment dynamics in a large tropical African river: the Upper Niger river basin. Journal of hydrology 250: 19-39. 2001.

[Rodgers, 2007]. Rodgers C, van de Giesen N, Laube W, Vlek P.L.G, Youkhana E. The GLOWA Volta project: A framework for water resources decision-making and scientific capacity building in a transnational West African basin. Water Resources Management 21:195-313. 2007.

[Sarma, 1986]. Sarma J.N. Sediment transport in the Burhi Dihing River, India. Drainage basin sediment delivery, IAHS Publ. 159: 199-215. 1986.

[Sloff, 1991]. Sloff C.J. Reservoir sedimentation: a literature survey. Communications on hydraulic and geotechnical engineering, Report no. 91-2. Faculty of Civil Engineering, Delft University of Technology. ISSN 0169-6548. June 1991.

[Sloff, 1997]. Sloff C.J. Sedimentation in reservoirs. Doctoral thesis, Faculty of Civil Engineering, Delft University of Technology. ISBN 90-9010530-1. 1997.

[Spott, 1994]. Spott D, Guhr H. The dynamics of suspended solids in the tidally unaffected River Elbe as a function of flow and shipping. Preprints of the International Symposium on particulate matter in rivers and estuaries. Reinbek 21-25:267-273. March 1994.

[Tiessen, 1991]. Tiessen H, Hauffe H.-K, Mermut A.R. Deposition of Harmattan dust and its influence on base saturation of soils in northern Ghana. Geoderma 49:285-299. 1991.

[Van de Giesen, 2001]. Giesen N. van de, Andreini M, Edig A, Vlek P. Competition for water resources of the Volta basin. Regional Management of Water Resources. IAHS Publ. no. 268. 2001.

[Van Rijn, 1993]. Rijn L.C. van. Principles of sediment transport in rivers, estuaries and coastal seas. Agua publications, Amsterdam. 1993.

[Van Sickle, 1983]. Van Sickle J, Beschta R.L. Supply-based models of suspended sediment transport in streams. Wat. Resour. Res. 19:786-778. 1983.

[Walling, 1974]. Walling D.E. Suspended sediment and solute yields from a small catchment prior to urbanization. Fluvial processes in instrumented watersheds, Inst. Br. Geog. (Spec. Publ.) 6:169-192. 1974.

[Walling, 1977]. Walling D.E. Limitations of the rating curve technique for estimating suspended sediment loads, with particular reference to British rivers. Erosion and solid matter transport in inland wateres (Proceedings of the Paris symposium, July 1977). IAHS Pbul. 122: 34-48. 1977.

[Walling, 1978]. Suspended sediment and solute response characteristics of the river Exe, Devon, England. Research in Fluvial Systems. Geoabstracts, Norwich, pp. 169-197. 1978.

[Wilson, 2010]. Wilson J.R. Minerals and rocks. Richard Wilson & Ventus Publishing ApS. ISBN 978-87-7681-647-6. 2010.

[Wood, 1977]. Wood P.A. Controls of variation in suspended sediment concentration in the River Rother, West Sussex, England. Sedimentology, 24:437-445. 1977.

Appendix A: Sediment transport formulas

A.1 General parameters:

$$u_* = \left(\frac{\tau_b}{\rho}\right)^{\frac{1}{2}}$$ = shear velocity (m/s)

$$\tau_b = -\rho g h \frac{\partial z_w}{\partial x}$$ = bottom shear stress (N/m^2)

$$\theta = \frac{u_*^{\,2}}{g\Delta D} = \frac{hi}{\Delta D} = \frac{u^2}{C^2 \Delta D}$$ = Shields parameter (-)

A.2 Meyer-Peter and Müller formula

Meyer-Peter-Müller (MPM, 1948) relates to bed load exlusively. The formula is mainly of an experimental nature, with an absence of suspended load. The maximum value of $\mu\theta$ in their tests was 0.2, while the grain diameter D was larger than 0.4 mm. As indication the formula mainly applies in situations where w_s/u_* >1 (De Vriend, 2004).

$$s = D^{3/2}\sqrt{(g\Delta)} \cdot 8\left(Y^{-1} - 0.047\right)^{3/2}$$ = bed load transport (m^2/s)

$$Y = \frac{\Delta D}{\mu h i}$$ = flow parameter (-)

$$\mu = \left(C / C_{90}\right)^{3/2}$$ = ripple factor (-)

$$C_{90} = 18 \log \frac{12h}{D_{90}}$$ = Chezy coefficient based on D_{90} (-)

$$D = \overline{D} = \sum^{i} \left(p_i / D_i\right) \sum^{i} p_i$$ = characteristic grain size (m)

A.3 Engelund-Hansen formula

Engelund-Hansen (EH, 1967) refers to the total bed material load (suspended load + bed load). The formula is semi-empirical; the measuring range of θ and D used for verification of the formula is respectively 0.07 <θ<6 and 0.19 mm<D_{50}<0.93 mm. These boundary conditions can limit the area of application of the formula. The formula proves especially applicable for the total load of relatively fine material, in which the suspended load plays a vital role: w_s/u_*<1 (De Vriend, 2004).

$$s = D^{3/2}\sqrt{(g\Delta)}\cdot 8\left(Y^{-1}-0.047\right)^{3/2}\cdot 0.05Y^{-5/2}$$ = Total load transport (m^2/s)

$$Y = \frac{\Delta D}{\mu hi}$$ = Flow parameter (-)

$$\mu = \left(C^2/g\right)^{2/5}$$ = Ripple factor 9-0

D = Critical grain diameter = D_{50} (m)

A.4 Van Rijn

Van Rijn (Van Rijn, 1993) derived separate formulas for bed load and suspended bed material load; total load = bed load + suspended load.
The formula is based on material in the following range: 200 μm < D < 700 μm

$S = s_b + s_s$

Bed load:

$$s_b = \Phi_b \cdot \sqrt{g \Delta D_{50}{}^3}$$ = bed load transport (excluding the pores with a porosity of 0.4) (m^2/s)

$$\Phi_b = 0.053 \frac{T^{2.1}}{D_*^{0.3}}$$ for T<3 (-)

$$\Phi_b = 0.1 \frac{T^{1.5}}{D_*^{0.3}}$$ for T ≥3 (-)

Suspended load:

$$s_s = F \bar{u} h c_a$$ = suspended sediment transport (m^2/s)

$$c_a = 0.015 \frac{D_{50}}{a} \frac{T^{1.5}}{D_*^{0.3}}$$ = reference concentration (-)

$$F = \frac{(a/h)^{Z'} - (a/h)^{1.2}}{(1 - a/h)^{Z'} (1.2 - Z')}$$ = shape factor (-)

$$D_* = D_{50} \left(\frac{\Delta g}{v^2} \right)^{\frac{1}{3}}$$ = particle diameter (-)

$$T = \frac{\tau_b{}' - \tau_{b,cr}}{\tau_{b,cr}}$$ = bed-shear stress parameter (-)

$$\tau_b' = \rho g \left(\frac{\bar{u}}{C'} \right)^2$$ = current–related effective bed-shear stress (N/m^2)

$$u_* = \frac{\sqrt{g}}{C} \bar{u}$$ = current-related overall bed-shear velocity (m/s)

$$C' = 18 \log \left(\frac{12h}{3D_{90}} \right)$$ = grain-related Chézy coefficient (m$^{0.5}$/s)

$$C = 18 \log \left(\frac{12h}{k_s} \right)$$ = overall Chézy coefficient (m$^{0.5}$/s)

$$\tau_{b,cr} = (\rho_s - \rho) g D_{50} \theta_{cr}$$ = critical bed-shear stress (N/m^2) according to Shields

$$\theta_{b;cr} = 0.04 D_*^{-0.1}$$ = Shields critical shear stress parameter (-)

$$Z' = Z + \Psi$$ = suspension number (-)

$$Z = \frac{w_s}{\beta \kappa u_*}$$ = suspension number (-)

$$\Psi = 2.5 \left(\frac{w_s}{u_*} \right)^{0.8} \left(\frac{c_a}{c_0} \right)^{0.4}$$ = stratification correction (-)

$$\beta = 1 + 2 \left(\frac{w_s}{u_*} \right)^2$$ = ratio of sediment and fluid mixing coefficient (β_{max} = 2) (-)

$$D_s = \left[1 + 0.011 (\sigma_b - 1)(T - 25) \right] D_{50}$$ = representative particle size of suspended sediment (m)
$D_s = D_{50}$ for $T \geq 25$

$$\sigma_s = \frac{1}{2} \left(\frac{D_{84}}{D_{50}} + \frac{D_{50}}{D_{16}} \right)$$ = geometric standard deviation of bed material (-)

In which:

s_s	= volumetric current-related suspended load transport (m^2/s)
u	= depth-averaged velocity (m/s) = Q/A
h	= water depth (m)
a	= reference level (m), a = ½ Δ or a =k_s
k_s	= overall roughness height (m)
Δ	= bed form height (m)
D_{50}	= median particle diameter of bed material (m)
D_{16}, D_{84}, D_{90}	= characteristics diameter of bed material (m)
w_s	= fall velocity of suspended sediment (based on d_s-value)
D_s	= representative particle size of suspended sediment (m)
c_0	= maximum concentration (=0.65)
S	= specific density (ρ_s /ρ)
ρ_s	= sediment density (2650 kg/m^3)
ρ	= fluid density (= 1000 kg/m^3)
v	= kinematic viscosity coefficient (= 1 $\cdot 10^6$ m^2/s)
κ	= constant von Karman (=0.4)
g	= acceleration of gravity (= 9.81 m/s^2)

Appendix B: Fieldwork

B.1 Research questions

The main objective of the field study (September–October 2011) was to make an estimation of the total yearly sediment load and the composition of the sediment and riverbed material. Another objective was to get insight into the morphological behaviour of the catchment area. In order to answer these questions, during the field study the following sub questions have been investigated:

Suspended sediment

- What is the quantity of sediment transported during the flood period in 2011?
    - What is the variation of the sediment concentration over the cross-section?
    - What is the relation between discharge and suspended sediment transport?
    - What is the proportion of wash load and bed material load in the suspended sediment?
    - What is the relation between depth-integrated measurements and surface-dip measurements?

Bed load

- What is the quantity of bed load transport during the flood period in 2011?
    - What is the variation of bed load over the cross-section?
    - Which theoretical formula is most suitable for predicting bed load?

Red Volta and White Volta branches

- What is the proportion of sediment transport in each river branch?
    - How do the sediment concentrations in the White and Red Volta branch compare?
    - How do the discharges in the White and Red Volta branch compare?

Erosion

- Is there a relation between Harmattan dust deposition and erosion of the catchment area?
    - Could sediment deposited on the floodplain be characterized as Harmattan dust?
    - What is the origin of sediment deposited on the banks?

Morphology

- Could the morphological behaviour of the catchment be explained based on the results and the observations and available literature of earlier studies?

B.2 Method

B.2.1 Measurement locations

Pwalugu

The measurement location of Pwalugu is a bridge over the White Volta River near the village of Pwalugu. During the period of fieldwork the main channel width is 80-100 m, the water depth is 2-7 m and the average flow velocity is 0.6-1.3 m/s. The weather in Pwalugu was predominantly dry with an occasional thunderstorm in the evening. The land use surrounding the measurement site is mainly cropland and open savannah woodland. The area is flat and the soil geology consists of biotite tonalite (HAP, 2009).

Figure B.1 White Volta River, Pwalugu

Figure B.2 Steep rightern bank, smooth left

The river bends slightly to the left at the location of the bridge, leading to an eroded steep right bank and a shallow inner left bank. Flow velocities are lowest on the left side (Figure B.1 and Figure B.2). There is a gauging station present with a staff gauge and an automatic water level recorder on the bridge (Figure B.3, Figure B.4 and Figure B.5).

Figure B.3 Pwalugu bridge

Figure B.4 Automatic water level recorder

Figure B.5 Staff gauge

A gauge reader records the water levels twice a day. This person lives in the village of Pwalugu and is commissioned by the VRA. The automatic water level recorder is not working. There is a stage-discharge relation available (HKV, 2011b), as shown in Figure B.36. During the flood year of 2011, three peaks occurred (Figure B.6). Upon arrival in early September the first flood wave of 2011 had just passed. While the water levels were dropping, sediment was deposited on the left riverbank, where flow velocities are low (Figure B.7 and Figure B.8). Within the period of measurements there were two more flood waves. After every peak sediment depositions were observed, but not as much as after the first peak. A canoe survey, conducted a few kilometres downstream of the bridge, shows that these sediment depositions occur frequently along the river reach. Most of the times the flooded land is situated in the inner bend of the river.

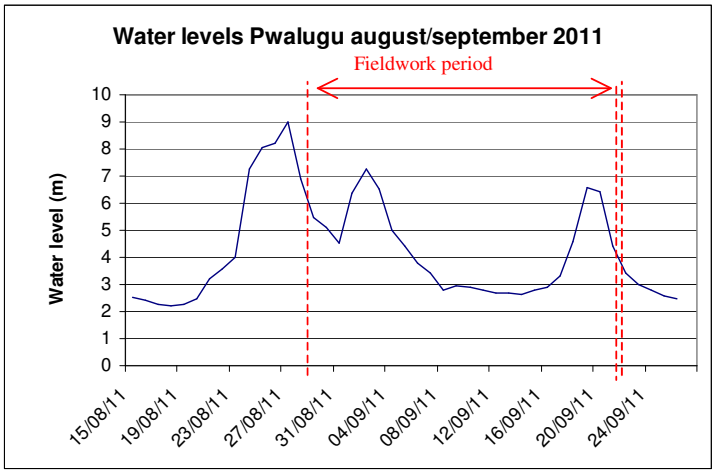

Figure B.6 Water levels Pwalugu August/September 2011

Figure B.7 Sediment deposition on left riverbank

Figure B.8 Four cm of deposited sediment

Nangodi

The measurement location is the bridge over the Red Volta River on the road Bolgatanga–Zebilla (Figure B.9). The main channel width is 25-30 m, the water depth 1-3 m. The water is fast flowing and turbulent with flow velocities of 1-1,5 m/s. A rating curve is available, but the gauging station has been washed away.

Figure B.9 Red Volta (Nangodi)

Figure B.10 Sediment deposition on the riverbank

The riverbed mainly consists of granite rocks. Along the river there are moderate hill slopes with small rocky streams draining into the river. These streams had fallen dry during the visits. There is no cropland along the banks, as is the case near Pwalugu, but dense vegetation instead. In the surrounding area there is rain forest.

After the first flood peak, sediment depositions on the riverbanks have been observed (Figure B.10). After the second flood peak, all sediment had disappeared and there appeared to be no deposition of new sediment.

Yarugu

The measurements are carried out from the bridge on the road between Zebilla and Bawku. Here, the main channel of the river is very wide (± 150 m) and shallow (0-2m) with low flow velocities (± 0.5 m/s). A sand bank is present in the middle of the river, dividing the river into two channels. This is probably caused by the changing of the main channel towards the right bank, due to large-scale morphological behaviour (Figure B.11 and Figure B.12). The surroundings are relatively flat savannah woodland and there are crops cultivated along the riverbanks.

Figure B.11 White Volta (Yarugu)

Figure B.12 Bridge over White Volta (Yarugu)

After the first flood, sediment deposition has been observed on the riverbanks but not as much as in Pwalugu (Figure B.13 and Figure B.14). After the 2nd flood the sediment had disappeared and there had not been any new deposition.

Figure B.13 Mud depositions at Yarugu

Figure B.14 Few centimetres of fine sediment on top of a sand layer

B.2.2 Frequency of measurements

Different types of measurements were executed:
- Depth-integrated measurements (objective: suspended sediment transport)
- Surface-dip measurements (objective: investigation of correction factor for surface-dip)
- Bed material measurements (objective: bed load transport)
- Riverbank material measurements (objective: origin of deposited sediment)
- Discharge measurements (objective: calculation sediment load)

The period of measurements is 29-8 till 23-9. Pwalugu has been visited most frequently (15 times). Nangodi and Yarugu have been visited once every week (4 times in total). The number of measurements taken during the fieldwork is presented in Table B.1.

Table B.1 Measurements taken during fieldwork 2011

Date	**Location**	**Depth-integrated suspended sediment**	**Surface dip suspended sediment**	**Bed material sample**	**Riverbank sample**	**Flow velocity measurements**
29-8	Pwalugu		1		1	
31-8	Pwalugu	3				
1-9	Pwalugu	3		1		
3-9	Pwalugu	5				
4-9	Nangodi, Yarugu	4 3			1 1	1 2
5-9	Pwalugu	3	1	1	1	3
6-9	Pwalugu	2		2		
9-9	Pwalugu	8			3	3
10-9	Nangodi, Yarugu	6 5		 1		2 3
17-9	Pwalugu	7	3			3
18-9 morning	Pwalugu	7				3
18-9 evening	Pwalugu	4	1			3
19-9	Pwalugu, Nangodi, Yarugu	7 4 4				3 2 3
20-9	Pwalugu	7	2			3
21-9	Pwalugu	6	2			
22-9	Pwalugu	6		3	3	3
23-9	Nangodi, Yarugu, Pwalugu	2 2		 2	2 2 3	2 2

B.2.3 Discharge measurements

The discharge is calculated by the velocity-area method (Luxemburg, 2007). This method multiplies the river cross-section with the flow velocity. For this reason, cross-sectional measurements and stream flow measurements have been conducted. The velocity measurements have been taken at three spots along the cross-section. The discharge is calculated with the following formula:

$$Q = \sum_{i=1}^{n} u_i \cdot A_i$$

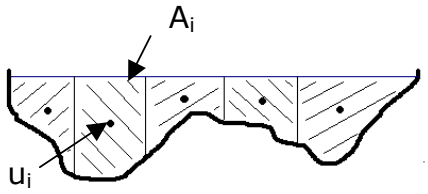

in which every velocity measurement (u_i) should be representative for the corresponding section (A_i). The number of sections depends on the local situation (page 90 and 91).

B.2.3.1 Cross-sectional measurements

For all measurement locations, the following procedure has been followed:

- First of all, the bridges have been discretized; One-meter marks were written with a waterproof marker on the railing of the bridge.
- The bottom depth relative to the bridge has been determined by lowering the suspended sediment sampler (10 kg) down to the bottom. On the suspension line a scale had been drawn, so the depth could be read easily (Figure B.15).
- The suspended sediment sampling equipment (10 kg) was lowered to the water level. First, the distance between the water level and the railing of the bridge was measured. Second, the sampler was lowered to the bottom of the river and the distance between the riverbed and the railing of the bridge was measured. The water depth was calculated by subtraction of these measurements.
- The measurements were preferably carried out at low flow conditions, because in fast flowing water the sampling device would be carried forward by the stream velocity, making depth estimation more difficult.
- In case the line was not suspended vertically due to high flows, the following correction formula has been used:

  $$x = c \cdot \cos\left(\arctan\left(b/a\right)\right)$$

  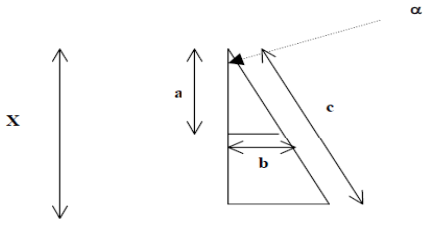

  in which:
  x = depth to bottom (m)
  a = depth to water level (measured) (m)
  b = horizontal distance where rope enters water (estimated) (m)
  c = length rope to bottom (m)

- The distance between the railing of the bridge and the water level has been measured at both ends of the bridge, in order to estimate the slope of the bridge. It is assumed that the water level is constant in the cross-section, because of the low flow velocities. For all bridges it appeared that the bridge is horizontal.

Figure B.15 Measurement of cross-section using the suspended sediment sampling device.

The cross-sections measured at Pwalugu, Nangodi and Yarugu are presented in Figure B.16, Figure B.17 and Figure B.18.

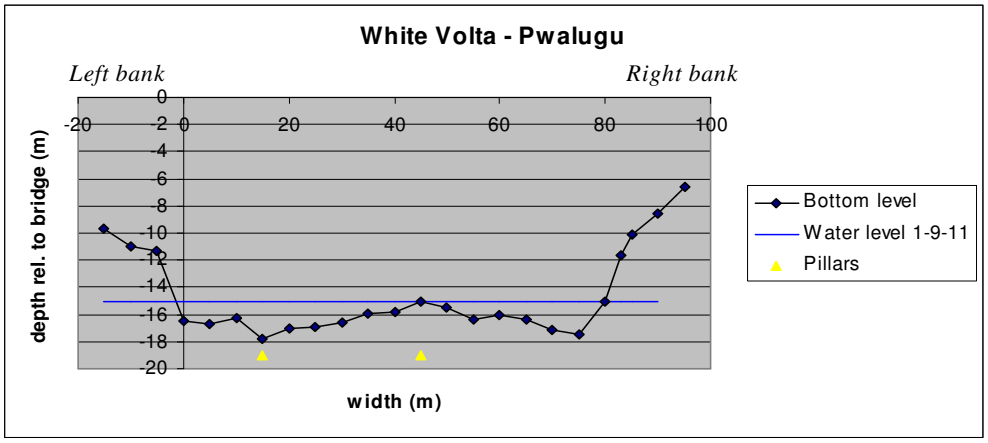

Figure B.16 Cross-section Pwalugu (White Volta) looking downstream

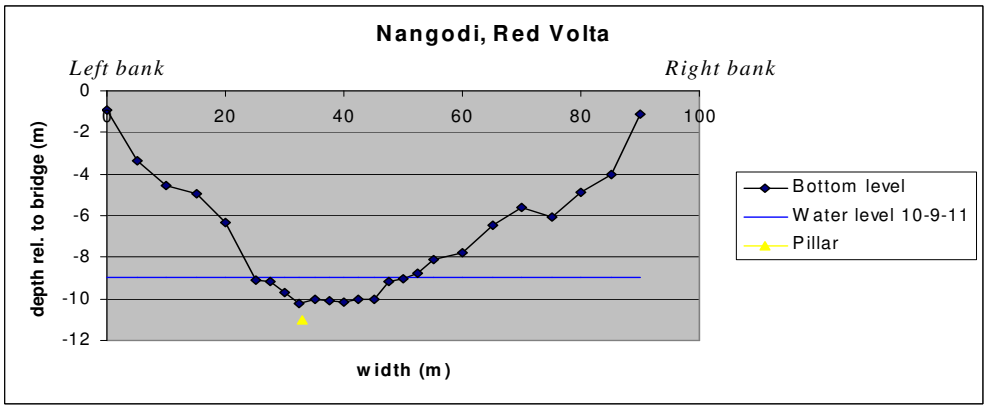

Figure B.17 Cross-section Nangodi (Red Volta) looking downstream

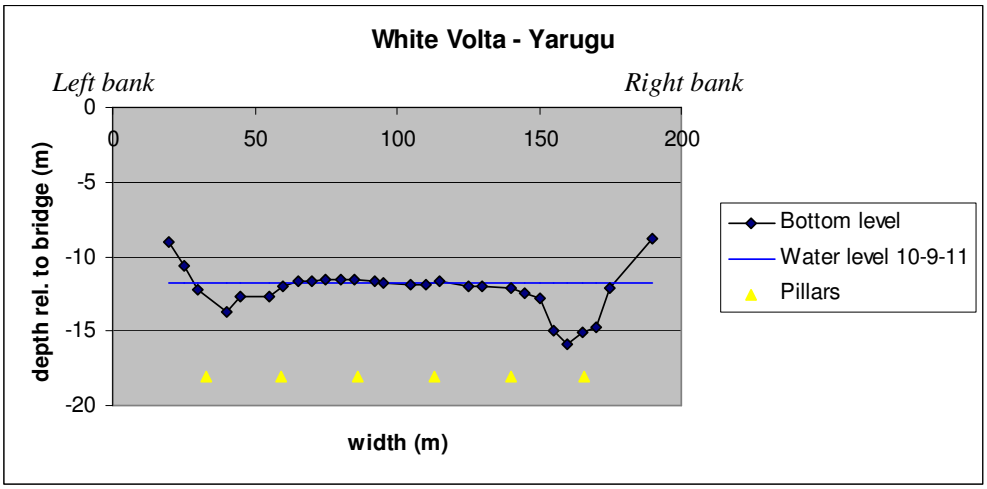

Figure B.18 Cross-section Yarugu (White Volta) looking downstream

B.2.3.2 Velocity measurements

The flow velocity has been measured using an improvised float method (Figure B.19). The float consisted of one empty bottle and a bottle filled with concrete tied together at 0.6 * the water depth. At this location underneath the water level, theoretically the average flow velocity occurs. The empty bottle is attached to a 75 m thin line. The velocity can be calculated by calculating the time it takes to unroll the entire line.

Figure B.19 Improvised float

Pwalugu

The bridge is built on pillars, which obviously affect the flow pattern as there is much turbulent movement around them. Therefore, the velocity measurements have been taken exactly in between of the pillars, where the pillars least affect the flow. The sections are not equally sized, but it is estimated that the flow at each measurement site represents the corresponding flow section. For Pwalugu, the three measurement sites are indicated in Figure B.20.

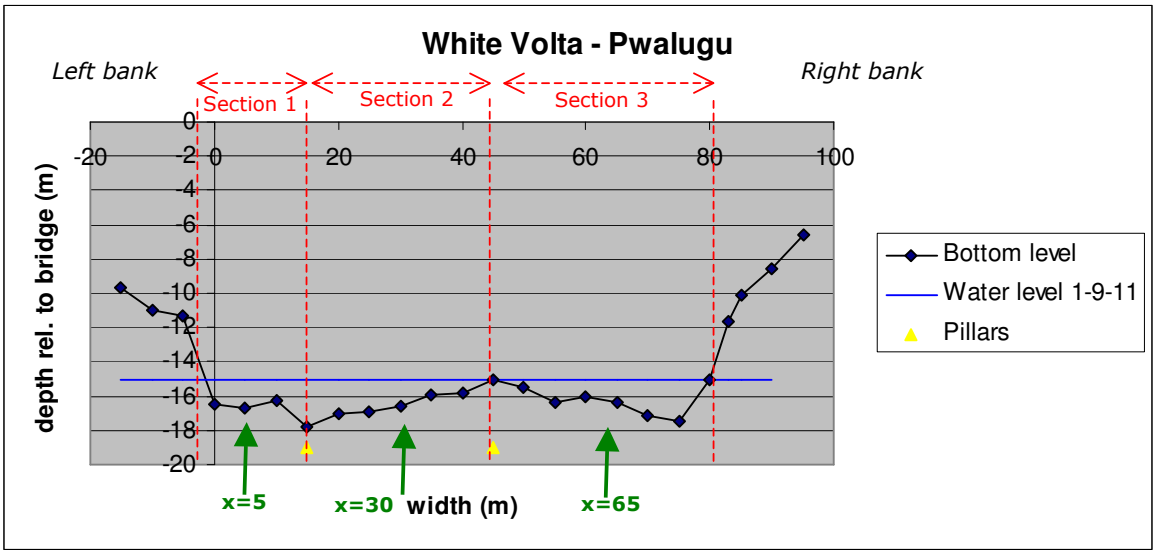

Figure B.20 Measurement locations Pwalugu

Nangodi

The bridge of Nangodi is built on one pillar, dividing the river into two sections. As the river is relatively narrow, only these two sections have been considered (Figure B.21).

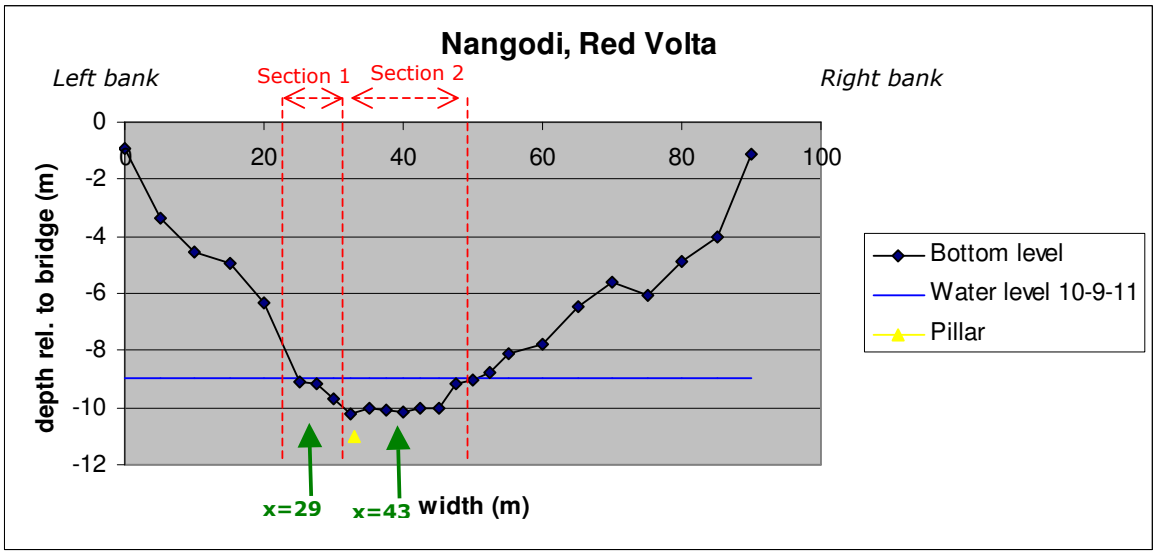

Figure B.21 Measurement locations Nangodi (green arrows)

Yarugu

The bridge is built on 6 pillars, which do influence the flow pattern but not as much as in Pwalugu or Nangodi because the flow velocity is much lower. In the middle section the riverbed is elevated. At low water levels a sand bank appears in the middle section, which divides the river into two flow channels (Figure B.22). The velocity measurements were taken in the centre of these channels. Unfortunately these points are located close to a pillar, but the flow doesn't seem to be influenced much at these points. The situation of two separate channels lasts until 50 m downstream of the bridge. At that point the sandbank has disappeared and the channels have merged together. This indicates that the flow velocity is not uniform along the longitudinal distance of measurement (75 m). Therefore the discharge measurements could be inaccurate.

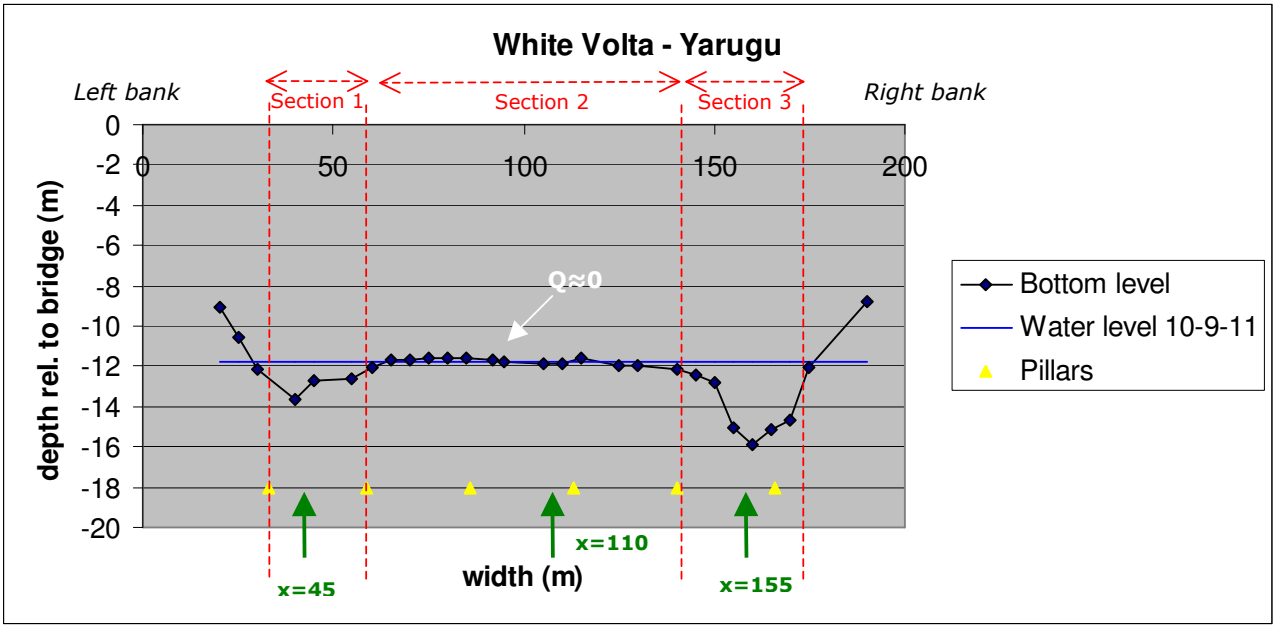

Figure B.22 Measurement locations Yarugu (green arrows)

B.2.4 Suspended sediment measurements

B.2.4.1 Sampling

For suspended sediment measurements, a depth-integrated (DI) sampling device has been used. By lowering this sampler from the water surface to the riverbed and back up again, a water sample of the entire depth could be taken, giving a depth integrated suspended sediment concentration in the vertical. The sampling equipment was a US DH 59 depth-integrating sampler containing a pint sized sampling bottle (0,48L) and an intake nozzle (Figure B.23). The time it takes to fill up the bottle depends on the water flow and was determined experimentally. Generally, the time it took to fill up the bottle was ± 1 minute.

Figure B.23 D-I suspended sediment sampler

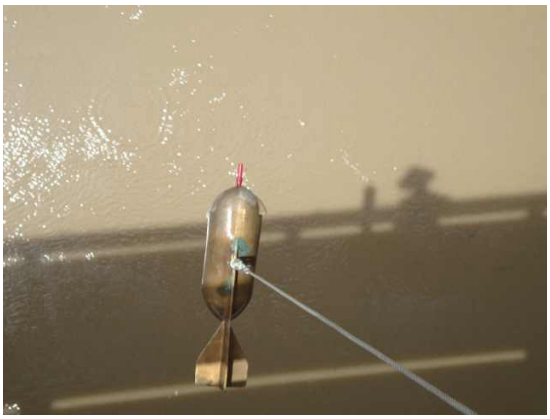

Figure B.24 Suspended from the bridge

The sampling device was suspended from the bridge at a steady rate until it reached the bottom. Then it was instantly reversed and slowly pulled back to the water surface within the required time (Figure B.24). To keep track of time, a voice-recording of the author counting was played. The samples were stored in 500 mL plastic water bottles. The measurement locations were the same spots as where velocity measurements were taken (Figure B.20, Figure B.21 and Figure B.22), so for Pwalugu and Yarugu there were three spots and for Nangodi there were two. Several measurements at every spot were taken in order to get a higher accuracy.

B.2.4.2 Analysis

The samples were analysed in the WRI-lab in Accra, using the evaporation method. This method is not a standard method and will therefore be described in detail.

- In each sample, one drip of a 50 % nitric acid solution has been added as a coagulant to enhance flocculation and sedimentation.
- The samples were stored for 5 days to wait for the sediment to settle. Application of Stokes formula on a settling height of 0.3 m shows that after 5 days all particles with $D<0.8$ μm had been settled. A portion of smaller particles would settle within 5 days: for many particles the starting height was lower than 30 cm, moreover the sedimentation rate increased due to the coagulant.
- After 5 days the sediment had been settled at the bottom of the water bottle (Figure B.25).

- The supernatant water was decanted in a beaker (Figure B.26). The sediment remained at the bottom of the bottle (Figure B.27).
- The remaining sediment was resuspended by adding some water and shaking the bottle (Figure B.28). Subsequently, this was poured into a 50 mL beaker (Figure B.29). The bottle was rinsed with some of the decanted water.
- The beaker was emptied in a Pyrex disc (Figure B.30) of which the tare weight had been measured. Funnel and beaker were rinsed with the decanted water, which had been taken with a pipette. The amount of water was chosen in a way that the total volume of liquid in the disc became 50 mL.
- The total volume of decanted water from the beaker is recorded. This was the total volume of water used, together with the 50 mL in the Pyrex disc. This value has been used to calculate the concentration of material that would still be in suspension ($D < 0.8$ µm).
- The Pyrex discs were dried in the oven for 3 hours at 105-110 °C (Figure B.31). The water evaporated and sediment remained at the bottom of the discs (Figure B.32).
- The beakers were weighed again and the total amount of sediment was calculated by subtracting the tare weight of the discs. The volume has been calculated by dividing the dry sediment by the total volume of the sample.

The sediment concentration of the supernatant water has also been analysed following the same procedure. This concentration appeared to be negligible, indicating that almost all sediment had indeed been settled.

Figure B.25 After 5 days the sediment has settled to the bottom of the water bottle.

Figure B.26 The supernatant water is decanted into a beaker.

Figure B.27 The sediment remained at the bottom of the bottle.

Figure B.28 The sediment is resuspended by shaking the bottle.

Figure B.29 The suspension is poured into a 50mL beaker.

Figure B.30 The small beaker is emptied in a pyrex disc.

Figure B.31 The pyrex discs are dried in the oven for 3 hours at 110°C

Figure B.32 The beakers containing dry sediment.

B.2.5 Bed material measurements

B.2.5.1 Sampling

Bed material measurements were carried out using an Ekman Birge Bottom sampler (Figure B.33 and Figure B.34). With a suspension line, the sampler was lowered to the riverbed where it grabbed 1-2 L of bottom material (sand). The samples could only be taken during low flow conditions, otherwise the device could not be suspended vertically.

Figure B.33 Bottom sampler

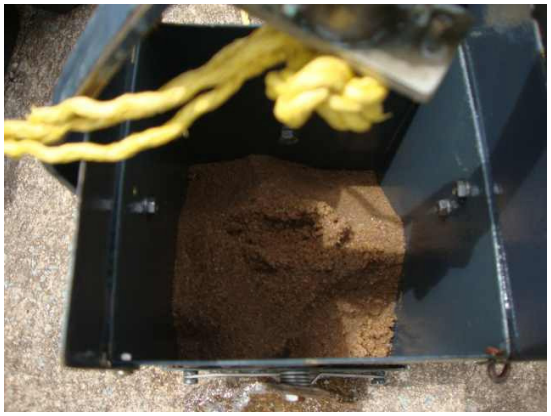

Figure B.34 Bottom material

B.2.5.2 Analysis

Texture-analysis of the sand samples took place in the WRI-laboratory in Accra. The particle size distribution was determined using the dry sieving method described in the British standard procedures (BS 1377: part 2:1990).

- Due to a renovation of the WRI laboratory, the samples could not be dried in the oven. Instead, they were dried for 2 days in open air (Figure B.35). Wind was very weak, so mixing of samples due to wind is considered negligible. Overnight the samples were stored inside the building.

Figure B.35 Air-drying of the riverbed and riverbank samples

- The sand samples were sieved through standard sieves (Table B.2 and Figure B.36).

Table B.2 Dry sieving method

	Mesh size (mm)	Material retained on sieve
1	5	Gravel
2	2,5	very coarse sand
3	1,25	coarse sand
4	0,63	coarse sand
5	0,5	medium sand
6	0,315	medium sand
7	0,25	fine sand
8	0,16	very fine sand
9	0,071	coarse silt
10	0,05	coarse silt
11	Bottom	medium silt, fine silt and clay

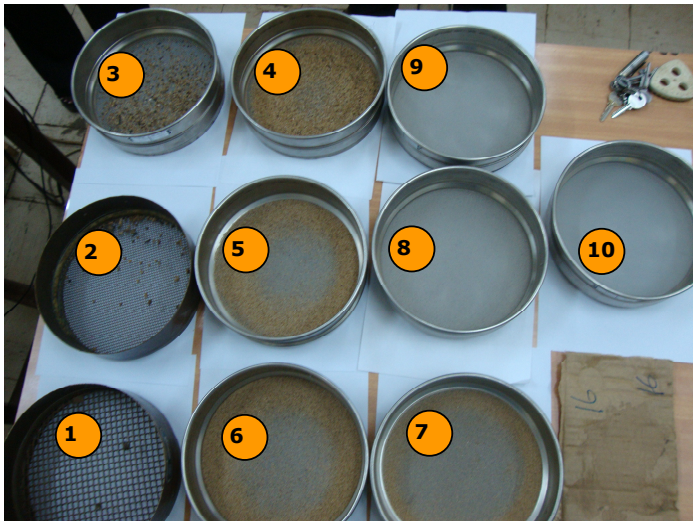

Figure B.36 Result after sieving

- For every sample the D_{84} was estimated and the amount of material to be sieved was selected such that normal accuracy would be reached, based on Figure B.37 (Jansen, 1979). For the White Volta River the D_{84} appeared to be in the range of 0.5-3 mm. For the coarsest samples, the sample size should be higher than 300 g. This was the case for all samples.

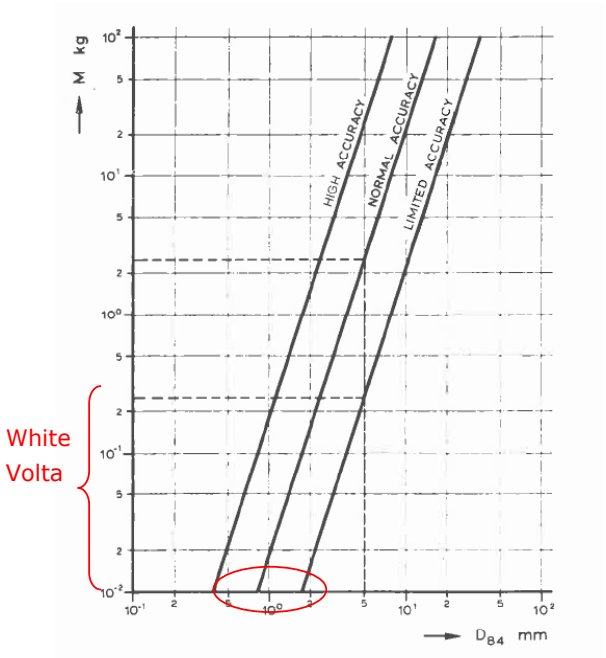

Figure B.37 Accuracy of dry sieving method (Jansen, 1979)

B.2.6 Riverbank samples

B.2.6.1 Sampling

After every flood peak soil samples have been collected from the riverbank. Using a spade the thickness of the sediment layer has been examined and the top few centimetres have been collected (Figure B.38).

Figure B.38 Collection of deposited sediment on the riverbank

B.2.6.2 Analysis

The samples were air-dried in Accra and transported to the Netherlands, where they were analysed on texture and mineralogy in the laboratories of soil mechanics and mechanical engineering at Delft University of Technology.

Texture

The riverbank samples consisted of clay, silt and sand. The particle size distribution in the clay and silt range (D<0.65 mm) has been analysed with the hydrometer method. Particles in the sand range (D>0.65 mm) were separately analysed by dry sieving. The analysis is conducted following a standard procedure described in British standard procedures (BS 1377: part 2:1990).

The method is summarized as follows:

- The dried riverbank samples have been dissolved in a dispersing solution in order to detach grains sticking to each other.
- The solution has been filtered through a 0.65 mm sieve where all sand particles have been retained. The sand fraction was dried in the oven and afterwards analysed by dry sieving.
- The suspension containing clay and silt particles has been transferred into a cylinder and was filled up to 1000 mL using distilled water. The density of the liquid has been monitored with a hydrometer. The sediment settled to the bottom and the density of the liquid decreased. The particle size distribution has been calculated using Stokes law.

Organic material has not been removed from the samples, as the amount is considered negligible. It is expected that the riverbank samples did not contain much organic material, because the material had only been deposited recently, so there has been not much time to accumulate organic material.

Mineralogy

With the x-ray diffraction method, riverbank samples have been analysed on mineralogy. Subsequently a semi-quantitative determination has been done in order to tell the quantity of minerals in each sample. The methods are further explained in Appendix H.

B.3 Results

B.3.1 Discharge

Pwalugu

The discharges measured with the method described in § B.2.3.2 in Pwalugu are presented in Table B.3.

Table B.3 Discharges measured in Pwalugu

Date	Section	Velocity (m/s)	Area per section (m^2)	Discharge per section (m^3/s)	Total discharge (m^3/s)	Total area (m^2)	Average velocity (m/s)
5/9/2011	1	0,34	87	29,6	238,8	365	0,65
	2	0,87	143	124,4			
	3	0,51	165	84,1			
7/9/2011	1	0,36	69	24,8	240,7	312	0,77
	2	0,68	113	76,8			
	3	1,07	130	139,1			
9/9/2011	1	0,34	61	20,7	165.6	275	0,60
	2	0,65	99	64,4			
	3	0,7	115	80,5			
17/9/2011	1	0,48	66	31,7	216,1	298	0,73
	2	0,80	108	86,4			
	3	0,79	124	98,0			
18/9/2011 morning	1	0,38	86	32,7	350,1	390	0,90
	2	1,06	141	149,5			
	3	1,03	163	167,9			
18/9/2011 evening	1	0,47	114	53,6	524,6	511	1,06
	2	1,23	181	222,6			
	3	1,15	216	248,4			
19/9/2011	1	0,36	135	48,6	521,6	577	0,90
	2	1,07	201	215,1			
	3	1,07	241	257,9			
20/9/2011	1	0,36	134	48,2	501,5	566	0,89
	2	1,06	200	212,0			
	3	1,04	232	241,3			
22/9/2011	1	0,51	69	35,2	225,2	312	0,72
	2	0,75	113	84,78			
	3	0,81	130	105,3			

The measured discharges for Pwalugu can be compared to discharge measurements carried out by Bayor (HKV, 2011b) (Figure B.39). From the measurements of Bayor it can be seen that hysteresis effects are significant at Pwalugu. The Q-h relation (red line) is based on measurements during rising stages. It is well visible that discharges are ± 100 m^3/s lower during falling stages with the same water level. The measurements carried out during the 2011 fieldwork, fit the curve well. Even the hysteresis effect is visible, as measurements during the rising stage lie on the red line, and measurements during the falling stage are in the left side of the cloud, except for one. The improvised float method appears to give accurate results. The measured values are used for calculation of the sediment load.

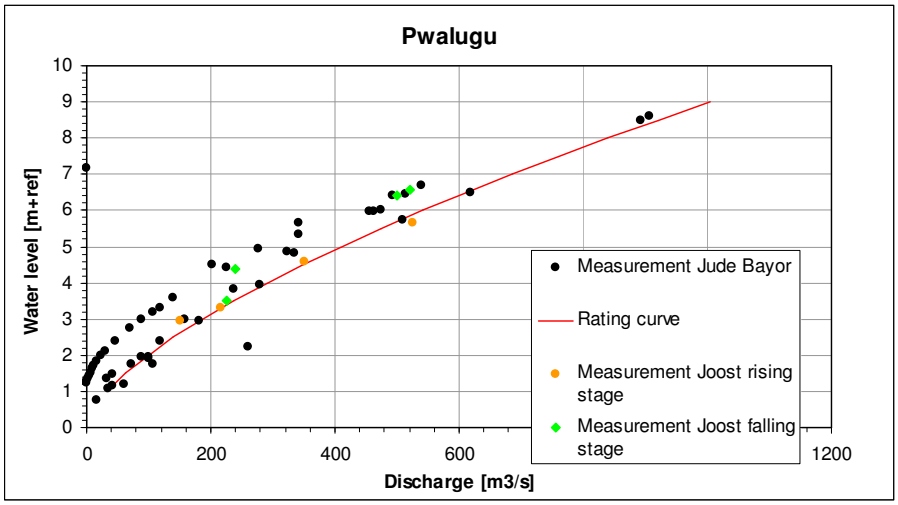

Figure B.39 Stage-discharge measurements carried out by Jude Bayor supplemented with those carried out by the author

The distribution of velocity at the three sections is presented in Figure B.40. As expected, the lowest flow velocities occur in the leftern section and the highest flow velocities occur either in the middle section or in the rightern section.

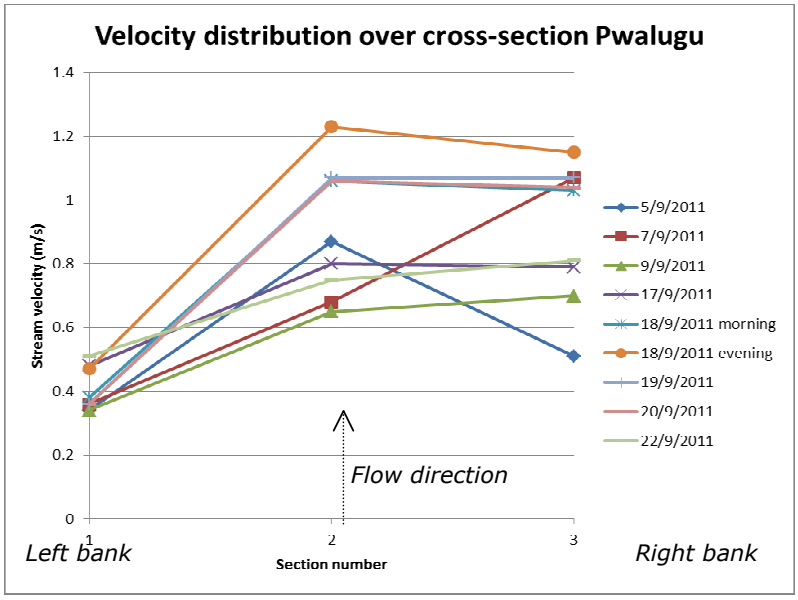

Figure B.40 Velocity distribution over cross-section in Pwalugu

Nangodi (Red Volta)

The discharges measured in Nangodi are presented in Table B.4. The discharge measured at September 4th is least accurate, as it is based on only one measurement.

Table B.4 Discharges measured in Nangodi

Date	Section	Velocity (m/s)	Area per section (m^2)	Discharge per section (m^3/s)	Total discharge (m^3/s)	Total cross-sectional area (m^2)	Average velocity (m/s)
4/9/2011	1	-	15	22,5	90	60	1,5
	2	1,5 m/s	45	67,5			
10/9/2011	1	0,75	10	7,5	44	43	1,03
	2	1,12	33	37,0			
19/9/2011	1	1,23	13,0	16,0	71	54	1,31
	2	1,34	41,2	55,2			
23/9/2011	1	1,30	4,0	5,2	22	20	1,12
	2	1,07	16,0	17,1			

Yarugu

The discharges measured in Yarugu are presented in Table B.5.

Table B.5 Discharges measured in Yarugu

Date	Section	Velocity (m/s)	Area per section (m^2)	Discharge per section (m^3/s)	Total discharge (m^3/s)	Total cross-sectional area (m^2)	Average velocity (m/s)
4/9/2011	1	0,60 m/s	36	21,6	89	133	0,67
	2	-	15	9,0			
	3	0,71 m/s	82	58,2			
10/9/2011	1	0,64	53	33,9	89	139	0,64
	2	-	0	-			
	3	-	86	55,0			
19/9/2011	1	0,76	54	41,0	168	211	0,80
	2	0,75	55	41,3			
	3	0,84	102	85,7			
23/9/2011	1	0,53	49	26,0	81	128	0,63
	2	-	-	-			
	3	0,69	79	54,5			

Comparison

The sum of the discharges measured in Yarugu and Nangodi can be compared with the discharge in Pwalugu, in order to estimate the relative contribution of the Red Volta to the discharge of the White Volta (Table B.6). To be able to compare the discharge the time lag, after which the water reaches Pwalugu, has been calculated. The velocity is chosen at 1 m/s, as

this is the average velocity during the field research in the White Volta River. The distance of the trajectories Yarugu-Pwalugu and Nangodi-Pwalugu are 150 and 115 km (HKV, 2012). The time lag is therefore ± 1.5 day. The discharge at Pwalugu is derived from interpolation (time of measurement plus 1.5 day).

Table B.6 Comparison discharge Yarugu and Nangodi

Date	Discharge Yarugu (m^3/s)	Discharge Nangodi (m^3/s)	Summed discharge (m^3/s)	Discharge Pwalugu (m^3/s) (timelag of 1.5 day)
4/9/2011	89	90	179	241
10/9/2011	89	44	133	160
19/9/2011	168	71	239	501
23/9/2011	81	22	103	210

The discharge in Yarugu is on average 107 m^3/s and the discharge in Nangodi is on average 57 m^3/s. The variation is quite high: the discharge in Yarugu ranges from 1 to 4 times the discharge in Nangodi. The average contribution of the Red Volta and White Volta branch are listed in Figure B.41.

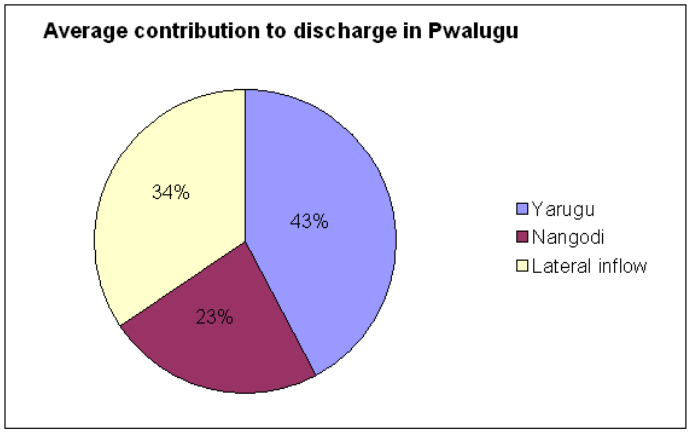

Figure B.41 Average contribution to discharge in Pwalugu

B.3.2 Suspended sediment

B.3.2.1 Pwalugu

The suspended sediment measurements have been taken at the same points as the velocity measurements (x = 5 m, x= 30 m and x= 65 m) (Figure B.20). The variation of sediment concentrations in the three sections is presented in Figure B.42.

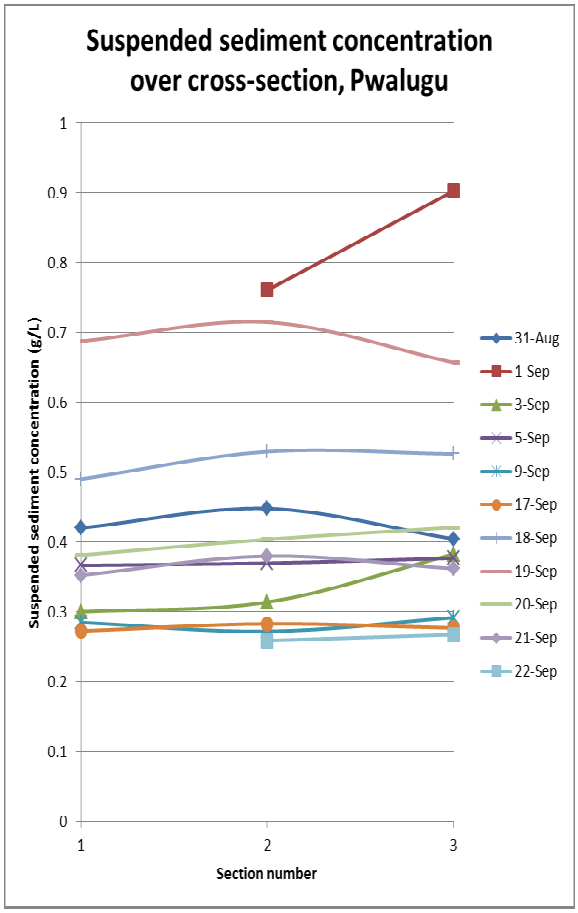

Figure B.42 Suspended sediment concentration over cross-section, Pwalugu

In general, the concentration is quite constant within the cross-section. The extreme value of September 1st occurred during high flow. There had been only one measurement in section 3, so this value is quite inaccurate. The measurements in section 2 are most reliable, as on this location most repetitive measurements have been carried out. The suspended sediment is calculated with the following formula:

Average sediment concentration = $\sum_{i=1}^{3} A_i \cdot c_i$

With:
A_i = Area section i / Total area
c_i = concentration in section i

The Total area = 85 m.
The sectional areas for sections 1, 2 and 3 are respectively 20, 30 and 35 m.

In some cases one or more measurements are missing. In that case, the available measurement is multiplied by a larger sectional area. As the suspended sediment measurements are not varying too much over the cross-section, this is considered permissible. The sediment concentration is plotted versus discharge in Figure B.43.

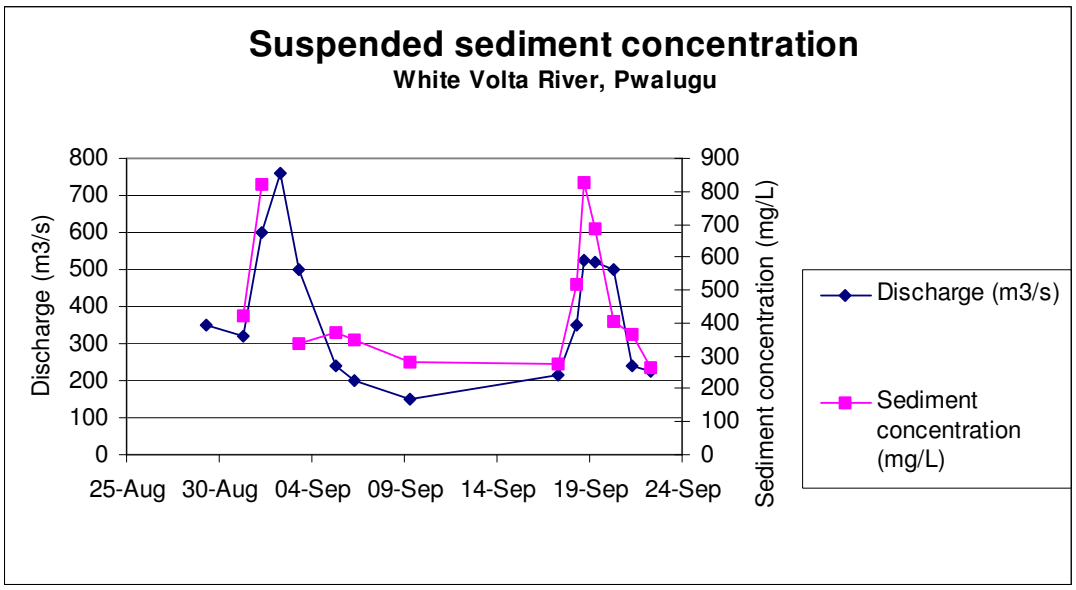

Figure B.43 Sediment concentration and discharge in Aug/Sep 2011, Pwalugu

The following is observed:
- Suspended sediment peaks are very sharp. The concentration peaks during rising stages and drops very fast as soon as the discharge drops.
- The measured concentrations are in the range of 200-800 mg/L.
- The sediment concentration on 3 September was higher than on 31 August, while the discharge was lower. This indicates a hysteresis effect: during rising stages, the sediment concentration is higher than during falling stages.

Note: On the day of maximum discharge (2 September) no sediment measurements were taken. Based on observations from the bridge it was observed that sediment concentrations on that day were higher than any other day. Therefore it is estimated that the sediment concentration would have reached a maximum on 2 September 2011.

The sediment load is calculated by the following formula:

*Sediment load = Sediment concentration * Discharge [kg/s]*

In case the discharge was not measured, the discharge was estimated from the stage-discharge relation in Figure B.39, taking into account the hysteresis effects for falling and rising stages. Based on the results presented in Figure B.43 the total sediment load in the period 31 August – 22 September was 275.000 ton.

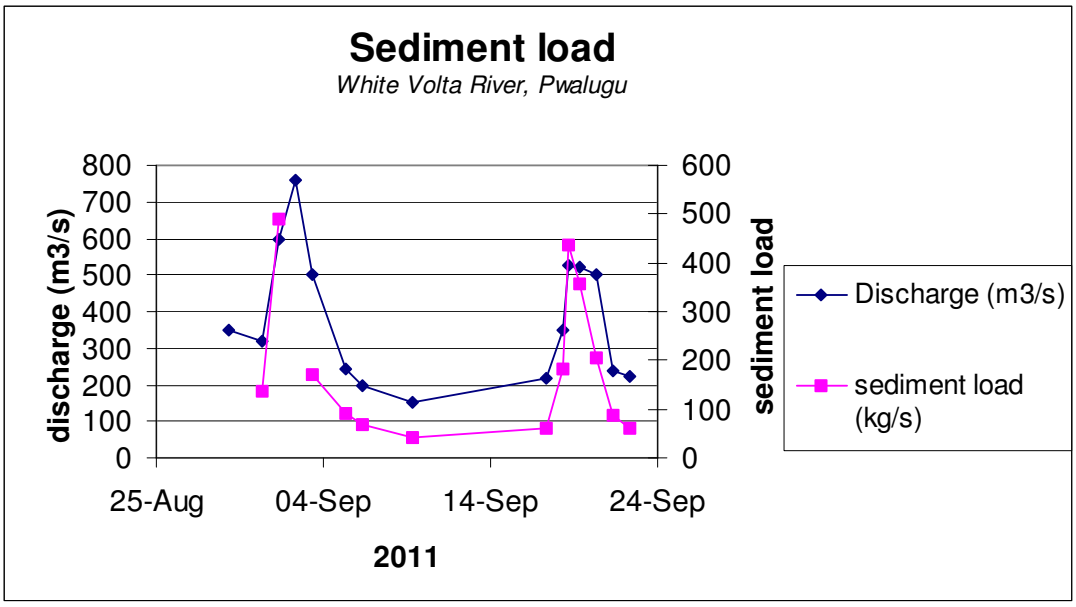

Figure B.44 Sediment load White Volta river Aug/sep 2011, Pwalugu

Surface dip measurements

In addition to the depth-integrated measurements, also surface dip measurements have been taken (Table B.7). The average correction factor between surface dip and depth-integrated measurements is 1.33. Even though few measurements have been taken, the accuracy of the measurements appears to be high, with standard deviations within a range of 0.01 and 0.1.

Table B.7 Comparison surface dip and depth-integrated measurements

	Surface dip (mg/L)	Depth-integrated (mg/L)	Factor
5/9/2011	0.31 (n=1)	0.38 (n=1)	1.22
17/9/2011	0.20 (n=3, sd = 0.02)	0.28 (n=3, sd=0.01)	1.4
18/9/2011	0.56 (n=1)	0.83 (n=4, sd = 0.1)	1.5
20/9/2011	0.33 (n=2, sd=0.01)	0.42 (n=3, sd = 0.04)	1.27
21/9/2011	0.29 (n=2, sd = 0.02)	0.36 (n=3, sd=0.03)	1.24
Average	0,34	0,45	1,33

Particle size distribution

The particle size distribution of the suspended sediment samples was not measured. However, the following has been observed:

- the samples consist mainly of silt/clay and a small fraction of sand (Figure B.45).
- the washload samples contain almost no sand particles.
- there is a difference in colour between different samples (Figure B.46). The darkest colours appear to have the highest sediment concentrations.

Figure B.45 Dried sediment samples

Figure B.46 Dried sediment sample

Sediment rating curve

A sediment rating curve has been produced, based on the results of the fieldwork supplemented with the results found by Nippon Koei (1966) and Akrasi (1994). This was done in order to have data in a wide range of discharges. In Figure B.47 it is shown that the measurements are in the same order of magnitude and are comparable, but that there appears to be much scatter.

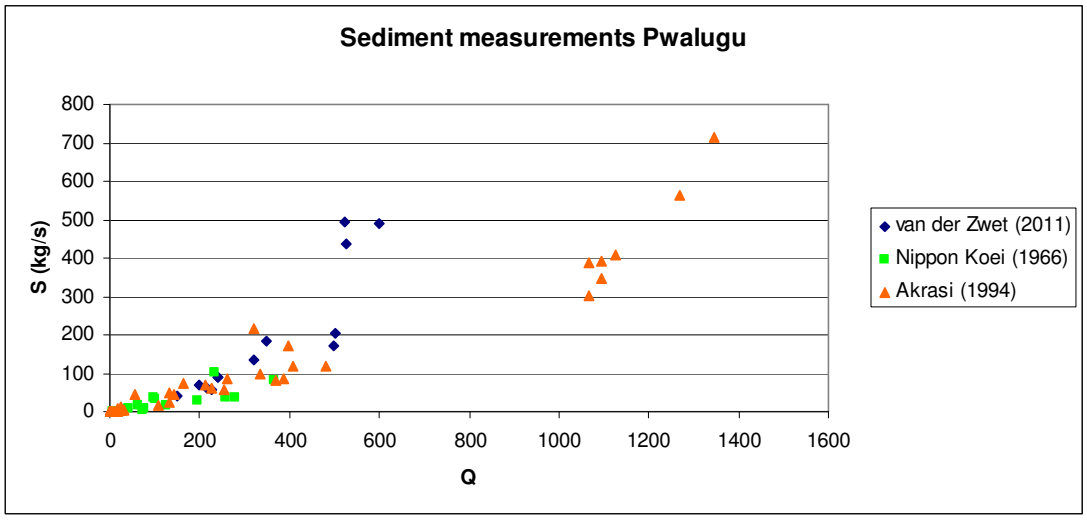

Figure B.47 Sediment measurements White Volta river, Pwalugu

The rating curve formula is presented in Figure B.48. The general formula for a rating curve is:

$\log(S) = \log(a) + b * \log(Q)$ which is equal to $S = a * Q^b$

Filling in the coefficients of the trend line, the following formula is obtained:

$\log(S) = -1.041 + 1.2078 * \log(Q)$ which is equal to $S[kg/s] = 0.091 * Q[m^3/s]^{1.2078}$

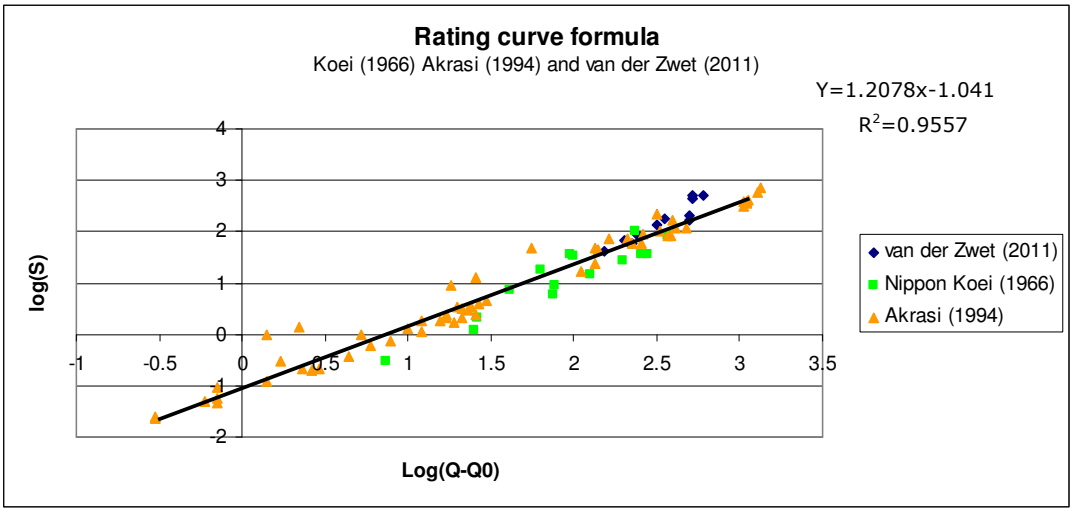

Figure B.48 Sediment rating curve, White Volta river, Pwalugu

When applying the rating curve to the 6 hourly discharge series for the period 2003-2007 (see chapter 3.1.4), the average yearly sediment load ≈ 1.1 M t/year. By dividing this by the correction factor of 1.33, the annual input of washload is 0.83 M t/year. With a porosity of 0.4 and a density of 2700 kg/m^3, the annual input of washload = 0.77 M m^3/year. The dead storage of the reservoir is 940 M m^3, so it would take 1223 years to completely fill up the dead storage. When averaging out the washload over the surface area ($A_{average}$ = 250 km^2), the annual siltation rate is 3 mm/year.

B.3.2.2 Nangodi

The suspended sediment concentration and load for Nangodi are calculated using the following formula:

$$S = \sum_{i=1}^{3} Q_i \cdot c_i$$

The results are presented in Table B.8 and the following can be observed:
- The average sediment concentration measured in Nangodi is 0.19 g/L.
- The sediment concentrations in sections 1 and 2 are quite similar.
- There are no large variations in sediment concentration between different dates.
- The difference in sediment load is mainly caused by higher discharges.

Table B.8 Suspended sediment concentration and load, Nangodi

Date	Section	Discharge per section (m^3/s)	Sediment concentration (g/L)	Sediment load (kg/s)
4/9/2011	1	22,5	0,19 (n=1)	18,5
	2	67,5	0,21 (n=3, sd=0,04)	
10/9/2011	1	7,5	0,13 (n=3, sd=0,01)	5,8
	2	37,0	0,13 (n=3, sd=0,006)	
19/9/2011	1	16,0	0,18 (n=2, sd = 0,03)	15,0
	2	55,2	0,22 (n=2, sd = 0,006)	
23/9/2011	1	5,2	-	4,7
	2	17,1	0,21 (n=2, sd = 0,05)	
Average all sections		**57**	**0,19**	**11**

B.3.2.3 Yarugu

The sediment load for Yarugu is calculated the same way and the results are presented in Table B.9.

Table B.9 Suspended sediment concentration and load, Yarugu

Date	Section	Discharge per section (m^3/s	Sediment concentration (g/L)	Total sediment load (kg/s)
4/9/2011	1	21,6	0,40 (n=1)	37
	2	9	0,50 (n=1)	
	3	58,5	0,40 (n=1)	
10/9/2011	1	34	0,21(n=2, sd = 0,01)	18
	2	-	-	
	3	55	0,20 (n=3, sd =0,003)	
19/9/2011	1	41,04	0,58 (n=2, sd = 0,01)	99
	2	41,3	-	
	3	85,7	0,60 (n=2, sd = 0,09)	
23/9/2011	1	26	-	27
	2	-	-	
	3	54	0,34 (n=2, sd = 0,04)	
Average all sections		**106.75**	**0.40**	**45**

- The average sediment concentration is 0,40 g/L.
- The sediment concentration appears to be quite constant over the cross-section.
- At 10/9 and 23/9 the concentrations were significantly lower than at the other dates.
- Concentration is highest on 19/9. On this day also the discharge was maximal.

B.3.2.4 Comparison

The sediment loads in Nangodi and Yarugu are compared in Table B.10. Again, for Pwalugu a time-lag of 1,5 day is applied.

Table B.10 Comparison sediment load Nangodi and Yarugu

Date	Sediment load Nangodi (kg/s)	Sediment load Yarugu (kg/s)	Sediment load (kg/s) (sum Nan+Yar)	Sediment load Pwalugu (kg/s)
4/9/2011	18	37	55	78
10/9/2011	6	18	24	45
19/9/2011	15	99	114	150
23/9/2011	5	27	32	60

The suspended sediment load in Yarugu is 2-6 times higher than in Nangodi. A substantial part of sediment load seems to be originated from lateral inflow (25 – 47 %). The average contribution of the Red Volta and lateral inflow to total suspended sediment transport in Pwalugu is presented in Figure B.49.

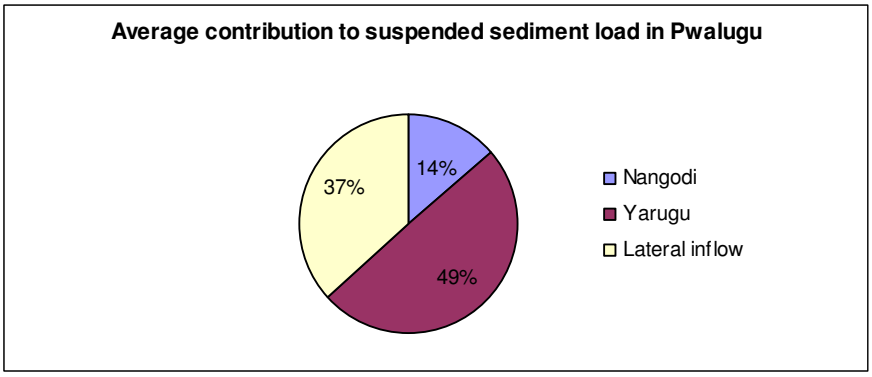

Figure B.49 Suspended sediment load

B.3.3 Bed material samples

B.3.3.1 Particle size distribution

The resulting particle size distribution curves of the bottom material can be found in Appendix A. The D_{16}, D_{50}, D_{84} and D_{90} values for Pwalugu are presented in Table B.11. The bottom material at site 1 (inner bend) consists of very fine sand, at site 2 (middle) of medium sized sand, and at site 3 (outer bend) of coarse sand/gravel. This can be explained by the flow velocity distribution over the cross-section; flow velocity is lowest in the inner bend (site 1) and highest in the outer bend (site 3). It can be seen that the particle size distribution is not the same on 6-9 and 22-9. This could be due to measurement errors in the analysis or due to morphological changes (sedimentation or erosion). It could also be the consequence of a lower discharge on the 22th compared to the 6th, because the higher the discharge the more coarse sand could be transported as bed load.

Table B.11 Particle size distribution Pwalugu

		D_{16} (mm)	D_{50} (mm)	D_{84} (mm)	D_{90} (mm)	Q (m^3/s)
Pwalugu Site 1	**6-9**	0.25	0.40	0.6	0.7	200
	22-9	0.30	0.44	0.7	0.8	266
Pwalugu Site 2	**5-9**	0.32	0.60	0.9	1	240
	22-9	0.51	0.80	1.1	1.4	266
Pwalugu Site 3	**6-9**	0.80	1.6	3	4	200
	22-9	0.7	1.3	3	5	266

The D_{16}, D_{50} and D_{84} values for Yarugu are presented in Table B.12. The bed material in Yarugu consists of fine sand (finer than in Pwalugu) and is more constant over the cross-section than in Pwalugu. The bed material in Nangodi could not be analyzed, as sampling was impossible due to a rock bed.

Table B.12 Particle size distribution Yarugu

		D_{16} (mm)	D_{50} (mm)	D_{90} (mm)	Q (m^3/s)
Yarugu Site 1	**23-9**	0.29	0.41	1	81
Yarugu Site 3	**10-9**	0.28	0.42	1.1	89
Yarugu Site 3	**23-9**	0.21	0.30	0.6	81

B.3.3.2 Bed load transport

Bed load transport is calculated using the theoretical formulas of Engelund-Hansen, Meyer-Peter –Muller and van Rijn (Appendix A). The average particle size distribution of the middle section is used as input (D_{50}=0.7mm and D_{90} =1.2 mm). The results are presented in Figure B.50.

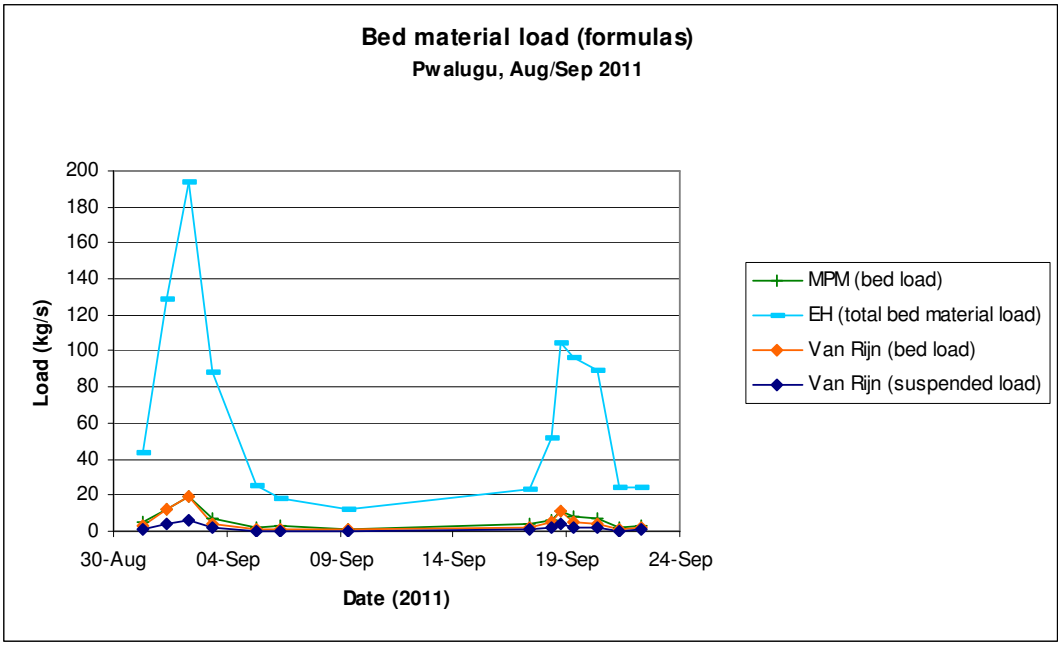

Figure B.50 Bed material load formulas, Pwalugu Aug/Sep 2011 with D_{50}=0.7 mm and D_{90}=1.2 mm

Criteria**:**

- Engelund-Hansen:
  - $0.07 < \theta < 6$: criteria met in all cases.
  - $0.19\ mm < D_{50} < 0.93\ mm$: criteria met in all cases.
  - $w_s/u^* < 1.$: Criteria met in all cases except for low flows at 9/9, 17/9 and 22/9.
- Meyer-Peter and Muller:
  - $\mu\theta < 0.2$: Criteria met in 50 % of the cases (during low flows).
  - D>0.4 mm: Criteria met in all cases.
  - $w_s/u^* > 1.$: Criteria met only for low flows at 9/9, 17/9 and 22/9.

According to the criteria, Engelund-Hansen can be used during high flows (Q>225 m^3/s). Meyer-Peter-Muller can be used during low flows (Q<400 m^3/s). It is not known whether the bed material of the middle section is representative for the whole river reach. The bed load predictions with bed material of the inner bend as input (D_{50}=0.42mm and D_{50}= 0.75 mm) is presented in Figure B.52.

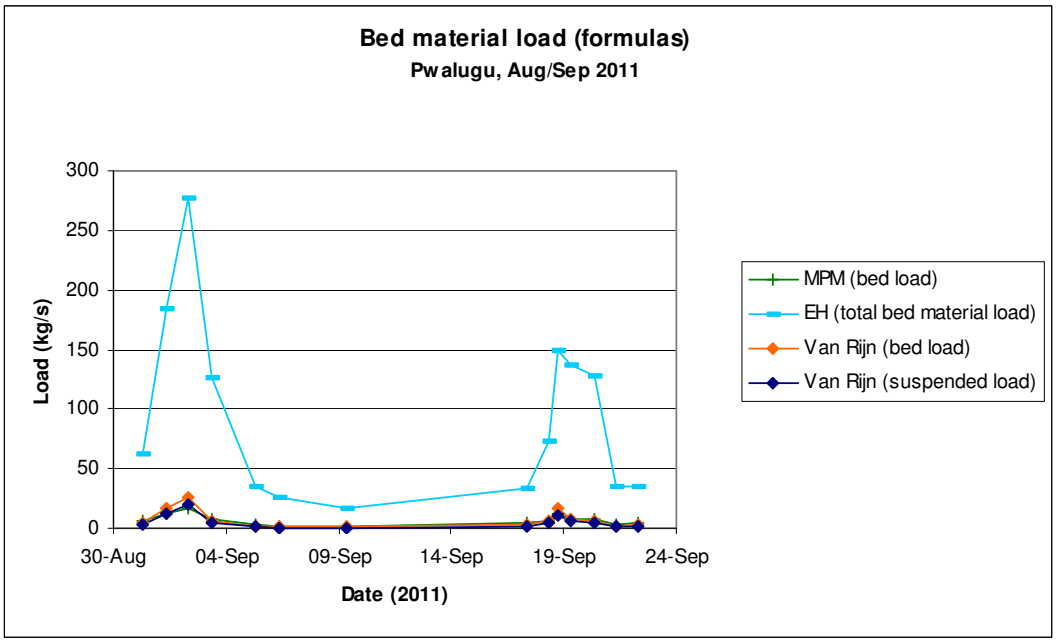

Figure B.51 Bed material load with D_{50} = 0.42 mm and D_{90} = 0.75 mm

The following parameters have been used as input into the formula:
h and Q follow from field measurements; i=0.0002; B=81 m and k=a=0.5.
The roughness values are plotted in Figure B.52.

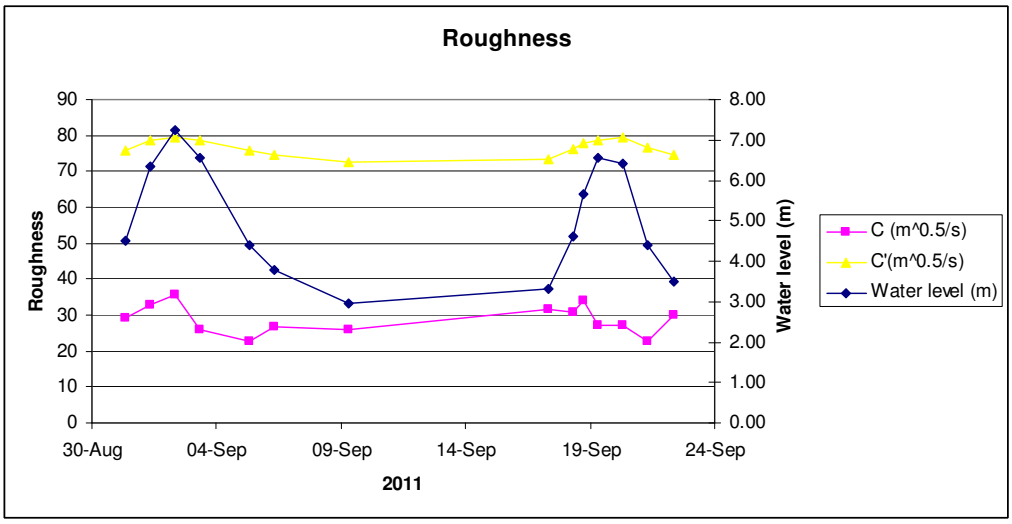

Figure B.52 Roughness values Pwalugu, 2011

The Shields numbers during the fieldwork and the critical Shields number are presented in Figure B.53. It can be observed that in September/August 2011 the Shields number exceeded the critical Shields number.

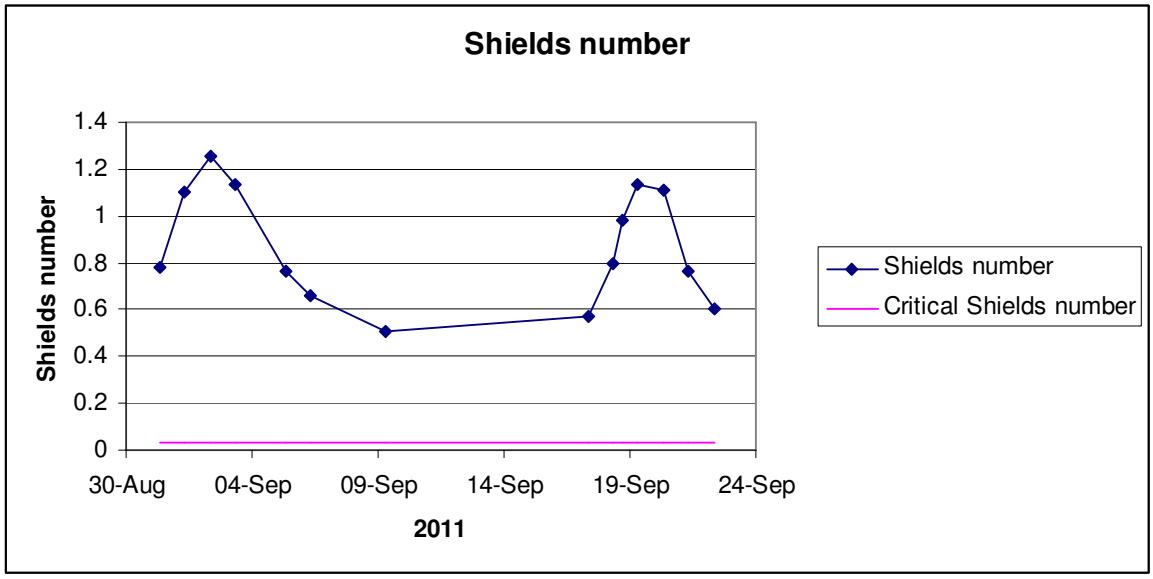

Figure B.53 Shields numbers and critical Shields number in August/September 2011

B.3.4 Riverbank samples

The hydrometer method requires the density of the sediment as input for the Stokes-formula. The density of very fine sand from Pwalugu, Nangodi and Yarugu has been analysed with a pyknometer and appeared to be 2700 kg/m^3. The particle size distribution of the riverbank samples is presented in Appendix C. The curves consist of two different parts. The left part is determined by the hydrometer method, the right part by dry sieving. The gap in between is due to the fact that the first density measurements can only be taken after 1 minute, because of instability of the suspension in the measurement tube. By that time, many of the silt particles have already settled to the bottom, and cannot be measured. The sand/silt/clay fractions of the riverbank samples are presented in Table B.13. The following classification rules are used:

- Clay: D<0.002 mm
- Silt: 0.002<D<0.065 mm
- Sand: 0.065<D<2 mm
- Gravel: D>2 mm

Table B.13 Particle size distribution riverbank samples

	Sand (%)	Silt (%)	Clay (%)
Pwalugu old bridge (after 1st flood wave)	14	63	23
Pwalugu bridge (after 1st flood wave)	12	58	30
Pwalugu bridge (after 2nd flood wave)	19	62	19
Nangodi (after 1st flood wave)	40	48	12
Nangodi (after 2nd flood wave)	80	14	6
Yarugu (after 2nd flood wave)	70	24	6

Pwalugu (White Volta)

- The sediment deposited on the banks at Pwalugu consists predominantly of silt and clay.
- The measurements at the two different sites near Pwalugu (bridge and old bridge) are similar.
- After the first flood wave, the clay fraction was higher than after the second flood wave.

Nangodi (Red Volta)

- After the first flood wave fine sand, silt and clay have been deposited on the banks.
- After the second flood wave the riverbanks are sandy (very fine sand). Little silt and clay has been deposited.

Yarugu (White Volta)

- The riverbank material at Yarugu is predominantly sandy. The clay fraction is small.
- Very little sediment has been deposited on the riverbanks after the second flood wave.
- Based on field observations, there had been deposited sediment on the riverbanks after the first flood, but no measurements were taken (Figure 2.10 and 2.11).

The results of the mineralogical analysis are presented in Table B.14.

Table B.14 Mineralogy riverbank samples 2011

	P1	P2	P3	R1	R2	Y1
	Pwalugu 5/9 (bank)	Pwalugu 22/9 (bank)	Pwalugu old site 23/9	Nangodi (4/9) (muddy)	Nangodi 23/9 (fine sand)	Yarugu 23/9
Quartz	67 %	62 %	71 %	80 %	72 %	47 %
Albite:	16 %	21 %	11%	20 %	16 %	40 %
Microcline:	4 %	10 %	3 %	0 %	13 %	13 %
Kaolinite:	13 %	7 %	14 %	0 %	0 %	0 %
D16 (mm)	<0.001	<0.001	<0.001	0.01	0.06	0.02
D50 (mm)	0.017	0.03	0.02	0.05	0.15	0.1
D84 (mm)	0.05	0.07	0.05	0.1	0.27	0.28
Clay	30 %	21 %	23 %	13 %	7 %	10 %
Silt	34 %	59 %	62 %	48 %	14 %	30 %
Sand	12 %	20 %	15 %	39 %	79 %	60 %

- Microcline is a potassium rich feldspar mineral. It is common in granite and pegmatites.
- Albite is a sodium-rich feldspar mineral. It is also common in granite and pegmatite.
- Quartz is the most-abundant mineral in the Earth's continental crust. It is a mineral that does not break down to clay minerals.
- Kaolinite is a clay mineral. It is a soft, earthy, usually white mineral, produced by the chemical weathering of aluminium silicate minerals like feldspar. Kaolinite clay occurs in abundance in soils that have formed from the chemical weathering of rocks in hot, moist climates—for example in tropical rainforest areas (Wilson, 2010)

Appendix C: Reservoir water balance model

The operation of the reservoir is modelled in Excel using the water balance. In evolutional form the equation reads:

$$V_{t+\Delta t} = V_t + (Q_{in} - Q_{evaporation} - Q_{leakage} - Q_{turbines} - Q_{spillway})\Delta t$$

with:

Δt: timestep of 6 hours.

Q_{in}: 6-hourly discharge series of Pwalugu for the period 2003-2007 are used.

$Q_{evaporation}$: Evaporation flux = Evaporation rate * Surface area. The evaporation rate is on average 1.134 m / year (prefeasability report, 1994). It is assumed that the rate is constant throughout the year. The surface area is not constant, as this depends on the water level. The A/h relation (Chapter 4.2.1) is used to convert water levels to surface area and subsequently to an evaporation flux at every time step.

$Q_{leakage}$: The leakage through the dam and infiltration of the subsurface is not known. The leakage is set at a low value of 2 m^3/s. That way there will always be a small discharge in the river downstream, which is a requirement for the SOBEK model.

$Q_{turbines}$: Flow through the turbines depends on the operational strategy. In this model it is possible to use a constant flow as well as a head-dependent flow. This flux is only active when $V_{minOL} < V < V_{maxOL}$

$Q_{spillway}$: For every timestep the reservoir level is checked. In case the level exceeds max OL, all excess water will be discharged through the spillway in the next timestep.

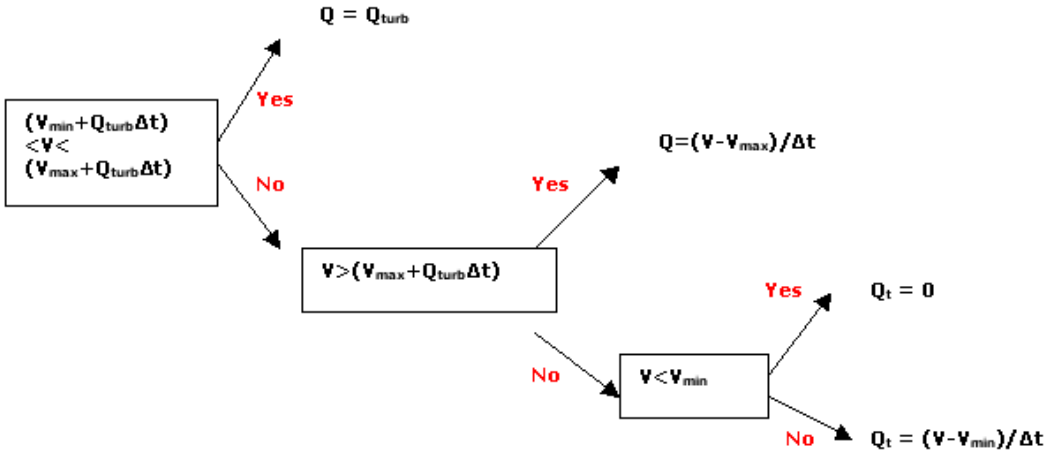

Excel script:
=IF(AND(V>(Vmin+Qturb*ΔT),Qturb<(Vmax+Qturb*ΔT)),Qturb,IF(V>(Vmax+Qturb*ΔT),(V-Vmax)/ΔT,IF(V<Vmin,0,(V-Vmin)/ΔT)))

Figure C.1 Water balance model scripts

The outflow through the turbines can either be constant, by manipulation of the gates, or a function of the water level using the formula for flow through turbines:

$$Q = B\mu w\sqrt{2g\left(H - \mu w\right)}$$

in which:

B: width = number of turbines in operation* width per turbine
μ: contraction coefficient = 0.7 (-)
w: vertical gate opening height (m)
H: energy level upstream with respect to gate level (m)
g: gravitational acceleration = 9,81 (m/s^2)

There will be two turbines in the future dam. The maximum discharge through both the turbines (at max OL) is 170 m^3/s (COB, 1993). The dimensions of the gates are not known. The width per turbine (B/2) is assumed to be 5 m. The gate opening is located at h = 145 m. That way the heads at Max OL and Min OL are 23 m and 9.4 m. The width follows from the formula; w= 1,25 m. With this gate opening width the flow at minimum operative level is Q_{min} = 105 m^3/s. The assumed dam dimensions used in the water balance model are schematised in Figure C.2.

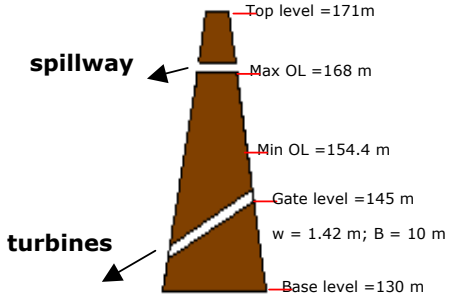

Figure C.2 Dam dimensions

Appendix D: SOBEK model I (sedimentation)

Slope

The average slope between minimum and maximum reservoir extent = 0.00034 (HKV, 2012).

River bed

The river profile at Yarugu has been used (Figure E.1). A schematisation is presented in Figure E.2.

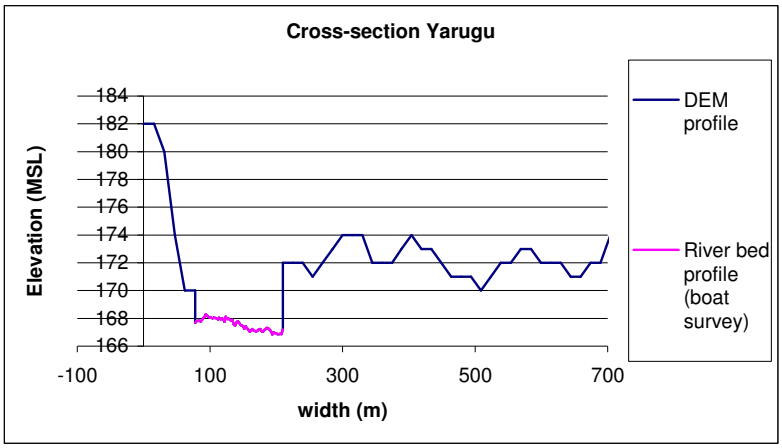

Figure E.1 Cross-section White Volta river at Yarugu

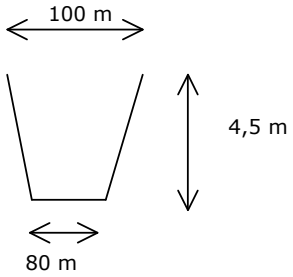

Figure E.2 Schematization of river bed

Floodplains

A representative cross-section of the floodplain has been drawn from a DEM map of resolution 20x20 (SRTM) at location WV 021, perpendicular to the centre line of the main channel (Figure E.3). It can be seen that surface levels of the floodplain are going both up and down, while SOBEK RE requires cross-sections in ascending order (Figure E.4). Therefore the elevations are sorted (Figure E.5). The average sorted slope equals (174-160)/3100 = 0.45 %. The reservoir at max OL does not become much wider than 3200 m, so from that width on the slopes are set vertically (Figure E.6).

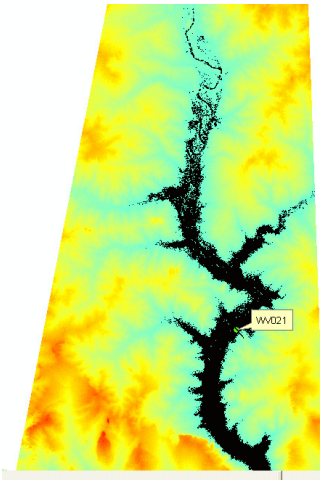

Figure E.3 Upstream reach of White Volta when reservoir is at max OL. Coordinates WV021 (decimal degrees): (-0.3538;10.7646)

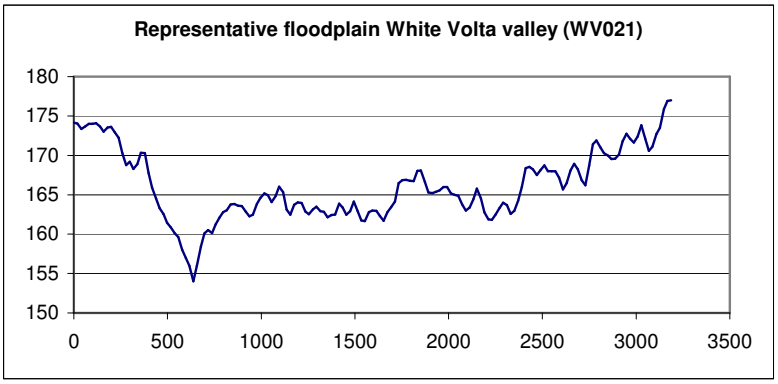

Figure E.4 Cross-sectione White Volta valley (WV021) derived from DEM map

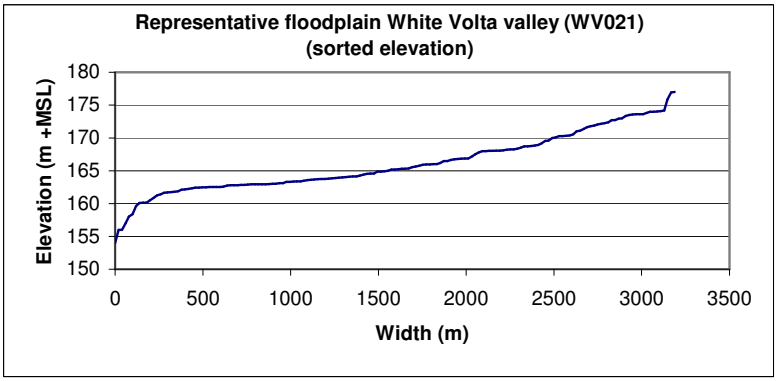

Figure E.5 Elevations of cross-section in ascending order

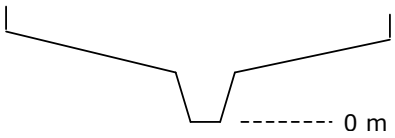

Water depth (m)	Width (m)
0	80
4.5	100
18.5	3200
25	3200

Figure E.6 Cross-section schematised based on sorted elevation.

Reach length:

The river reach between minimum and maximum reservoir extent is equal to 40 km. As backwater effects could also cause sedimentation, the reach has been extended for 80 km in upstream direction. In downstream direction the reach has been extended with 30 km.

Slope:
The average slope between maximum and minimum reservoir extent = 0.00034 (HKV, 2012). The riverbed elevation at x = 0 is 190.7 m+NLD. The floodplain level of 168 m (max OL) is reached after 80km. 40 km further downstream the floodplain level is at 154.4 (min OL).

Boundary conditions:
Upstream, flow: Discharge series Yarugu, period 2003-2007. This series is repeated 10 times, 50 years in total.
Upstream, sediment transport: Constant riverbed level. It is assumed that at the upstream boundary the velocity is not influenced by the backwater curve and bed aggradation won't occur.
Downstream, flow: Series of water levels in the reservoir for the period 2003-2007 with time steps of 6 hours. These values are derived from the water balance model.

Friction
Main channel: Chezy roughness = 50 $m^{1/2}/s$. This is the average roughness value. The total range is between 20 and 80 $m^{1/2}/s$ (see Chapter B.3.3).
1st floodplain: Nikuradze value of k_N = 1 m. Along the riverbanks of the White Volta River bushes are present with an estimated roughness value of k_N = 1 m.
2nd floodplain: Nikuradze k_N = 0.5 m. On the main floodplain savannah grassland with sparse trees is present, with an estimated roughness value of k_N = 0.5 m.

Transport formula
The Engelund Hansen formula is used (Appendix A). This formula estimates total transport and meets the flow criteria in most cases (Appendix B).

Initial conditions:
Flow: automatically defined
Bed material: $D_{0.5}$ = 0.35 mm and $D_{0.9}$ = 0.6 mm (Chapter 0)

Grid definition:
Δx = 500m

Run time data:
Start: 2003/01/01;00:00:00
End: 2053/01/01;00:00:00
Computation time step: 06:00:00

Appendix E: SOBEK model II (erosion)

Geometry

In this model the cross-sectional profile at Pwalugu is used (Figure D.1). This is a representative cross-section for the river section downstream of the dam. The cross-section has been schematised by sorting the levels (Figure D.2).

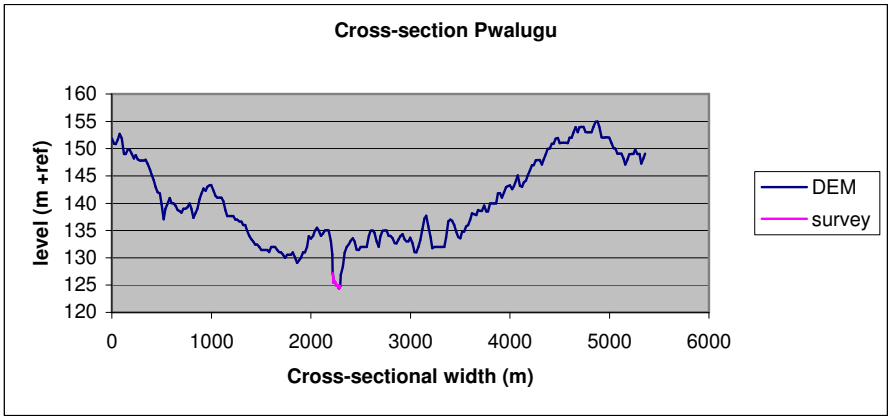

Figure D.1 Cross-section Pwalugu (river bed and floodplain)

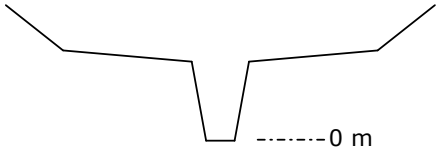

Water depth (m)	Width (m)
0	65
7	80
7.5	2500
22	5000

Figure D 2 Schematised cross-section Pwalugu

Slope:

The average slope over the first 20 km downstream of the dam is = 0.000182 (HKV, 2012).

Reach length:

The riverbed level downstream of the dam is 130 m. The water level in Lake Volta = 80 m and the bed level at that location is 75 m. Given a constant slope, this results in a total reach length of (130-75)/0.000182=302198 m ≈ 300 km.

Boundary conditions:

Upstream, flow: Released discharge through the dam, which is the output of the water balance model. This 2003-2007 series is repeated 10 times (50 years in total)

Upstream, sediment transport: The sediment load of the inflow is zero, as all sediment has been trapped in the reservoir.

Downstream, flow: Water level in Lake Volta, which in reality varies between 75 to 85 m. As the distance between Pwalugu and Lake Volta (300km) is long, water level variation downstream will not influence the erosion near the dam. An average water level of 80 m has been selected.

Friction:

Main channel: Chezy roughness = 25 $m^{1/2}/s$. This is the average roughness value. The total range found during the fieldwork is between 10 and 35 $m^{1/2}/s$ (see Chapter B.3.3).

1st floodplain: Nikuradze value of k_N = 1 m. On the riverbanks of the White Volta river bushes are present with an estimated roughness value of k_N = 1 m.

2nd floodplain: Nikuradze k_N = 0.5 m. On the main floodplain savannah grassland with sparse trees is present, with an estimated rougness value of k_N = 0.5 m.

Transport formula

The Engelund Hansen transport formula is used. This formula estimates total transport and meets the flow criteria in most cases (chapter B.3.3).

Initial conditions:

Flow: automatically defined

Bed material: $D_{0.5}$ = 0.7 mm and : $D_{0.9}$ = 1.1 mm (Chapter B.3.3)

Grid definition:

0- 30 km: grid = 50 m

30-300 km: grid = 250 m

Run time data:

Start: 2003/01/01;00:00:00

End: 2053/01/01;00:00:00

Computation time step: 06:00:00

Appendix F: Particle size distribution bed material samples

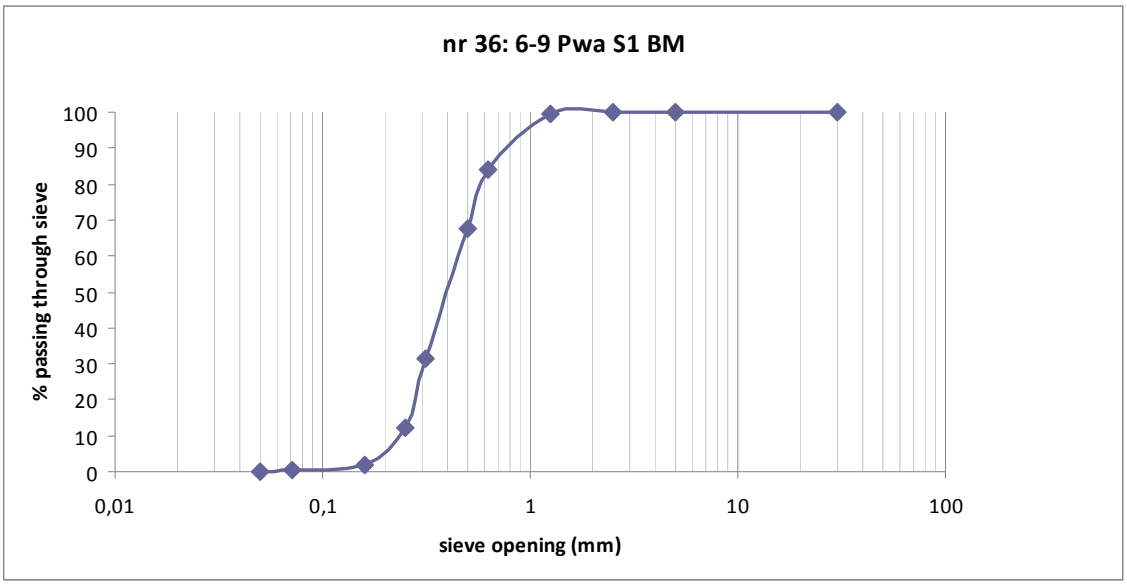

Figure F.1 6/9 Pwalugu site 1

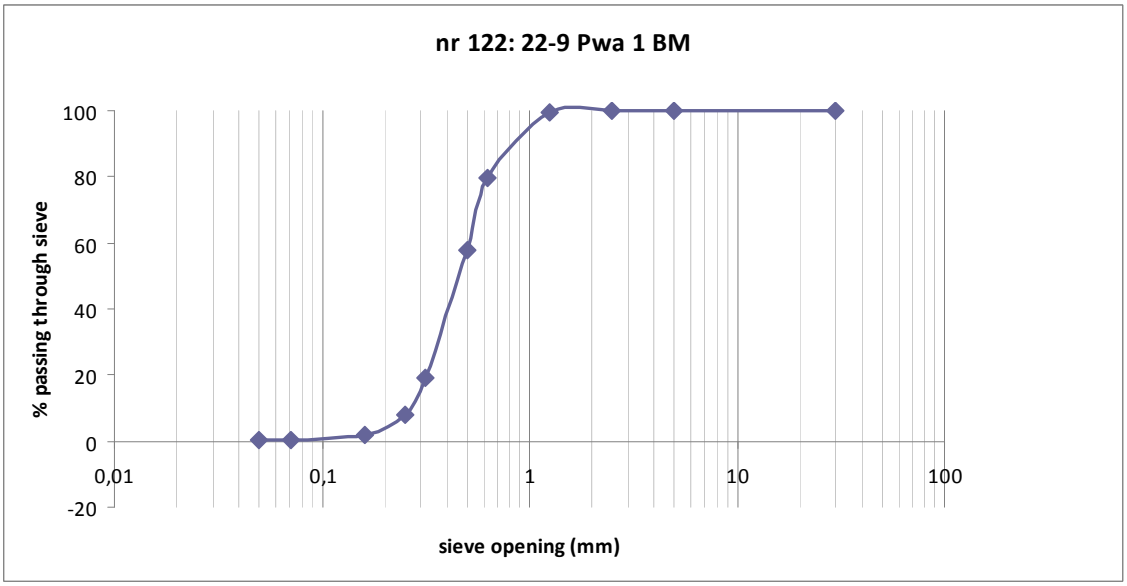

Figure F.2 22/9 Pwalugu site 1

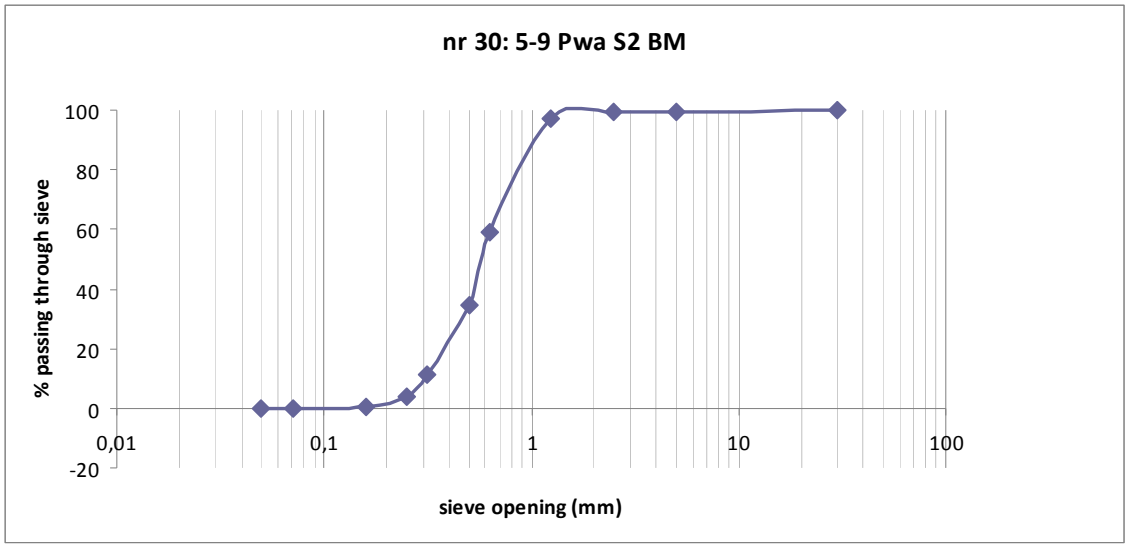

Figure F.3 5/9 Pwalugu site 2

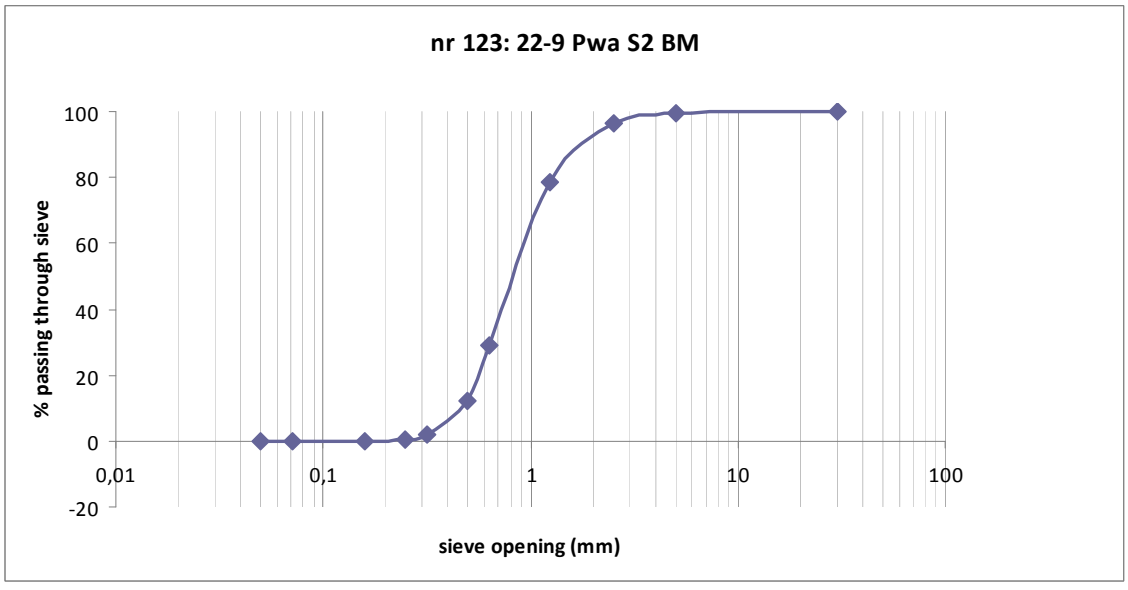

Figure F.4 22/9 Pwalugu site 2

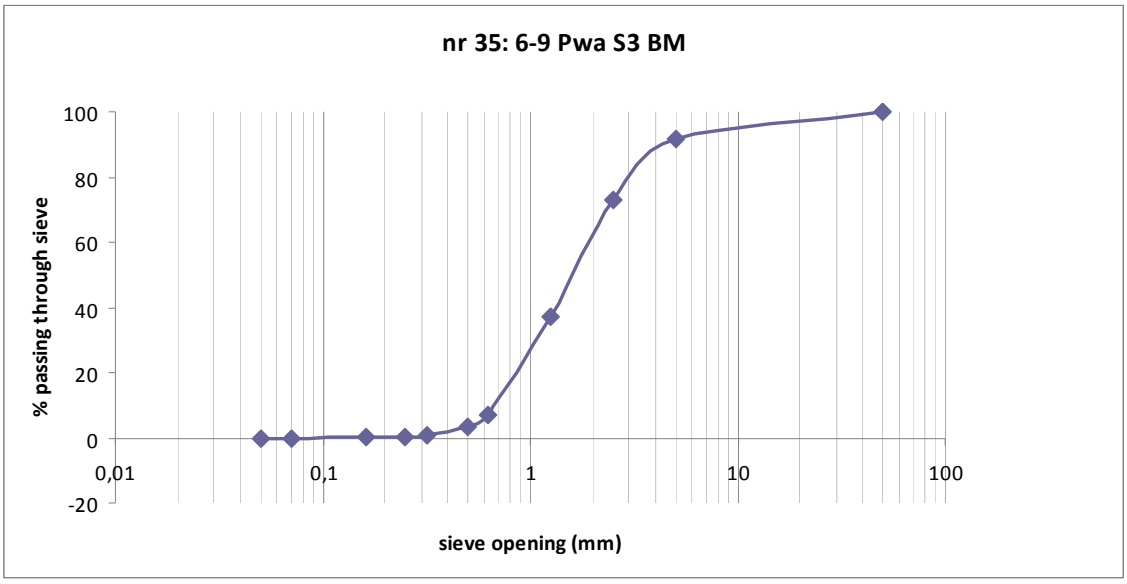

Figure F.5 6/9 Pwalugu site 3

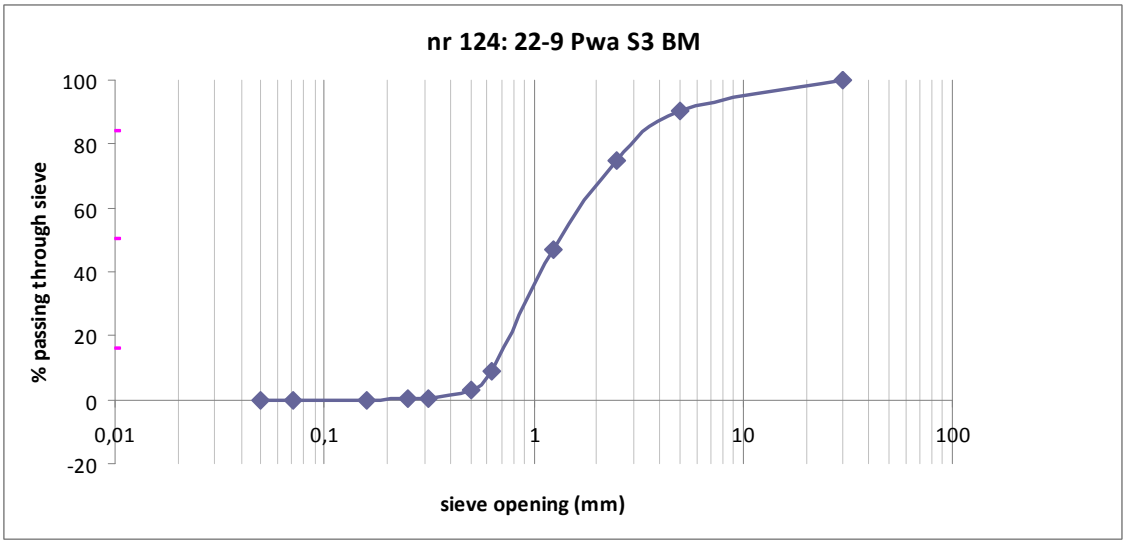

Figure F.6 22/9 Pwalugu site 3

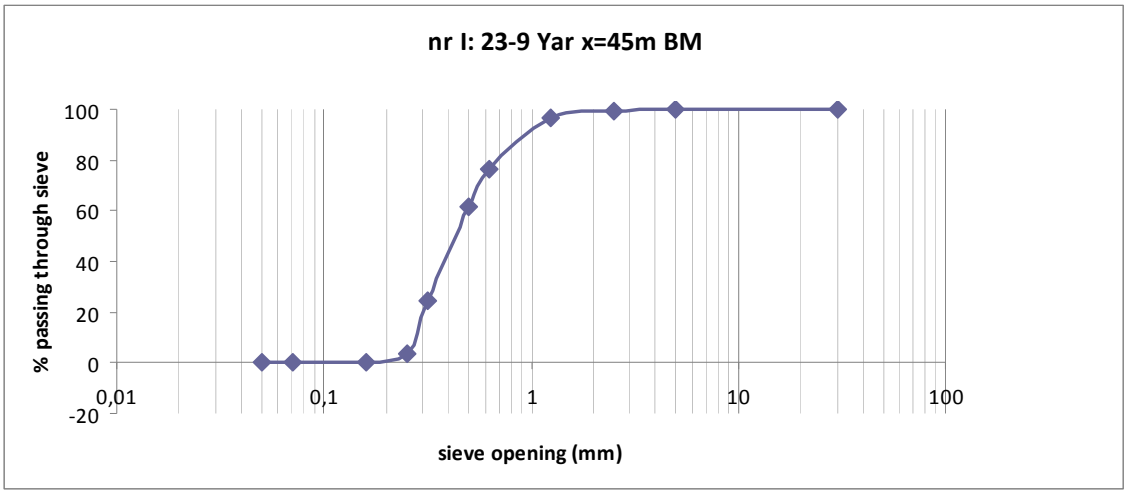

Figure F.7 23/9 Yarugu site 1

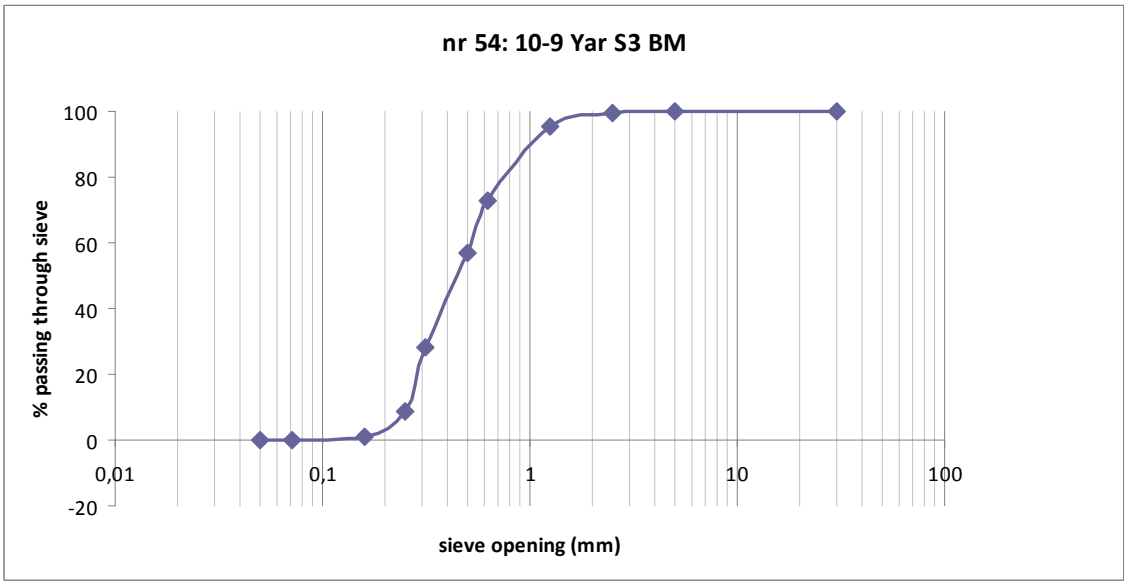

Figure F.8 10/9 Yarugu site 3

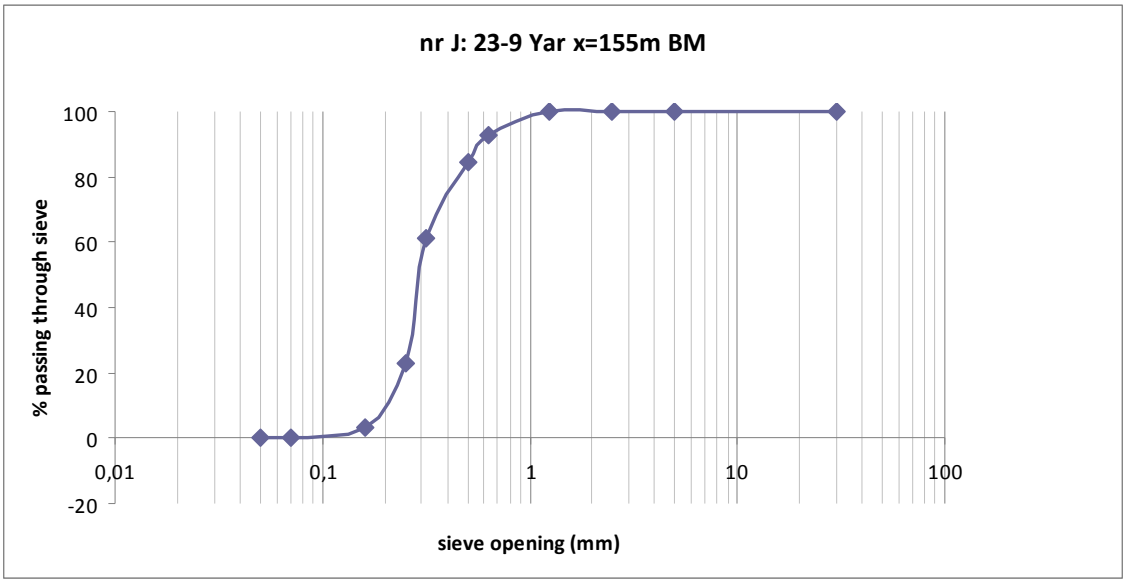

Figure F.9 23/9 Yarugu site 3

Table F.1 Overview particle size distribution river bed samples

Location	Date	D_{10} (mm)	D_{50} (mm)	D_{90} (mm)
Pwalugu S1	6/9/2011	0.2	0.4	0.8
Pwalugu S1	22/9/2011	0.2	0.5	0.7
Pwalugu S2	5/9/2011	0.3	0.6	1
Pwalugu S2	22/9/2011	0.5	0.8	1.5
Pwalugu S3	6/9/2011	0.6	1.5	4
Pwalugu S3	22/9/2011	0.6	1	4
Yarugu S1	23/9/2011	0.3	0.4	0.9
Yarugu S3	10/9/2011	0.2	0.4	1

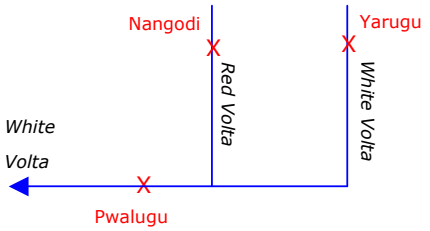

Appendix G Particle size distribution riverbank samples

Sample nr 22: 4/9 Red Volta Riverbank (muddy)

D_{16} = 0.01 mm **D_{50} = 0.05 mm** **D_{84} = 0.1 mm**

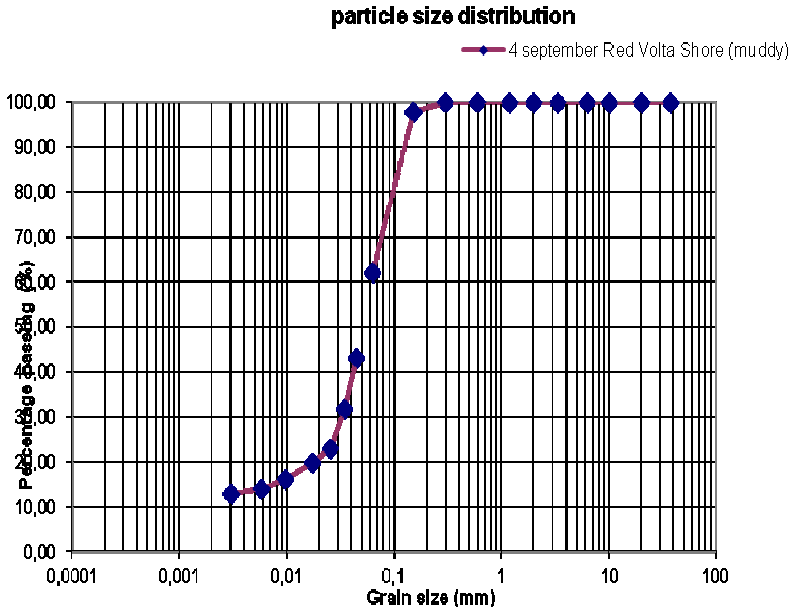

Sample nr 31: 5/9 Pwalugu riverbank

D_{16} <0.001 mm **D_{50} = 0.017 mm** **D_{84} = 0.05 mm**

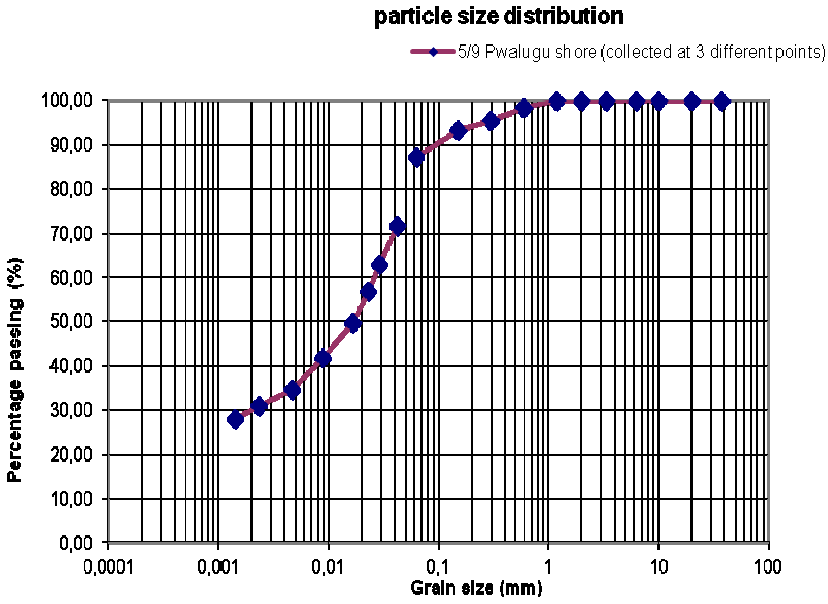

Sample nr A: 23/9 Yarugu Riverbank 1

D_{16} =0.06 mm **D_{50} = 0.18 mm** **D_{84} = 0.3 mm**

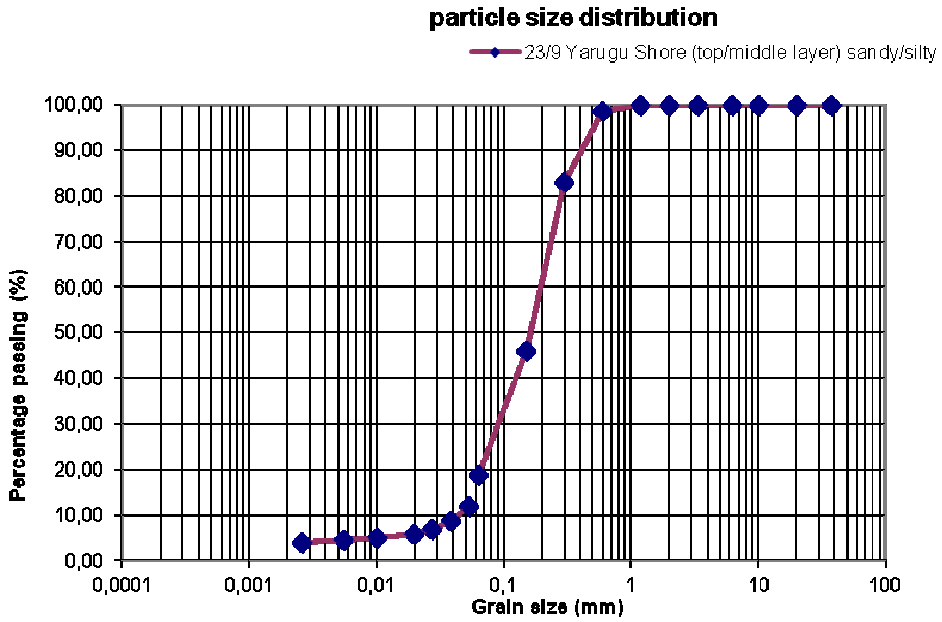

Sample nr B: 23/9 Yarugu Riverbank 2

D_{16} =0.02 mm **D_{50} = 0.10 mm** **D_{84} = 0.28 mm**

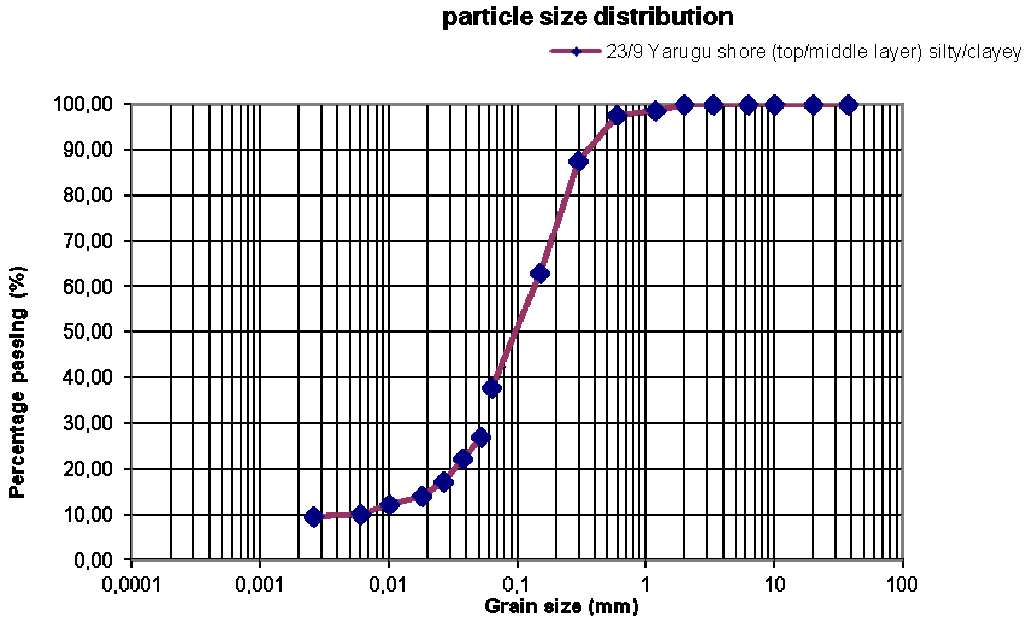

Sample nr D: 23/9 Pwalugu Old site 1

D_{16} < 0.001 mm **D_{50} = 0.02 mm** **D_{84} = 0.05 mm**

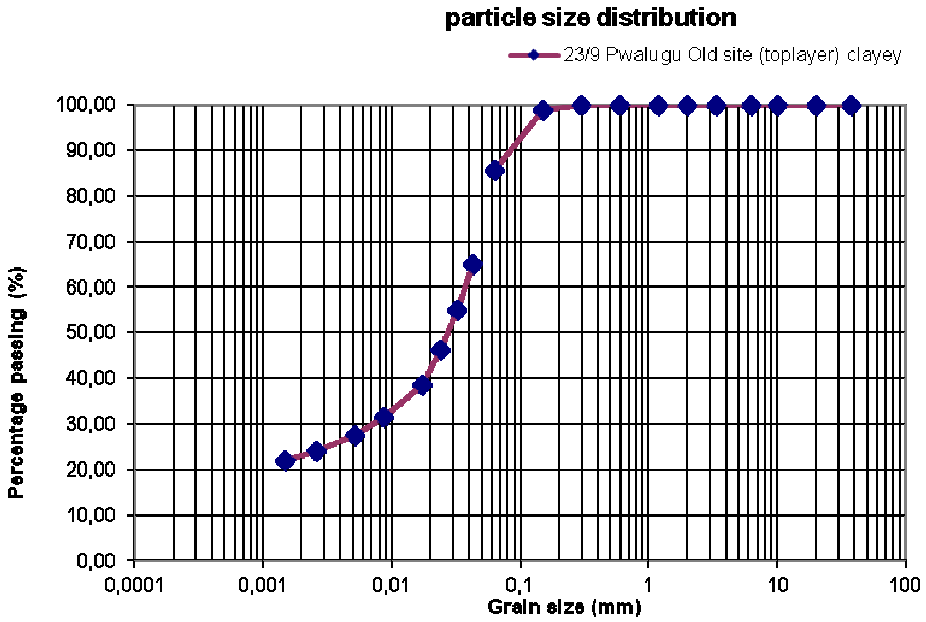

Sample nr E: 23/9 Pwalugu Old site 2

D_{16} < 0.001 mm **D_{50} = 0.03 mm** **D_{84} = 0.05 mm**

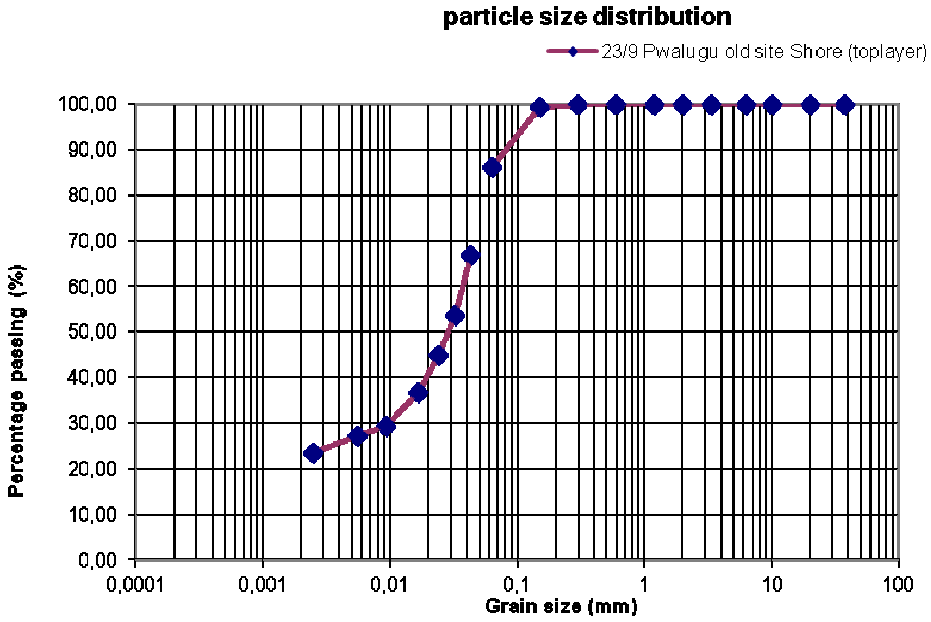

Sample nr F: 23/9 Nangodi riverbank (sandy)

D_{16} =0.06 mm **D_{50} = 0.15 mm** **D_{84} = 0.27 mm**

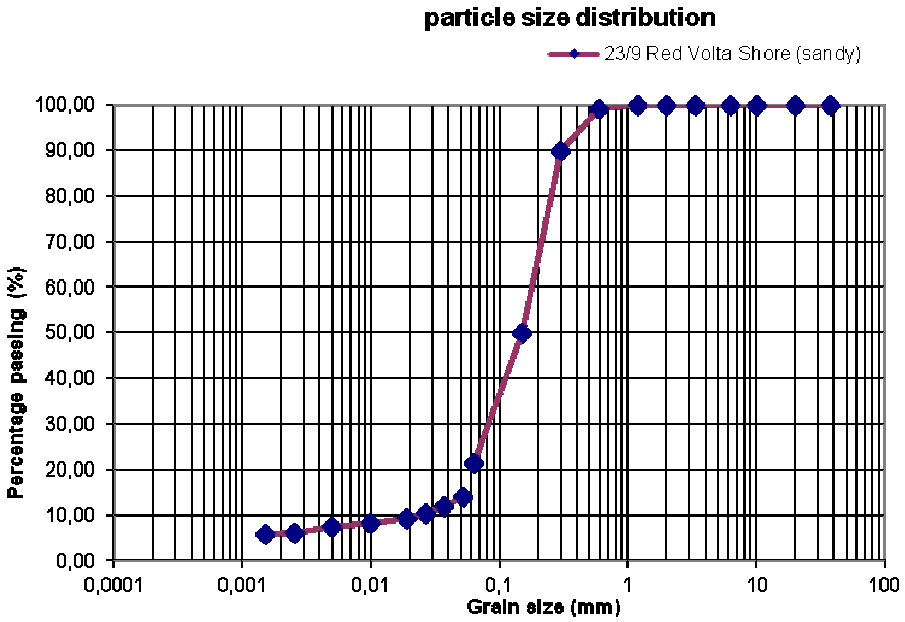

Sample nr Labda: Yarugu - Right bank

D_{16} =0.06 mm **D_{50} = 0.09 mm** **D_{84} = 0.18 mm**

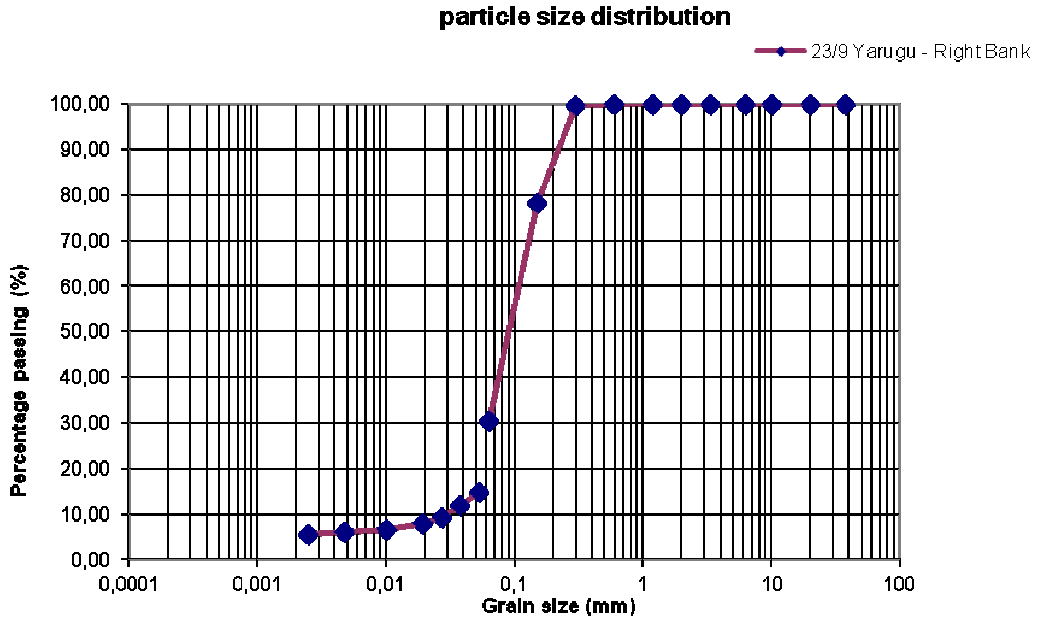

Sample nr NN1: 22/9 Pwalugu riverbank

D_{16} < 0.001 **D_{50} = 0.04 mm** **D_{84} = 0.07 mm**

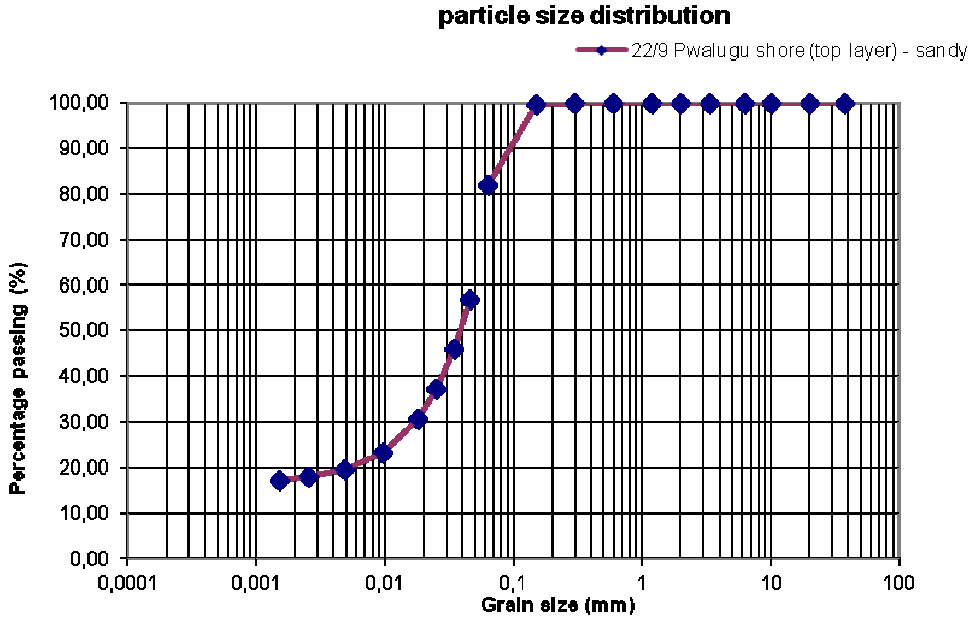

Sample nr NN2: 22/9 Pwalugu riverbank

D_{16} < 0.001 **D_{50} = 0.03 mm** **D_{84} = 0.07 mm**

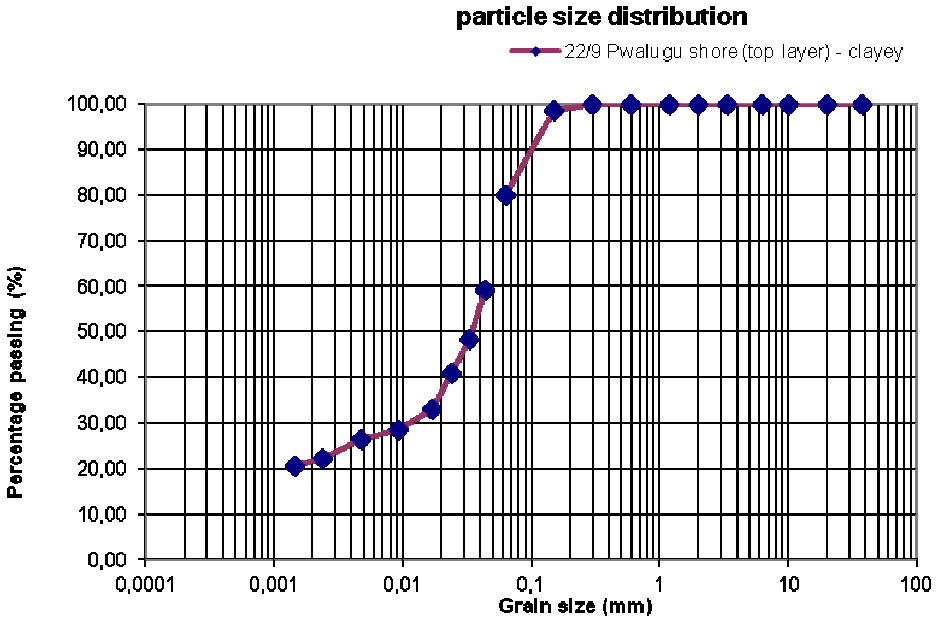

Table H.1 Overview riverbank samples

Location	Date	D_{16} (mm)	D_{50} (mm)	D_{84} (mm)
Pwalugu left bank	5/9/2011	<0.001	0.017	0.05
Pwalugu left bank	22/9/2011	<0.001	0.04	0.07
Pwalugu left bank	22/9/2011	<0.001	0.03	0.07
Pwalugu old site 1	23/9/2011	<0.001	0.02	0.05
Pwalugu old site 2	23/9/2011	<0.001	0.03	0.05
Nangodi (muddy)	4/9/2011	0.01	0.05	0.1
Nangodi (sandy)	23/9/2011	0.06	0.15	0.27
Yarugu right bank 1	23/9/2011	0.06	0.09	0.18
Yarugu right bank 2	23/9/2011	0.06	0.18	0.3
Yarugu right bank 3	23/9/2011	0.02	0.10	0.28

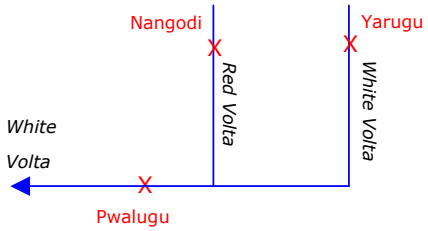

Appendix H: Mineralogy riverbank samples

Materials Science and Engineering
TUDelft, Faculty of 3mE
Mekelweg 2
2628 CD Delft, The Netherlands
Tel/ Fax 032 15 278 2255/ 6730
Email: R.W.A.Hendrikx@tudelft.nl

X- ray diffraction facilities

XRD-identificatie van 6 poederpreparaten:

Client: Joost van der Zwet, CITG
Datum: 23jan 2012
Operator: Ruud Hendrikx

Meetcondities:

X-ray poeder diffractie (XRPD) patronen werden opgenomen in een Bragg-Brentano geometrie met een Bruker D5005 diffractometer uitgerust met een Huber monochromator in de invallende bundel en een Braun PSD detector. De scans werden opgenomen met behulp van monochromatische Cu Kα1 straling (λ= 0.154056 nm) in het 2θ gebied tussen 5° en 90° , stapgrootte 0.038° 2θ. Alle monsters zijn gemeten onder identieke omstandigheden. De monsters werden geroteerd tijdens de meting. Data-analyse werd gedaan met het Bruker programma EVA.

Op de volgende pagina's staan XRD patronen met in zwart de gemeten XRD patronen. De gekleurde sticks geven de piekposities en -intensiteiten van de geïdentificeerde fasen aan, zoals gevonden met behulp van de ICDD pdf4 database. Alle XRD patronen zijn "background subtracted" dwz dat de ondergrond welke een gevolg is van voornamelijk luchtscatter en fluorescentie van het gemeten patroon is afgetrokken.

Resultaten:

Kwarts en albiet lijken in alle 6 preparaten aanwezig te zijn. In het onderstaande lijstje staan de overige mogelijk geïdentificeerde verbindingen genoemd.

Compound Name	Formula
Quartz alpha	SiO2
Albite	NaAlSi3O8
Microcline, ordered	KAlSi3O8
Corundum, syn	Al2O3
Microcline	KAlSi3O8
Kaolinite-1A	Al2Si2O5(OH)4

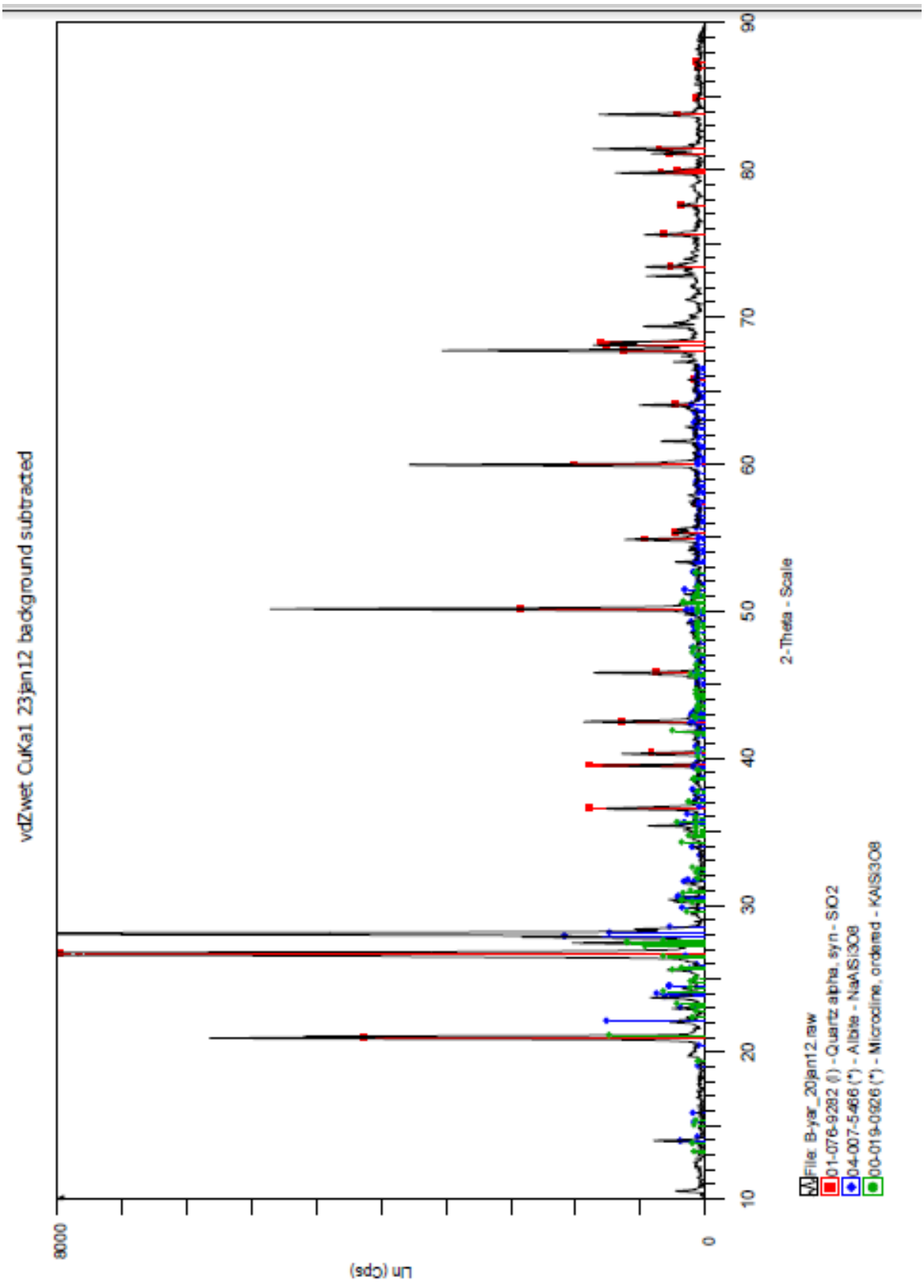

Figure H.1 Yarugu (White Volta) 23/9/2011

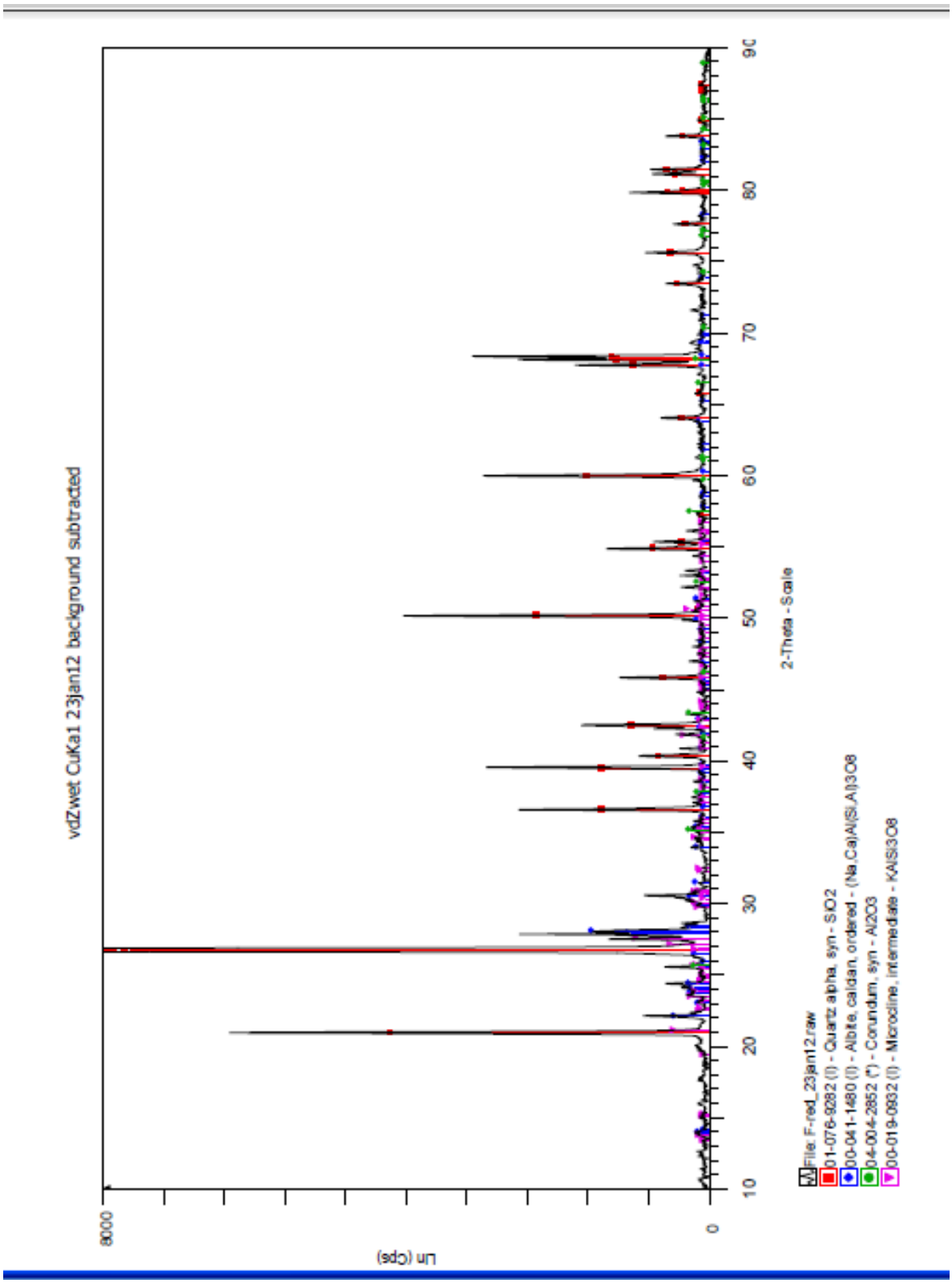

Figure H.2 Nangodi (Red Volta) 23/9/2011

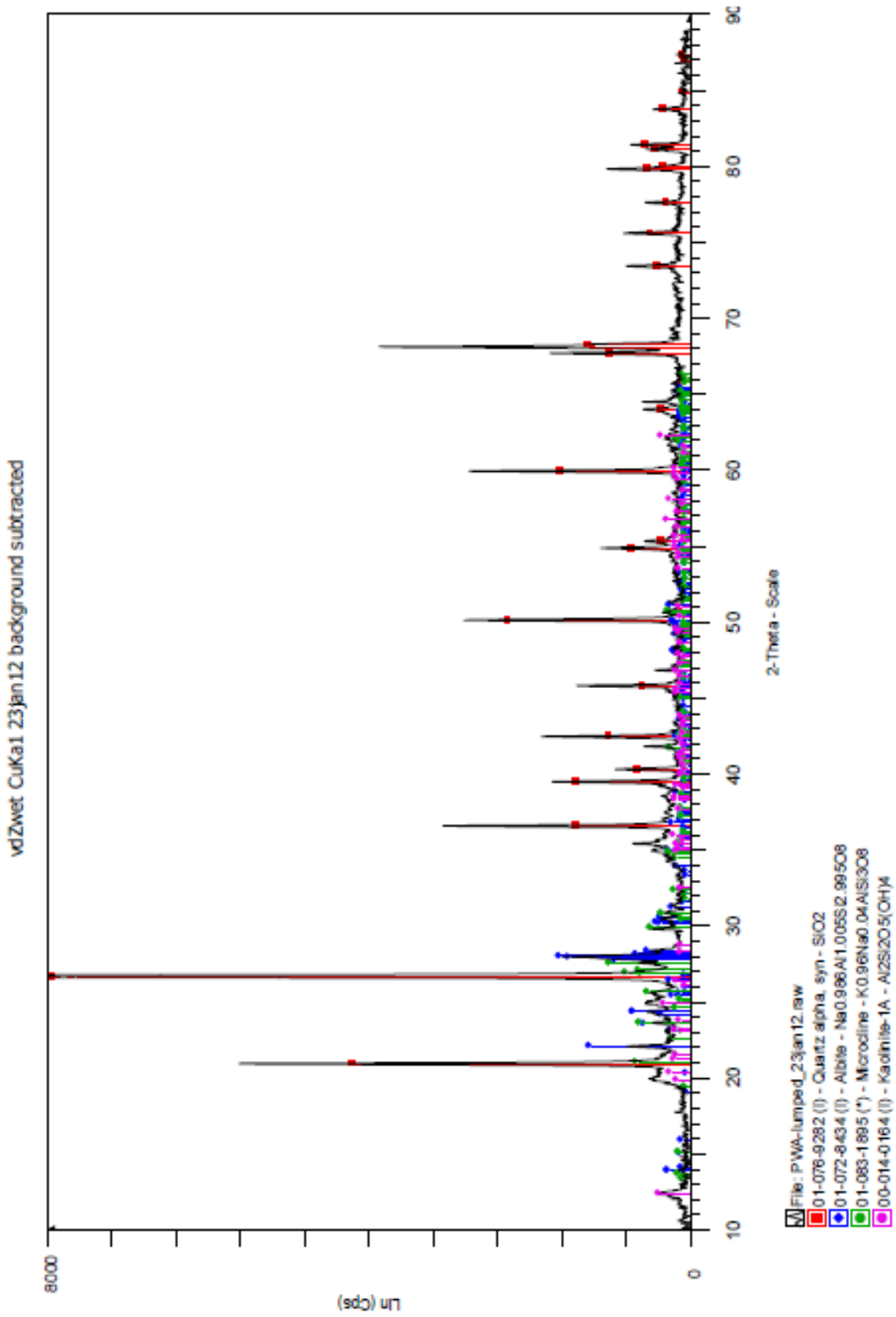

Figure H.3 Pwalugu (White Volta) 5/9

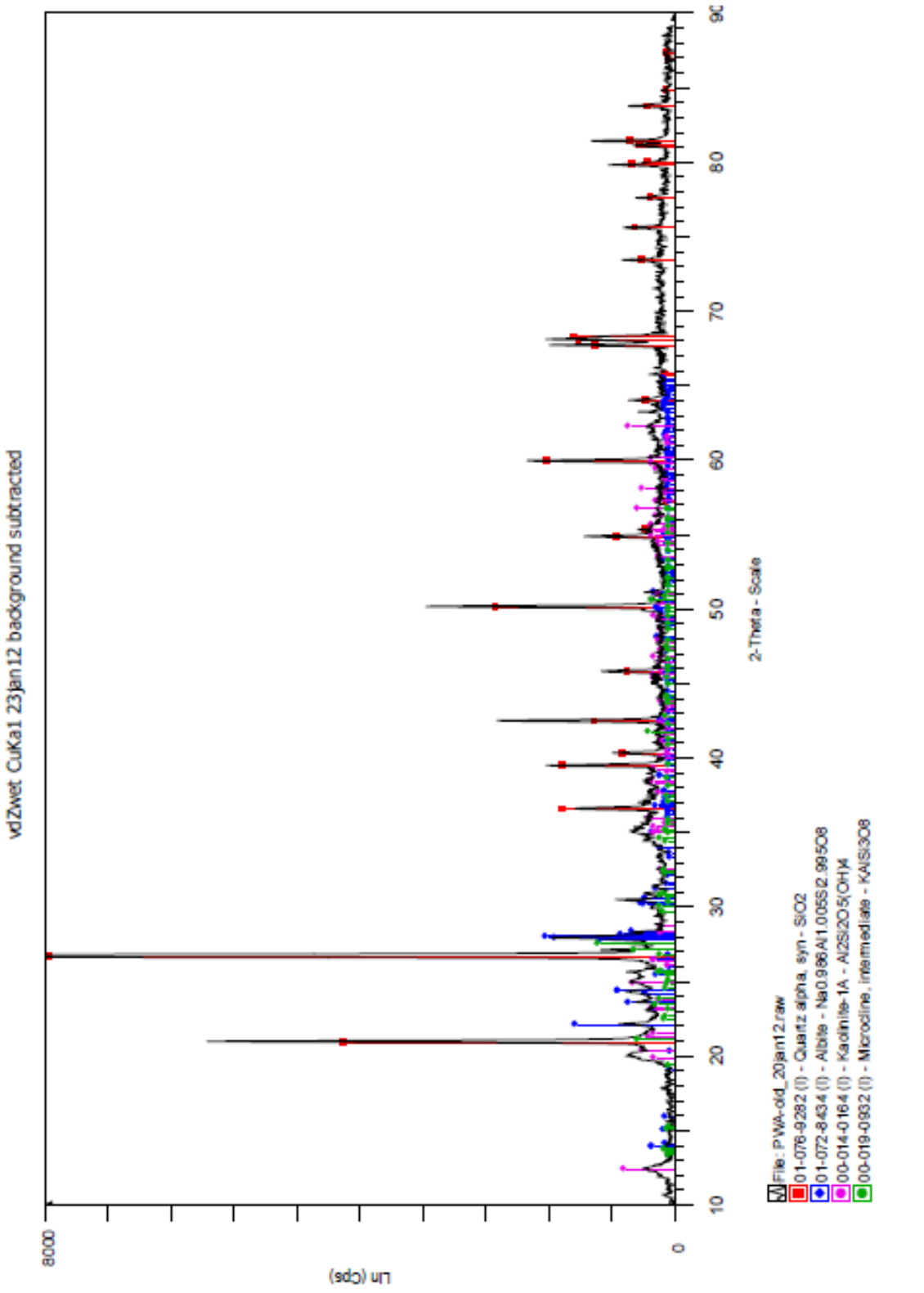

Figure H.4 Pwalugu old site (White Volta) 23/9

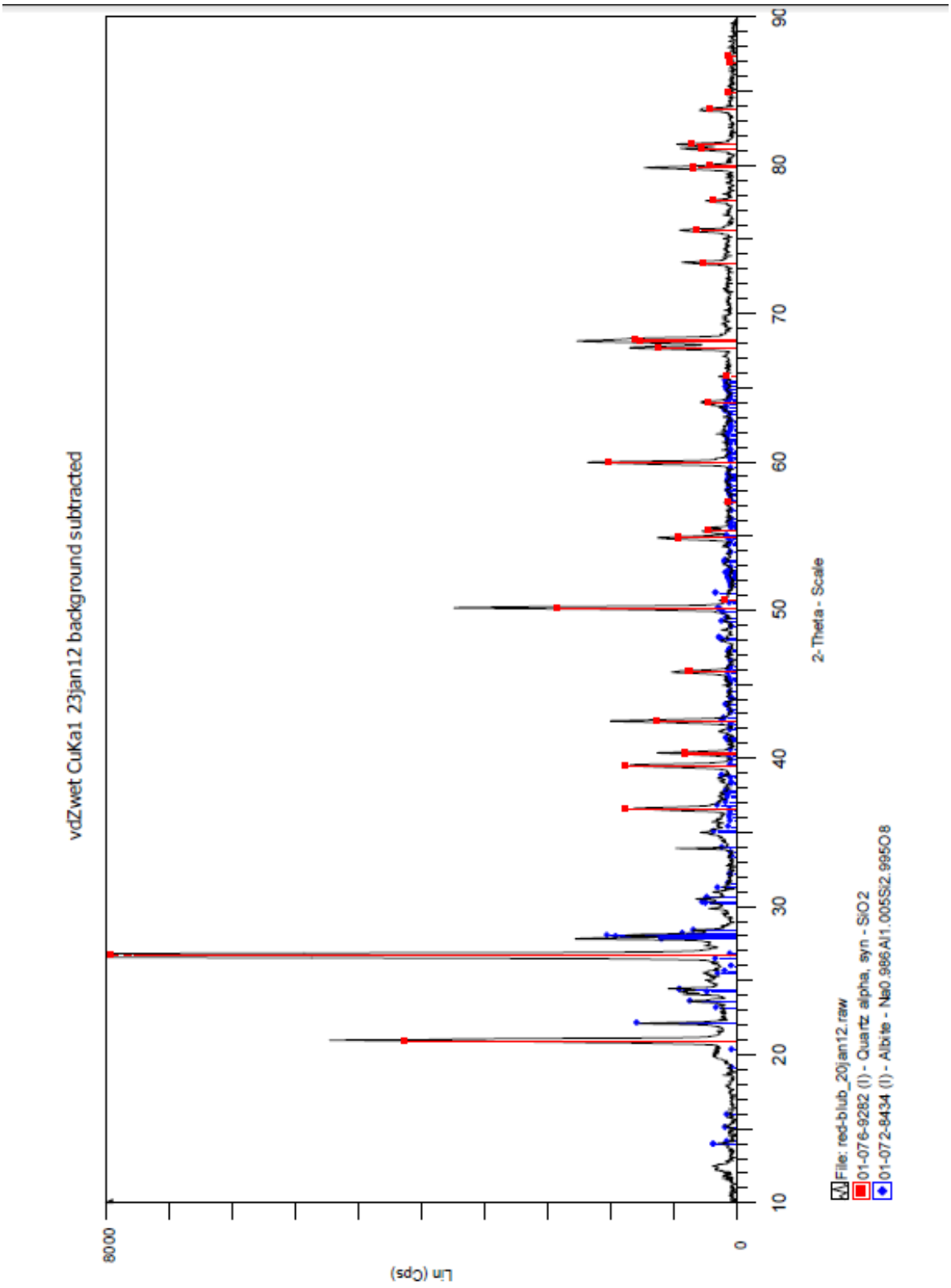

Figure H.5 Nangodi (Red Volta) 4/9

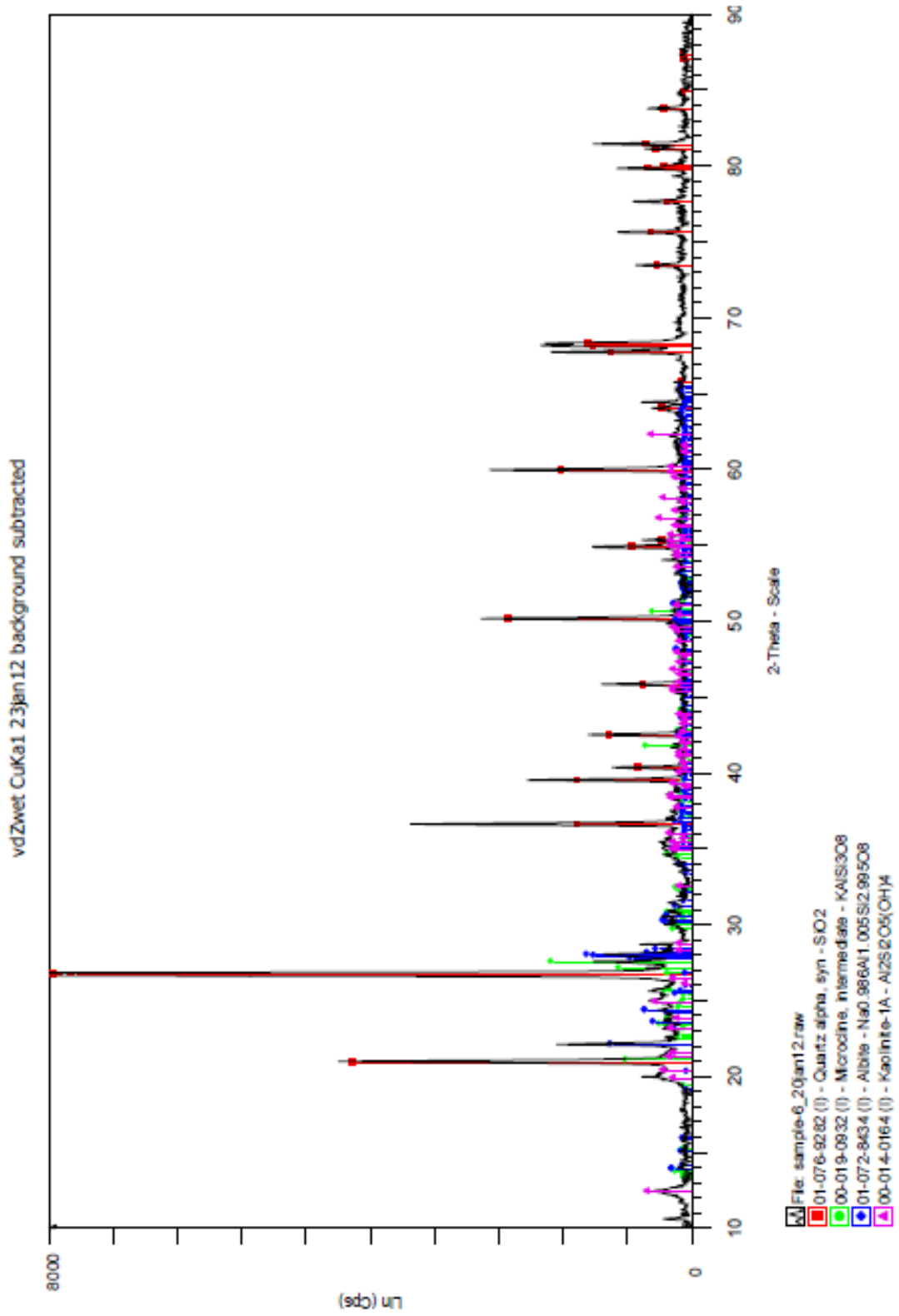

Figure H.6 Pwalugu (White Volta) 22/9

Appendix I: XRD Quantitative analysis

XRD Semi-quantitive determination .

The numbers in wt% are not absolute! Matrix effects are not corrected for, therefore the compositions should only be compared one sample relative to the other. Unidentified phases are neglected. Texture is not taken into account
The (integral) intensities and peak positions are determined with program Eva.

The mineral data are obtained from the ICDD-Pdf4 database.

sample	compound	2theta	Raw Area cpsxdeg	Raw Area counts	Raw Area composition corrected	wt%
B-yar_20jan12.raw	Quartz	26.612	3852	98769	28965	47
	Microcline	27.362	186.2	4774	8092	13
	Albite	13.887	80.61	2067	24466	40 sum

sample	compound	2theta	Raw Area cpsxdeg	Raw Area counts	Raw Area composition corrected	wt%
PWA-lumped_23jan12.raw	Quartz	26.65	3117.1	79926	23439	67
	Microcline	27.52	35.27	904	1533	4
	Albite	22.029	111.4	2856	5558	16
	Kaolinite-1A	12.322	155.9	3997	4595	13 sum

sample	compound	2theta	Raw Area cpsxdeg	Raw Area counts	Raw Area composition corrected	wt%
F-red_23jan12.raw	Quartz	26.65	4433.7	113685	33339	72
	Microcline	27.459	136.4	3497	5928	13
	Albite	22.054	146.5	3756	7309	16 sum

sample	compound	2theta	Raw Area cpsxdeg	Raw Area counts	Raw Area composition corrected	wt%
red-blub_20jan12.raw	Quartz	26.64	4052	103897	30468	80
	Albite	22.049	148.5	3808	7409	20 sum

sample	compound	2theta	Raw Area cpsxdeg	Raw Area counts	Raw Area composition corrected	wt%
PWA-old_20jan12.raw	Quartz	26.676	3141	80538	23618	71
	Microcline	27.496	25.43	652	1105	3
	Albite	22.083	73.72	1890	3678	11
	Kaolinite-1A	12.344	157.7	4044	4648	14 sum

sample	compound	2theta	Raw Area cpsxdeg	Raw Area counts	Raw Area composition corrected	wt%
sample-6_20jan12.raw	Quartz	26.679	4549.5	116654	34209	62
	Microcline	27.51	127.7	3274	5550	10
	Albite	22.057	227.9	5844	11371	21
	Kaolinite-1A	12.337	136.4	3497	4020	7 sum